



**UNIVERSITÀ DEGLI STUDI DI NAPOLI
“FEDERICO II”**



PhD Thesis

**“Design and identification of bio-compounds to
increase shelf-life and food safety”.**

Coordinator

Prof. Paolo De Girolamo

Candidate

Dott.ssa Lorena Gratino

Tutor (CNR)

Dott.ssa Gianna Palmieri

Tutor (UNINA)

Prof. Aniello Anastasio

“A chi vive di coraggio,
senza mai smettere di avere paura”

Index

Abbreviations	8
List of figures	12
List of tabs	19
Abstract	21
CHAPTER I	
1. INTRODUCTION	25
1.1 The oxidative stress	26
1.2 Oxidants and free radical production	26
1.2.1 Physiological Activities of Free Radicals	28
1.2.2 Reactive Oxygen Species (ROS).	30
1.2.3 Deleterious effects on food of oxidative stress	32
1.3 Antioxidant defence systems	39
1.3.1 Superoxide Dismutase enzymes	42
1.3.2 Extremophilic organisms	45
1.3.2.1 <i>Archaea</i>	47
1.3.2.1.1 <i>Aeropyrum pernix</i>	51
2. MATERIALS AND METHODS	53
2.1 Cloning of <i>Aeropyrum pernix</i> K1 Mn/Fe-SOD Coding DNA Sequences (CDS)	53
2.2 Cloning of <i>SOD_{Ap}</i> in Plant Expression Vectors	54
2.3 Genetic Transformation of Tomato Plants by <i>Agrobacterium</i> <i>Tumefaciens</i>	56
2.4 Molecular Analysis of the Tomato Transformed Lines	59
2.5 Production of Tomato Cell Extracts	60

Index

2.6	SOD and NBT Assays	61
2.7	Molecular Mass Determination	62
2.8	SDS-PAGE and Western Blot Analyses	63
2.9	ORAC Assay	63
2.10	Sampling Preparation	64
2.11	Colour Measurements	66
2.12	Histamine and Nitrate Determination in Tuna Fillet	67
2.12.1	Color reagent	67
2.12.2	Reduction of nitrate to nitrite	68
2.12.3	Nitrite determination	69
2.13	Statistical Analysis	69

3. RESULTS AND DISCUSSION 70

3.1	Expression of SOD _{Ap} in Tomato Cell Cultures	70
3.2	Biochemical characterization of SOD _{Ap}	76
3.3	Activity of SOD _{Ap} -tomato cell extracts on tuna slices	79
3.4	Activity of SOD _{Ap} -tomato cell extracts on myoglobin oxidation	86

4. CONCLUSIONS 88

5. REFERENCES 90

CHAPTER II

1. INTRODUCTION 98

1.1	Food safety and Food Security	99
1.2	Food spoilage	100

Index

1.2.1	Microbial food spoilage	102
1.2.1.1	<i>Listeria monocytogenes</i>	105
1.2.1.2	<i>Salmonella</i> spp.	106
1.2.1.3	<i>Staphylococcus aureus</i>	107
1.2.1.4	<i>Escherichia coli</i>	109
1.2.1.5	<i>Campylobacter</i> spp.	110
1.2.1.6	<i>Yeasts and moulds</i>	111
1.3	Food preservation	114
1.3.1	Active packaging	115
1.3.1.1	Antimicrobial packaging	116
1.4	Antimicrobial peptides	119
1.4.1	Classification	120
1.4.2	Mechanism of action	126
1.4.3	AMPs applications and future perspectives	132
2.	RESULTS OF RESEARCH GROUP	133
3.	MATERIALS AND METHODS	137
3.1	ANTIMICROBIAL PEPTIDE 1018K6	137
3.1.1	Production of 1018K6	137
3.1.2	Atmospheric Plasma Treatment and 1018K6 Immobilization on Polymer Surfaces	138
3.1.3	1018K6 release test	139
3.1.4	Sample preparation	139
3.1.5	pH and water activity measurements	140
3.1.6	Microbiological analyses	141
3.1.7	Challenge test	142
3.1.8	Colourimetric analyses	143
3.1.9	TBARS, Total volatile basic nitrogen and trimethylamine	

Index

	analyses	144
3.1.10	Sensory testing	146
3.1.11	Statistical analyses	147
3.2	ANTIMICROBIAL PEPTIDE RiLK1	148
3.2.1	Production of RiLK1	148
3.2.2	Circular Dichroism and Fluorescence Spectroscopies of RiLK1	148
3.2.3	The effect of Ionic Strength on RiLK1 Stability	149
3.2.4	Antimicrobial assay	152
3.2.5	Antifungal assay	153
3.2.6	Evaluation of Cell Morphology and <i>In Vitro</i> Cytotoxicity Assays	153
3.2.7	Preparation of Model Membranes: Multilamellar Vesicles (MLVs)	155
3.2.8	Lipid Binding Assay	157
3.2.9	Steady-State Tryptophan Fluorescence	158
3.2.10	Statistical Analyses	158
4.	RESULTS AND DISCUSSION	159
4.1	ANTIMICROBIAL PEPTIDE 1018K6	159
4.1.1	1018K6 Immobilization on PP Surface	159
4.1.2	Effects of 1018K6-PP on physical properties and on microbiological quality of Salmon fillets	162
4.1.3	Instrumental colour analysis of salmon fillets	168
4.1.4	Effect of 1018K6-PP on chemical parameters of Salmon fillets	171
4.1.5	Panelists' sensory evaluation	175
4.1.6	Microbial challenge testing of <i>L. monocytogenes</i> on salmon fillets packaged with 1018K6-PP.	177
4.1.7	Evaluation of 1018K6-PPs slides on physico-chemical, microbial and sensorial properties of <i>Sarda sarda</i> burgers	179
4.2	ANTIMICROBIAL PEPTIDE RiLK1	186
4.2.1	Conformational characterization of RiLK1	186
4.2.2	In Vitro Antimicrobial Activities of RiLK1	193

Index

4.2.3	In Vitro Antifungal Activities of RiLK1	198
4.2.4	Evaluation of Detrimental Effects of RiLK1 on Mammalian Cells	201
4.2.5	Peptide binding to Multilamellar vesicles (MLVs) and lipid binding assay	203
5.	CONCLUSIONS	207
6.	REFERENCES	209

Abbreviations

AAPH	2,2'-Azobis(2-amidinopropane) dihydrochloride
ACSSuT	Ampicillin, chloramphenicol, streptomycin, sulfonamides, and Tetracycline
AD	Alzheimer's disease
ADI	Acceptable Daily Intakes
ALEs	Advanced lipid oxidation end-products
ALOA	Agar Listeria acc. to Ottaviani & Agosti
ALS	Amyotrophic Lateral Sclerosis
AMP	Ampicillin,
AMP	Antimicrobial Peptides
APD3	Antimicrobial Peptide Database
ATCC	American Type Culture Collection
AUC	Area Under Curve
BA _s	Biogenic amines
BHA	t-Butyl-4-HydroxyAnisole
BPW	buffered peptone water
BSA	Bovine Serum Albumin
CAMP	Collection of Anti-Microbial Peptides
CAT	Catalase
CAZ	Ceftazidime
CD	Circular Dichroism
cDNA	Complementary DNA
CDS	Coding DNA Sequence
CFU	Colony forming units
CHL	Chloramphenicol
CIP	Ciprofloxacin
CL	Cardiolipin
CLSI	Clinical and Laboratory Standards Institute
CM	Commercial Brine Solution
CSI	Chemical spoilage index
CST	Colistin sulfate
CTX	Cefotaxime
DMA	Dimethylamine
DMEM	Dulbecco's modified Eagle's medium
DMSO	Dimethyl-sulfoxide
dNTP	Deoxyribonucleotide Triphosphate
DOPE	1,2-dioleoyl-sn-glycero-3-phosphoethanolamine
DSMZ	Deutsche Sammlung von Mikroorganismen und Zellkulturen
ECDC	European Centre for Disease Control
EDTA	Ethylenediaminetetraacetic Acid
EFSA	Food Safety Authority

Abbreviations

EGFP	Enhanced Green Fluorescent Protein
EHEC	E. enterohemorrhagic coli
ERR	Rough Endoplasmic Reticulum
FAO	Food & Agriculture Organization
FR	Free Radical
GEN	Gentamicin
GPX	Glutathione Peroxidase
GSH	Glutathione
HDPs	Host Defense Peptides
HEPES	(4-(2-hydroxyethyl)-1-piperazineethanesulfonic acid)
HIV	Human immunodeficiency virus
HNE	4-hydroxynonenal
HRP	Horseradish Peroxidase
IC50	Half-maximal inhibitory concentrations
ICMSF	International Commission on Microbiological Specifications for Foods
ISS	Istituto Superiore di Sanità
JECFA	Joint FAO-WHO Committee on Food Additives
KAA	Kanamycin Aesculin Azide
LAB	Lactic Acid Bacteria
LPS	Lipopolysaccharides
Mb	Myoglobin
MBC	Minimum Bactericidal Concentration
MDA	Malondialdehyde
MDR	Multidrug resistant
MES	Ethanesulfonic Acid
MFC	Minimum Fungicidal Concentration
MIC	Minimum inhibitory concentration
MLVs	Multilamellar Vesicles
MRS	Man, Rogosa, Sharpe
MRSA	Methicillin-resistant S. aureus
MS	Member States
MS	Murashige and Skoog
MWCO	Molecular Weight Cut-off
NAA	1-Napthaleneacetic Acid
NAC	N-Acetylcysteine
NAL	Nalidixic acid
NBT	Nitro Blue Tetrazolium
NR	Neutral Red
NRU	Neutral Red Uptake
ORAC	Oxygen Radical Absorbance Capacity
ORF	Open Reading Frame

Abbreviations

OxyMb	Oxymyoglobin
PA	phosphatidic acid
PBS	Phosphate-Buffered Saline
PBS	Phosphate Buffered Saline
PC	Phosphatidylcholine
PCA	Plate Count Agar
PCR	Polymerase Chain Reaction
PE	Phosphatidylethanolamine
PET	Polyethylene terephthalate
PFA	Paraformaldehyde
PFGE	Pulsed Field Gel Electrophoresis
PG	Phosphatidylglycerol
PI	Phosphatidylinositol
POPE	Palmitoyl-2-oleoyl-sn-glycero-3-phosphoethanolamine
POPG	1-palmitoyl-2-oleoyl-sn-glycero-3-phosphatidylglycerol ()
PP	polypropylene
PrAMPs	Proline-Rich Peptides
PS	Phosphatidyl serine
PUFA	Polyunsaturated Fatty Acids
PVDF	Polyvinylidene Fluoride
ROS	Reactive Oxygen Species
RP-HPLC	Reverse-Phase High-Performance Liquid Chromatography
RT-PCR	Real-time Polymerase Chain Reaction
SCF	Scientific Committee for Food
SDS-PAGE	Sodium Dodecyl-Sulfate Polyacrylamide Gel Electrophoresis
SE	Standard error
SM	N-Acyl-D-sphingosine-1-phosphocholine
SOD	Superoxide dismutase
SSOs	Specific spoilage microorganisms
STEC	Shiga-toxin producing Escherichia coli
SXT	Trimethoprim-sulfamethoxazole,
TAB	Total aerobic bacterial
TBA	Thiobarbituric acid
TBARS	Thiobarbituric acid reactive substance
TBX	Tryptone Bile X-glucuronide
TCA	Trichloroacetic acid
TEMED	Tetramethylethylenediamine
TET	Tetracycline
TFA	Trifluoroacetic acid
TMA	Trimethylamine
TRP	Tryptophan
TSP	Total Soluble Proteins

Abbreviations

TTBS	Tris-Tween Buffered Saline
TVB-N	Total volatile basic nitrogen
UE	European Union
VOCs	Volatile organic compounds
VRBG	Violet Red Bile Glucose
VRBL	Violet Red Bile Lactose
VSP	Vacuum Skin Packaging
WB	Western Blot
WHO	World Health Organization
WT	Wild Type
YEP	Yeast Extract Peptone

List of figures

CHAPTER I

Fig. 1: Oxidative stress definition according to Helmut Sies (1995).

Fig. 2: Schematic representation of a stable molecule and a free radical. A free radical is an atom or group of atoms that has at least one unpaired electron and is therefore unstable and highly reactive.

Fig. 3: Schematic representation of formation sources, and molecular targets of free radicals. Free radicals can be formed either naturally in the body through normal metabolic processes or from external factors such as X-rays, cigarette smoking, air pollutants, industrial chemicals, and even diet.

Fig. 4: Schematic representation of the adverse effects of free radicals to human health.

Fig. 5: Schematic representation of the effects of free radicals on biological molecules such as lipids, proteins, and DNA. Free radicals react largely in a nonspecific manner with nucleic acids, proteins, and membrane lipids causing cell injury through various mechanisms as shown.

Fig. 6: Oxidative stress effects on food products.

Fig. 7: Schematic representation of oxidation of polyunsaturated fatty acids (PUFAs) and production of lipid radicals. The first step is the generation of lipid radicals (initiation), followed by the propagation caused by the generation of new lipid radicals, such as Malondialdehyde (MDA) and 4-hydroxynonenal (HNE). These highly reactive chemicals, can bind biomolecules involved in fundamental processes in the cells, leading to cell death. The final step is termination, either by antioxidants or another radical.

Fig. 8: Effects of lipid peroxidation on different food products. A) Rancid butter; B) rancid meat; C) rancid fruit and D) Rancid seafood.

Fig. 9: Schematic representation of possible effects of protein oxidation.

Fig. 10: Schiff base formation from proteins interaction with aldehydic products.

Fig. 11: How antioxidants reduce the free radicals.

Fig. 12: Subcellular non-enzymatic antioxidants targets. Within the cell, non-enzymatic antioxidants are distributed according to their subcellular target. The mitochondria are protected from oxidative stress by CoQ10, MitoQ, carnosine, and Vit C. In the cytoplasm, the antioxidant system includes GSH, NAC, and UA. Vit E is found in cytoplasmic, ER, and mitochondrial membranes, as well as in lysosomes. (Figure created in BioRender.com).

Fig. 13: Antioxidant enzyme systems. They catalyze reactions to neutralize free radicals and reactive oxygen species. These enzymes, including superoxide dismutase, glutathione peroxidase, glutathione reductase and catalases, metabolize oxidative toxic intermediates

List of figures

and represent the body's endogenous defence mechanisms to help protect against free radical-induced cell damage.

Fig. 14: Superoxide dismutase reaction.

Fig. 15: Classes of Superoxide dismutase enzyme.

Fig. 16: Representative idealized cross section of Earth's crust showing the diversity of extreme environments and their approximate location. (Merino N. 2019).

Fig. 17: A schematic diagram of extremophilic microorganisms which grow in reported extreme conditions.

Fig. 18: A phylogenetic tree of living things, based on RNA data and proposed by Carl Woese, showing the separation of bacteria, archaea, and eukaryotes. By This vector version: Eric Gaba (Sting – fr: Sting) – NASA Astrobiology Institute, found in an article, Public Domain.

Fig. 19: Ultrathin section of *Aeropyrum pernix* K1. Bar, 0.2 μm . (Sako Y. et al.,1996).

Fig. 20: Coding DNA sequences (CDS) of SODAp extremozyme inserted in the subcloning pSCB vector.

Fig. 21: Schematic representation of pBICK-SODAp. The vector was assembled by introducing between the HindIII/EcoRI restriction sites of the original pBI121 binary vector the expression cassette from pCK expression vector encoding gene of interest (pCK-SODAp_{ter}K3S described in Materials and Methods) under the control of double-enhancer 35S (2x) promoter and a transcription leader sequence (TL). Transcription stops thanks to the terminator of CaMV 35S. 2x enh. CaMV35S-pro: double-enhancer 35S (2x) promoter from Cauliflower mosaic virus 35S; 35Ster: Cauliflower mosaic virus 35S terminator; SODAp: *Aeropyrum pernix* SuperOxide Dismutase; NPTII (kanr): neomycin phosphotransferase II gene for kanamycin resistance; NOS: nopaline synthase; RB: right border and LF: left border.

Fig. 22: Scheme of the experimental procedure for the sampling and preparation of tuna fillets (filleting, brine injection, and vacuum skin packaging-VSP).

Fig. 23: Transgenic calli production from tomato cotyledones (cv MicroTom). (A) callus induction in leaf pieces; (B) callus formation from hypocotyls on MS medium containing NAA and kinetin; (C) callus lines regenerated; (D) transgenic clones characterized for the presence and the expression of etherologous SOD.

Fig. 24: Semi quantitative RT-PCR analysis of transgenic SODAp gene. Ladder: 1 Kb DNA ladder (Promega); WT: untransformed tomato calluses; 18S: amplification product of 18S gene (internal standard).

List of figures

Fig. 25: SDS-PAGE, NBT-PAGE and western blot analyses of total protein extracts from transgenic tomato cell lines. (A) Total protein extracts (30 μ g) were electrophoresed on 12% SDS-polyacrylamide gel and detected with Coomassie blue staining. (B) Total protein extracts (15 μ g) obtained from tomato cell lines untransformed (WT) or transformed with SODAp gene, were electrophoresed on Native-PAGE (10%). Following Native-PAGE, protein bands were detected by in-gel SOD activity staining using the Riboflavin-NBT assay. The results are representative of three independent experiments on three different proteins. (C) Total proteins were extracted from the tomato cell lines, separated by SDS-PAGE and transferred to PVDF membrane. WT: untransformed tomato cells; SODAp#1, SODAp#2 and SODAp#3: callus lines transformed with SODAp gene. SODEC: purified SOD used for comparative quantification of the relative intensity of band of interest (indicated with *).

Fig. 26: Gel filtration chromatography of partially purified SODAp. Size-exclusion chromatogram of partially purified SODAp on Superdex 200 column in 50 mM Tris-HCl buffer pH 7.5 containing 50 mM NaCl. The absorbance was measured at 280 nm. Insert: calibration curve of Superdex 200 column using protein standards of known molecular masses: Thyroglobulin (670 kDa), Bovine g-globulin (158 kDa), Chicken ovalbumin (44 kDa), Equine myoglobin (17 kDa), Vitamine B12 (1.35 kDa).

Fig. 27: Electrophoretic analyses followed by enzyme activity staining. SDS-PAGE (10%) (left) and Native-PAGE (10%) (right) analyses of SODAp fraction obtained after gel filtration chromatography. MW: molecular markers. Following electrophoretic analyses, protein bands were detected by in-gel SOD activity staining using the Riboflavin-NBT method. The results are representative of three independent experiments on three different protein preparations.

Fig. 28: Biochemical analysis of transgenic extracts: Effects of (A) temperature and (B) NaCl on SODAp activity. Fold increase was calculated as ratio between SOD activity in crude protein extracts from wild-type plants/SOD activity in crude protein extracts from transgenic plants, using the NBT assay. All experiments were performed in triplicate on three different protein preparations. Data were expressed as means \pm standard deviation. Standard deviation values lower than 5% were not shown.

Fig. 29: Biochemical properties of SODAp: Effect of (A) temperature and (B) NaCl on SODAp activity. The activity at the optimal temperature or NaCl concentration was defined as 100%. The SOD activity was measured using the NBT assay and all experiments were performed in triplicate on three different protein preparations. Data were expressed as means \pm standard deviation. Standard deviation values lower than 5% were not shown.

Fig. 30: Analyses of total color difference (ΔE) and variation in a^* (Δa^*) in *Thunnus albacares* and *Thunnus thynnus* fillets during the storage (4 ± 1 °C) for 10 days. (A) ΔE and (B) Δa^* values in *Thunnus albacares* fillets injected with aqueous solutions containing: water only (CTR: blue); extracts from tomato cell lines non-transformed with sodAp (WT: light red); extracts from tomato cell lines transformed with sodAp (SODAp: green); commercial brine (CM: red). (C) ΔE and (D) Δa^* values of *Thunnus thynnus* fillets injected with aqueous solutions containing: water only (CTR: blue); extracts from tomato cell lines

List of figures

non-transformed with sodAp (WT: light red); extracts from tomato cell lines transformed with sodAp (SODAp: green). The measurements were carried out on the inner surface of the tuna fillets after 10 minutes of exposure to air. Results are means of three independent experiments and error bars represent the standard error (sem). *Significant difference ($p < 0.05$) between the treated and the control samples. *** Significant difference ($p < 0.001$) between the treated and the control samples.

Fig. 31: Appearance of *Thunnus thynnus* slices stored for 10 days at refrigerated temperature (4 ± 1 °C). The samples were injected with aqueous solutions containing water only (CTR); extracts from tomato cell lines non-transformed with sodAp (WT); extracts from tomato cell lines transformed with sodAp (SODAp).

CHAPTER II

Fig. 1: Examples of contaminated foods: fruit, meat and bread.

Fig. 2: Representative scheme of food spoilage caused by microbial agents. The enzymes of microorganisms growing on foods, lead to by-products formation which are responsible of the spoilage and alteration of organoleptic characteristics.

Fig. 3: Notification rates and reported numbers of confirmed human cases of zoonoses in the EU, 2019 (EFSA and ECDC, 2021).

Fig. 4: Image of *Listeria monocytogenes* produced by microscope.

Fig. 5: Image of *Salmonella* produced by microscope.

Fig. 6: Image of *Staphylococcus aureus* produced by microscope.

Fig. 7: Image of *Escherichia coli* produced by microscope.

Fig. 8: Image of *Campylobacter* produced by microscope.

Fig. 9: Representative plates of the (A) mould *Aspergillus Flavus* and (B) yeast *Candida*.

Fig. 10: Classification of active packages.

Fig. 11: Different strategies of incorporation to the polymeric film and mode of release of antimicrobial agents in foods: (A) inclusion of the bioactive molecule in the polymer before extrusion and release from the material with gradual diffusion from the material into the headspace; (B) incorporation into the plastic film prior to extrusion and gradual diffusion from the material into the food by direct contact; (C) surface coating on the film and release into the headspace by gradual diffusion; (D) surface coating on the film and gradual diffusion from the material into the food by direct contact; (E) edible film and gradual diffusion from the material into the food by direct contact.

List of figures

Fig. 12: Classification of AMPs.

Fig. 13: Different structures of AMPs.

Fig. 14: Schematic representation of the "barrel-stave" model. Hydrophilic and hydrophobic portions of peptides are represented in blue and red respectively.

Fig. 15: Schematic representation of the "toroidal" model. The hydrophilic and hydrophobic portions of the peptide molecules are represented in blue and red respectively.

Fig. 16: Schematic representation of the "carpet" model. The hydrophilic and hydrophobic portions of the peptide molecules are represented in blue and red respectively.

Fig. 17: Representative scheme of AMPs action mechanisms involving interaction with intracellular targets.

Fig. 18: Immobilization yield (%) of 1018K6 on PP surfaces determined by RP-HPLC chromatography on a C18 column after the coupling reaction. PP surfaces pre-activated by plasma treatment, were incubated with a water solution of 1018K6 (100 μ M). After the coupling reactions, the supernatants were recovered and analysed by RP-HPLC. The peptide solution (100 μ M) at time 0 ($t = 0$) was used as control. The reported chromatograms are representative of three independent experiments.

Fig. 19: Representative scheme of the experimental preparation of salmon fillets.

Fig. 20: Effects of 1018k6-PP surfaces on the Chemical Quality of *Salmon salar* fillets. Changes in TVB-N (A), TMA-N (B), and TBARS (C) of *Salmon salar* fillets packaged in active 1018K6-PP films during storage at 4 °C. CTR (blue lines): PP films without 1018K6; 1018K6-PP (green lines): PP films functionalized with 1018K6. Results are means of three independent experiments and error bars represent the standard error (sem). Different letters at each sampling time are used for significantly different samples, according to Tukey test (uppercase letters: $p < 0.01$; lowercase letters: $p < 0.05$).

Fig. 21: Changes in colour (A), odour (B), and overall appearance (C) of salmon fillets during storage period. CTR (blue lines): PP films without 1018K6; 1018K6-PP (green lines): PP films functionalized with 1018K6.

Fig. 22: Bactericidal activity of polymer functionalized with 1018K6 against *L. monocytogenes* on salmon fillets. Negative control: untreated salmon fillets; Positive control: salmon fillets treated with not-functionalized PP; Treated control: salmon fillets treated with 1018K6-PP.

Fig. 23: Representative scheme of preparation of *Sarda sarda* burgers employed in the microbiological and physico-chemical analyses. (A) Burgers of *Sarda sarda* treated with

List of figures

PPs films not-functionalized with 1018K6 (CTR); (B) Burgers of *Sarda sarda* treated with PPs films functionalized with 1018K6 (1018K6-PP).

Fig. 24: (A) Analysis of Δa^* variation (Δa^*) in bonito fish burgers during the storage period. Results are means of three independent experiments and error bars represent the standard error (sem). CTR (blue): PP films without 1018K6; 1018K6-PP (green): PP films functionalized with 1018K6. (B) Photos of *Sarda sarda* burgers packaged with the control and functionalized slides at each sampling time.

Fig. 25: Effects of 1018K6-PP slides on the Chemical Quality of *Sarda sarda* burgers. Changes in TVB-N (A), TMA-N (B), and TBARS (C) of *Sarda sarda* burgers packaged in active 1018K6-PP films during storage at 4 °C. CTR (blue lines): PP films without 1018K6; 1018K6-PP (green lines): PP films functionalized with 1018K6. Results are means of three independent experiments and error bars represent the standard error (sem). Different letters at each sampling time are used for significantly different samples, according to Tukey test (uppercase letters: $p < 0.01$; lowercase letters: $p < 0.05$).

Fig. 26: Changes in colour (A), odour (B), and overall appearance (C) of bonito fish burgers during storage period. CTR (blue lines): PP films without 1018K6; 1018K6-PP (green lines): PP films functionalized with 1018K6.

Fig. 27: Time-dependent effect of SDS on the secondary and tertiary structure of RiLK1 monitored by spectroscopic analyses. (A) Far-UV Circular Dichroism (CD) spectra of the peptide (0.1 mg/mL) were recorded in 10 mM Tris-HCl buffer pH 7.0 in the presence or absence of SDS (3 mM) over the time at 25 °C. (B) Intrinsic fluorescence emission spectra of RiLK1 (0.1 mg/mL) in 10 mM Tris-HCl buffer, pH 7.0 in the presence or absence of SDS (3 mM) over the time at 25 °C.

Fig. 28: Effect of the temperature on the secondary structure of RiLK1. Far-UV CD spectra of the peptide (0.1 mg/mL) were acquired in 10 mM Tris-HCl buffer pH 7.0 in the presence of 3 mM SDS at three different temperatures (4 °C, 25 °C, and 90 °C) after 24 h incubation.

Fig. 29: Effect of pH on the secondary structure of RiLK1. Far-UV CD spectra were obtained by incubating the peptide (0.1 mg/mL) in buffers at different pHs for 24 h at 25 °C, and in the presence of SDS at a final concentration of 3 mM.

Figure 30: Stability in saline solution of RiLK1 determined by Reverse-Phase High-Performance Liquid Chromatography (RP-HPLC) on a C18 column. The peptide at final concentration of 50 μ M was incubated in the presence of NaCl (1M) until 9 days at 25 °C. At each incubation time, the peptide solutions were recovered and analyzed by RP-HPLC. The solution at time 0 ($t = 0$) was used as control. The chromatograms are representative of three independent experiments.

Figure 31: Dose-response effect of RiLK1 on the survival of different foodborne pathogens. Bacteria were incubated in the presence of increasing concentrations of the peptide. Data were determined by enumeration of the surviving colony forming units

List of figures

(CFU) on plates seeded with the pathogen incubated with the different peptide concentrations. Results were expressed as the percentage of colony forming units (CFU) survival, with respect to the colony counted in the control plates. The half-maximal inhibitory concentrations (IC50) and Minimal Bactericidal Concentration (MBC) values of the tested peptide against each bacterial strain were calculated using GraphPad Prism version 6.00. Data are presented as means \pm standard deviation (s.d.) of three separate experiments performed in triplicate.

Fig. 32: Antibacterial activity of RiLK1 against different foodborne pathogens: (A) *S. Typhimurium*, (B) *L. monocytogenes*, (C) *S. aureus*, and (D) *E. coli*. CTRL: each tested pathogen without treatment. Bacterial cultures treated, or not, with different concentrations of peptides were seeded on selective plates. The photographs are representative of three independent experiments performed in triplicate.

Figure 33: Antifungal activity of RiLK1 and 1018-K6 against pathogenic fungi. (A, B) *Aspergillus brasiliensis* and (C, D) *Candida albicans*. The fungal cultures untreated (CTRL) or treated with the peptides at 25 μ M concentration were seeded on DG18 (Dichloran 18% Glycerol Agar) plates. The photographs are representative of three independent experiments performed in triplicate.

Fig. 34: Morphological observation of different human cell lines treated with RiLK1 under phase-contrast microscope. Keratinocyte (HaCAT), embryonic (WI38), and fetal (TIG3) lung fibroblastic cell lines were incubated at 37 °C for 24 h in absence (CTRL) or in presence (treated) of RiLK1 at the maximum concentration tested (10 μ M). The microscope images are representative of three independent experiments performed in triplicate. Bar is equal 100 μ m.

Fig. 35: Saturation binding assay curves and Scatchard plots transformation for fluorescence spectroscopy data of Rilk1 in model membranes of (A) eukaryotic cell, (B) zwitterionic lipids, (C) *S. aureus*, (D) *S. Typhimurium*. Results are means of three independent experiments.

List of tables

CHAPTER I

Table 1: Radical and non-radical species of ROS.

Table 2: Comparison of structural and metabolic features in bacteria, eukaryotes, and Archaea. (Youssouf S. et al., 2019).

Table 3: Primer sequences used in this study.

Table 4: Primer sequences used in this study. Restriction sites are underlined.

Table 5: Primer sequences used in this study to amplify the SODAp.

CHAPTER II

Table 1: List of the physicochemical properties calculated and predicted for the designed peptide RiLK1 in comparison with those of the parent AMP 1018-K6.

Table 2: Membrane lipid composition in eukaryotic and prokaryotic organisms (% mol).

Table 3: Evaluation of microbiological counts [Log (CFU/g)] in salmon fillets packaged in active PP films functionalized with 1018K6 by storage time.

Table 4: Changes in colour indices of the salmon fillets packaged in active PP films functionalized with 1018K6 by storage time.

Table 5: Evaluation of microbiological counts (Log CFU/g) in *Sarda sarda* burgers packaged in active PP films functionalized with 1018K6 by storage time.

Table 6: Changes in colour indices of *Sarda sarda* burgers packaged in active PP films functionalized with 1018K6 by storage time.

Table 7: Secondary structure contents of RiLK1 in the absence or presence of SDS (3 mM) determined by BeStSel (Beta Structure Selection) and DichroWeb server.

Table 8: Secondary structure contents of RiLK1 at different temperatures in the absence or presence of SDS (3 mM) determined by BeStSel and DichroWeb server.

Table 9: Secondary structure contents of RiLK1 at different pH values determined by BeStSel and DichroWeb server.

Table 10: IC50 and MBC values of the tested peptides against the bacterial strains.

Abstract

All living organisms need food to survive, grow and get energy but it can constitute a possible hazard to human health, as it can contain pathogens, toxins or chemicals.

In the last few decades, there has been a rapid increase in the incidence of foodborne infections and diseases due to contamination that, can occur at any point along the food chain during production, processing, distribution, or preparation. Actually, there is a growing need to develop new and effective strategies to preserve foods and prevent foodborne illness thus satisfying the consumer demand for healthier and safer food products.

In this context, the aim of my PhD thesis was:

1) To investigate on antioxidant properties of an extremophilic Superoxide dismutase (SOD) heterologously expressed in transgenic tomato cell cultures, with the aim to evaluate the antioxidant potential of the extremozyme-enriched plant extracts in food preservation as promising natural ingredients able to protect against the deleterious effects of oxidation, (described in *Chapter I*)

2) To evaluate the effects of an active packaging functionalized with the antimicrobial peptide 1018K6 (already projected and characterized by the research group), on microbial growth, physicochemical properties and the sensory attributes of a highly perishable food like raw salmon fillets, with the aim to find alternative solutions to overcome existing challenges that are associated with fish spoilage (described in *Chapter II*).

Abstract

3) To further characterize a novel antimicrobial decapeptide, named RiLK1, which was rationally designed and preliminary studied by the research group, with the aim of developing a new class of short and multitask antimicrobial agents (described in *Chapter II*).

4) To study the interaction of RiLK1 with different model bacterial lipid membranes in order to investigate on the mode of action of this compound (described in *Chapter II*).

CHAPTER I

1. INTRODUCTION

In addition to the need, the sensory properties of foods are the principal reason that induce people to eat. Appearance, flavour, texture, smell and even the sounds of food can impart a desire to eat or cause us to dismiss the food as unappetizing, stale, or even inappropriate from a cultural standpoint [Chambers, E., 2019]. In fact, in the food industry, sensory analysis can be useful to direct marketing decisions concerning for example product positioning with respect to competitors, but also market segmentation, customer relationship management, advertising strategies and price policies [Iannario, M. *et al.*, 2012].

Nutritional values, colour, texture, and edibility of foods are susceptible to spoilage. So, the food preservation, that includes growing, harvesting, processing, packaging, and distribution of products, is an important element to prevent the alteration of organoleptic characteristics and to guarantee the food safety. [Rahman, M.S., 2007]. After microbial spoilage, the oxidation is the second most important cause of food impairment. As targets of reactive oxygen species (ROS), proteins and lipids are oxidatively modified through multiple mechanisms and pathways, leading to the loss of organoleptic and nutritional properties, especially in highly perishable foods [Lindley, M.G., 1998].

1.1 The oxidative stress

The concept of oxidative stress was introduced for the first time thirty years ago by H. Sies, which defined it as “a disturbance in the prooxidants - antioxidant balance in favour of the former, leading to potential damage” [Sies, H., 1985; Lushchak VI, Storey KB, 2021]. Nevertheless, the definition of oxidative stress is continuously in update. Later, the same authors updated the definition of oxidative stress in “an imbalance between oxidants and antioxidants in favour of the oxidants, potentially leading to damage”(Figure 1) [Sies, H., 1997].



Fig. 1: Oxidative stress definition according to Helmut Sies (1995).

1.2 Oxidants and free radical production

In the oxidative stress phenomena, an important role is played by free radicals (FRs), which were discovered at the beginning of the 20th century by Moses Gomberg [Gomberg, M., 1900].

From the chemical point of view, FRs can be defined as an atom or molecule that contains one or more unpaired electrons in valence shell or outer orbit and is able to exists in independent way (Figure 2). The odd number of electron(s) of a free radical makes it unstable, short lived and highly reactive, allowing to take electrons from other compounds

Chapter I

to become stable. Therefore, the attacked molecule loses its electron and turns into a free radical itself, beginning a chain reaction cascade, which finally damages the living cell [Mukherji, S.M., 1986; Phaniendra, A. *et al.*, 2015].

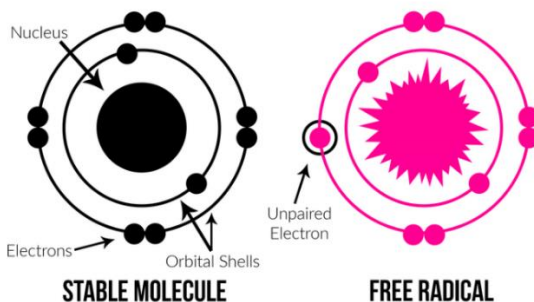


Fig. 2: Schematic representation of a stable molecule and a free radical. A free radical is an atom or group of atoms that has at least one unpaired electron and is therefore unstable and highly reactive

The FRs are normally produced by cellular metabolism and they can be generated from both exogenous (i.e environmental pollutants, heavy metals, several drugs, chemical solvents, smoke, meat, used oil, fatty acids, cigarette smoke, alcohol, and radiations) [Valko, M. *et al.*, 2007] and endogenous (i.e mitochondria, immune cell activation, inflammation, ischemia, infection, cancer, excessive exercise, mental stress, and aging) sources (**Figure 3**) [Frei, B., 1997].

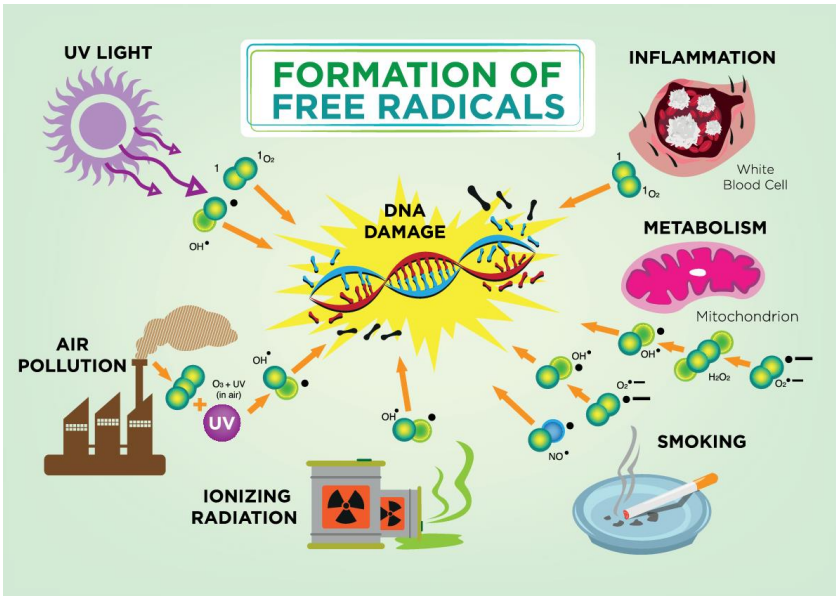


Fig. 3: Schematic representation of formation sources, and molecular targets of free radicals. Free radicals can be formed either naturally in the body through normal metabolic processes or from external factors such as X-rays, cigarette smoking, air pollutants, industrial chemicals, and even diet.

1.2.1 Physiological Activities of Free Radicals

At low or moderate concentrations, FRs have beneficial effects, such as the synthesis of some important cellular structures and the defence against pathogens [Pizzino, G. *et al.*, 2017]. In fact, phagocytes synthesize and store free radicals, in order to release them to destroy pathogenic microbes that invade the organism [Droge, W., 2002; Young, I. and Woodside, J., 2001]. Moreover, FRs play a key role in many cellular signalling pathways in different cell types, such as fibroblasts, endothelial cells, vascular smooth muscle cells, cardiac myocytes, and thyroid tissue [Pacher, P. *et al.*, 2007; Halliwell, B.,

2007]. Nevertheless, FRs are involved, at high concentrations, in harmful processes that can damage molecules and cellular structures. In fact, when an imbalance exists between free radical formation and the capability of cells to clear them, oxidative stress phenomena take place, causing, several diseases, both chronic and degenerative [Pizzino, G. *et al.*, 2017], if not strictly controlled.

It has been widely reported that oxidative stress is involved in cancer development, producing a variety of modifications on DNA structure, for example, base and sugar lesions, DNA-protein cross-links, strand breaks, and base-free sites [Valko, M. *et al.*, 2007]. During the last years, both *in vivo* and *ex vivo* studies pointed out an association between oxidative stress and cardiovascular diseases, such as atherosclerosis, ischemia, hypertension, cardiomyopathy, cardiac hypertrophy, and congestive heart failure [Droge, W., 2002; Bahorun, T. *et al.*, 2006; Chatterjee, M. *et al.*, 2007; Ceriello, A., 2008]. Moreover, it is known that oxidative stress is involved in the onset and/or progression of neurological (i.e., Parkinson's disease, Alzheimer's disease (AD), amyotrophic lateral sclerosis (ALS), multiple sclerosis, depression, and memory loss), and respiratory (i.e., asthma and chronic obstructive pulmonary disease, determined by systemic and local chronic inflammation) diseases, as well as in Rheumatoid arthritis, and in many others pathologies (**Figure 4**) [Valko, M. *et al.*, 2007; Halliwell, B., 2001; Butterfield, D. A., 2002; Caramori, G. and Papi, A., 2004; MacNee, W., 2001; Walston, J., 2006; Mahajan, A. and Tandon, V. R., 2004; Akovou, E. and Kourti, M. A., 2002].



Fig. 4: Schematic representation of the adverse effects of free radicals to human health

1.2.2 Reactive Oxygen Species

In all living aerobic organisms, the Reactive Oxygen Species (ROS) represent the most important class of radical species. They can be classified into radical and non-radical species and are reported in **Table 1** [Caimi, G. *et al.*, 2004; Rahman, T. *et al.*, 2012].

Chapter I

Table 1: Radical and non-radical species of ROS

Radicals	Non-radicals
Superoxide anion (O_2^-)	Hydrogen peroxide (H_2O_2)
Hydroxyl (OH^-)	Hypochlorous acid (HOCl)
Peroxy (RO^{2-})	Hypobromous acid (HOBr)
Alkoxy (RO^-)	Ozone (O_3)
Hydroperoxyl (HO_2^-)	Singlet Oxygen ($^1\text{O}_2$)

ROS are generated during normal metabolism and derive from oxygen, that is a biradical containing two unpaired electrons [Halliwell, B., 2001]. Specifically, oxygen is required for cellular respiration, acting as a terminal electron acceptor in oxidative phosphorylation. During this process, in which cells use up oxygen to generate energy, water molecules should be formed as product, but most times free radicals are created as consequence of ATP production by mitochondria [Diplock, A.T. *et al.*, 1998].

ROS(s) are highly reactive and toxic compounds involved in many inflammatory processes that generate human diseases (as described above).

Especially, ROS(s), being by-products of many degenerative reactions in several tissues, can impair the regular metabolism by damaging the cellular components [Foyer, C.H. and Noctor, G., 2002]. Generally, the detrimental effects of ROS(s) cause DNA damage, lipid peroxidation, protein oxidation and inactivation of specific enzymes, oxidating their cofactors. These reactions can affect intrinsic membrane properties like fluidity, ion transport, loss of enzyme activity, and so forth ultimately resulting in cell death (**Figure 5**).

Chapter I

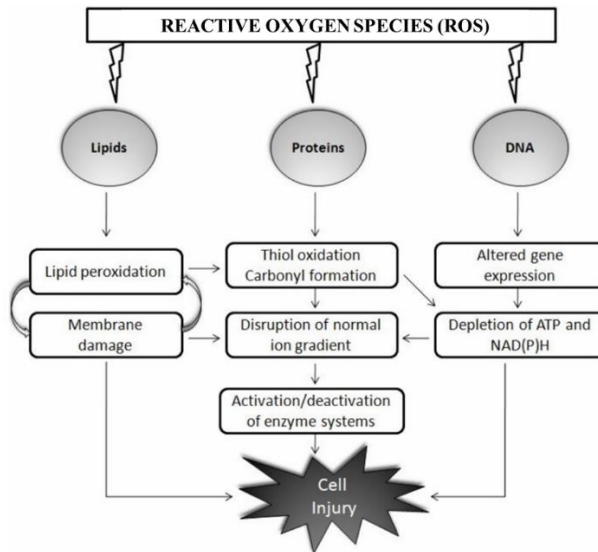


Fig. 5: Schematic representation of the effects of free radicals on biological molecules such as lipids, proteins, and DNA. Free radicals react largely in a nonspecific manner with nucleic acids, proteins, and membrane lipids causing cell injury through various mechanisms as shown.

1.2.3 Deleterious effects on food of oxidative stress

Food spoilage by chemical oxidation represents one of the major problems for society. This process often involves ROS(s) production, in fact, the exposure of foods or beverages to oxygen can trigger a chain of chemical reactions on proteins, pigments, fatty acids, and lipids, which results in the alteration of organoleptic and nutritional properties (**Figure 6**) [Decker, E.A. *et al.*, 2010].

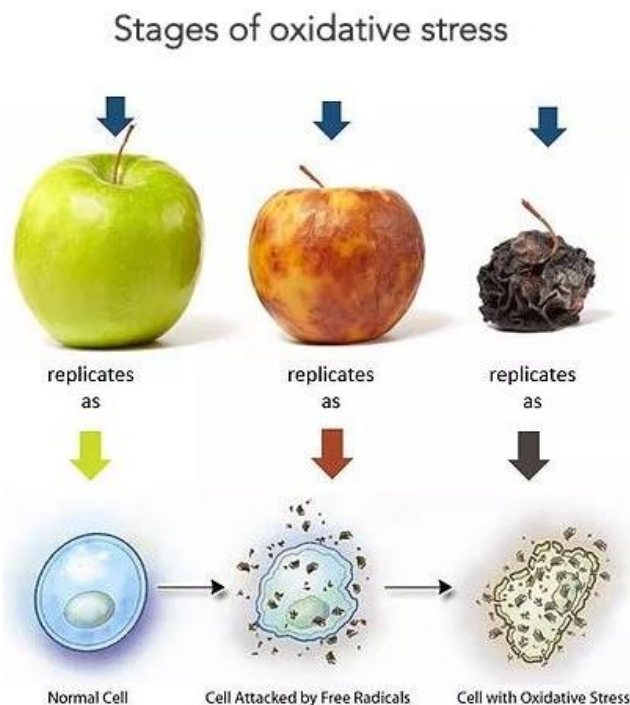


Fig. 6: Oxidative stress effects on food products

Specifically, lipid oxidation is classified as the major deterioration process affecting both the nutritional and sensory quality of foods causing rancidity and/or loss of the nutritional value, colour, flavour, texture and safety of the products [Shahidi, F. and Zhong Y., 2005].

The lipid oxidation can occur by three main complex reactions such as autoxidation, enzymatic-catalysed oxidation and photo-oxidation, which involve free radicals and/or other reactive species as intermediates [Shahidi, F., 2000; Vercellotti, J.R., 1992].

Lipid oxidation has long been accepted as a classic free radical chain reaction mechanism with initiation, propagation, and termination stages (e.g., lipid radicals, $R\cdot$; alkoxy, $RO\cdot$; peroxy, $ROO\cdot$; and

Chapter I

hydroxyl, $\bullet\text{OH}$), leading to the formation of hydroperoxides and conjugated dienes (or trienes) as primary unstable oxidation products, that can be further break down to secondary oxidation products, such as alcohols, aldehydes, ketones, hydrocarbons, volatile organic acids and epoxy compounds (**Figure 7**).

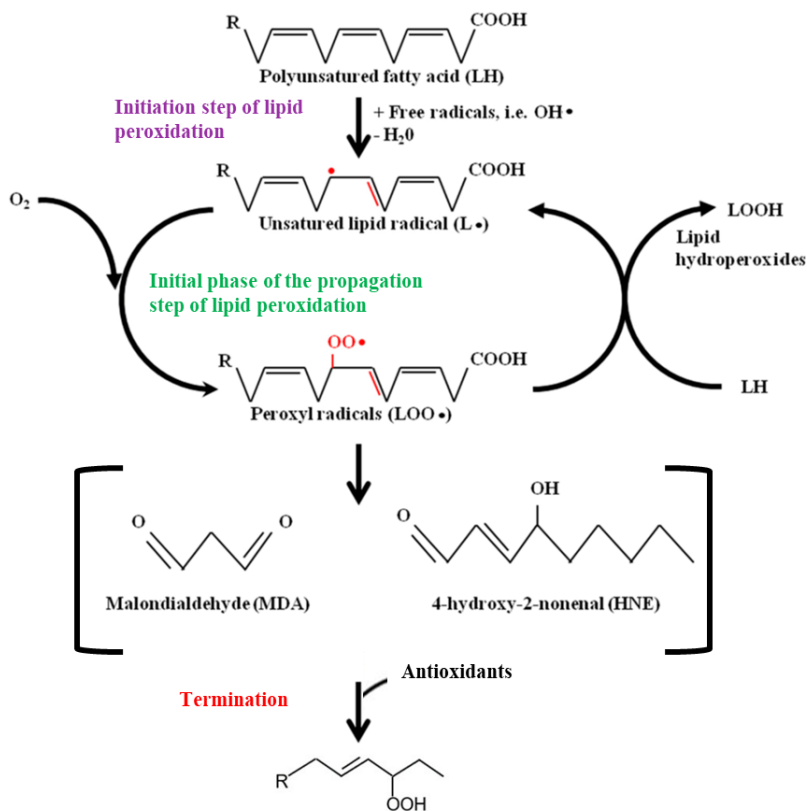


Fig. 7: Schematic representation of oxidation of polyunsaturated fatty acids (PUFAs) and production of lipid radicals. The first step is the generation of lipid radicals (initiation), followed by the propagation caused by the generation of new lipid radicals, such as Malondialdehyde (MDA) and 4-hydroxynonenal (HNE). These highly reactive chemicals, can bind

Chapter I

biomolecules involved in fundamental processes in the cells, leading to cell death. The final step is termination, either by antioxidants or another radical.

Some of these compounds give rise to a bad odour at very low threshold values and are responsible for the “off-flavour” notes of oxidatively deteriorated foods as occurs in butter, margarine, and salad/cooking oils [Lyras, L., 1997; Scott, G., 1997].

Lipid oxidation also causes quality deterioration of meat [Min, B., D.U. 2005], dairy products [Collomb, M. and Spahni, M., 1996], fruits and vegetable crops and seafood products (**Figure 8**) [Secci, G. and Parisi, G., 2016].



Fig. 8: Effects of lipid peroxidation on different food products. A) Rancid butter; B) rancid meat; C) rancid fruit and D) Rancid seafood.

Specifically, the oxidation of poly-unsaturated fatty acids (PUFA), results in significant generation of dietary advanced lipid oxidation end-products (ALEs), which are in part cytotoxic and genotoxic compounds. The gastrointestinal tract is constantly exposed to

oxidized food compounds, some of which are absorbed into the lymph or directly into the bloodstream after digestion. After ingestion of oxidized fats, animals and human have been shown to excrete in urine increase amounts of malondialdehyde but also lipophilic carbonyl compounds. Some of the dietary ALEs, that are absorbed from the gut to the circulatory system, could act as injurious chemicals that activate an inflammatory response, affecting also organs, such as liver, kidney, lung, and the gut itself. Therefore, the repeated consumption of oxidized fats in the diet poses a chronic threat to human health [Kanner, J., 2007].

Moreover, FRs formed during lipid peroxidation, such as peroxy radicals, could participate into protein oxidation processes, increasing the chain reactions (**Figure 8**) [Hellwig, M. *et al.*, 2014; Schaich, K., 2008; Nagy, P., 2009]. Compared to lipid peroxidation, intramolecular propagation reactions can occur in proteins owing to the many diverse functional groups in the side-chains of protein-bound amino acids. Indeed, during protein oxidation process, the microenvironment of a given residue may alter the redox potential, influencing the oxidation of other amino acids (**Figure 9**) [Davies, M. J., 2016; Robinson, S. *et al.*, 1998; Hawkins, C. L. and Davies, M. J., 2001].

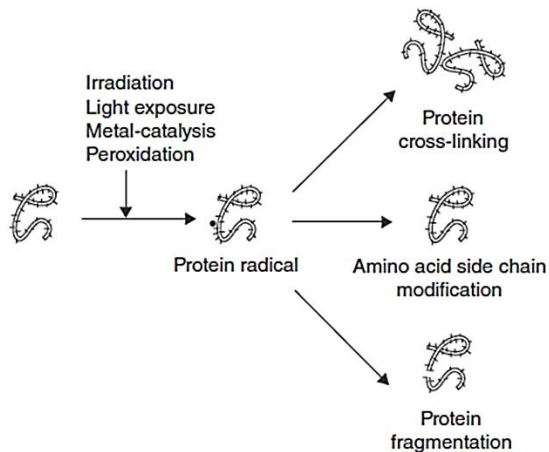


Fig. 9: Schematic representation of possible effects of protein oxidation.

The interaction of the aldehydic products of lipid oxidation with the amino groups in the side chains of proteins (such as lysine) can give rise to Schiff bases which emit fluorescence (**Figure 10**) [Kagan, V.E., 1988].

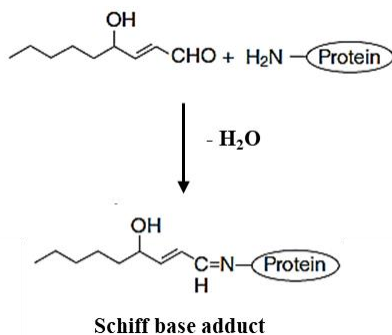


Fig. 10: Schiff base formation from proteins interaction with aldehydic products.

Chapter I

The accumulation of these intracellular auto fluorescent materials (called lipofuscin, ceroid or age pigment) has been characterized in different organs, mainly in striated muscles, either during the ageing process or associated with pathologies linked with oxidative processes [Grune, T. *et al.*, 2004, Seehafer, S.S and Pearce, D.A., 2006].

The formation of pigments whose fluorescence characteristics are similar to those of lipofuscins was observed also during refrigerated storage of bovine meat [Renerre, M. *et al.*, 1996].

The Schiff bases between protein and lipid oxidation products could be implicated in the changes of functional and biochemical properties of meats [Smith, D.M., 1987], leading to off-flavours and off-colours. Progressive conjugation or crosslinking of such molecules can cause protein denaturation, polymerization, aggregation, and insolubilization. Severe oxidation of proteins may cause changes in hydrophobicity, conformation, solubility and an altered susceptibility of protein substrates to proteolytic enzymes [49, 50] that could have negative effects on meat tenderness [Rowe, L. J. *et al.*, 2004] and may lead to loss of nutritional value of muscle food. Moreover, protein aggregation can also affect digestibility of meat proteins [Kamin-Belsky, N. *et al.*, 1996, Liu, G. and Xiong, Y.L., 2000]. In fact, several amino acids, following oxidation, pass the intestinal barrier and they can be mis-incorporate into proteins during biosynthesis [Estèvez, M. and Luna, C., 2017]. This has been regarded as a major cause for the low digestibility and hence, lesser nutritional value of oxidized proteins [Morzel, M. *et al.*, 2006].

Beyond to reactions between aldehydic products with protein, also oxidation *via* radical transfer between proteins is a form of reaction that has received some attention and can affect the food quality, even if the mechanism is rather poorly understood.

Hence, both protein oxidation and lipid peroxidation processes are involved in several disorders of human health and, for this reason, studies aimed at developing strategies to counteract the effects induced by oxidative stress phenomena are increasing [Morzel, M. *et al.*, 2006; Kanner, J., 2007].

1.3 Antioxidant defence systems

All aerobic organisms possess antioxidant defence systems responsible for the removal of reactive oxygen species (ROS) produced as a result of aerobic respiration. Removing them is essential to avoid adverse effects on biological macromolecules and thus on human health [Matés, J.M. and Sánchez-Jiménez, F., 1999]. Halliwell and Gutteridge define "antioxidant" as "any substance that, when present at low concentrations compared to that of an oxidizable substrate, significantly delays or inhibits oxidation of that substrate" (**Figure 11**) [Halliwell, B. and Gutteridge, J. M. C., 1989].

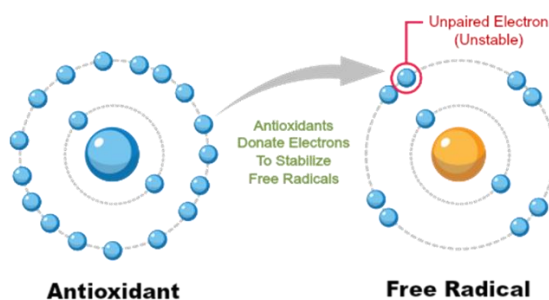


Fig. 11: How antioxidants reduce the free radicals

The protection against ROS production is certainly a first line of defence against their formation, i.e., prevention. In biology, there are numerous strategies designed to evade oxidative stress, ranging from the plankton that descends from the surface of the seawater to lower levels of solar irradiation, to the packaging of DNA in chromatin to shield the genetic material by providing alternate targets, etc [Sies, H., 1993].

However, these and other strategies are not completely preventative, because they operate by decreasing the yield of a given challenging agent with less than 100% efficiency.

In this regard, a wide array of non-enzymatic (**Figure 12**) and enzymatic (**Figure 13**) systems exist in cells and body fluids which work in concert to control the level of reactive species which otherwise might generate a cascade of products leading, in turn, to attacking oxidants [Matés, J.M. and Sánchez-Jiménez, F., 1999]. To the first class belong intercepting chain-breaking antioxidants, which are often phenolic compounds, such as (R, R, R)- α -Tocopherol [Burton, G. W. *et al.*, 1986]. These molecules transfer the radical

Chapter I

function away from further potential targets, stopping the radical chain reaction [Sies, H., 1993]. Another suitable ROS-scavenging system comprises carotenoids, that operate as efficient biological quenchers for singlet molecular oxygen [Foote, C. S. and Denny, R. W., 1968].

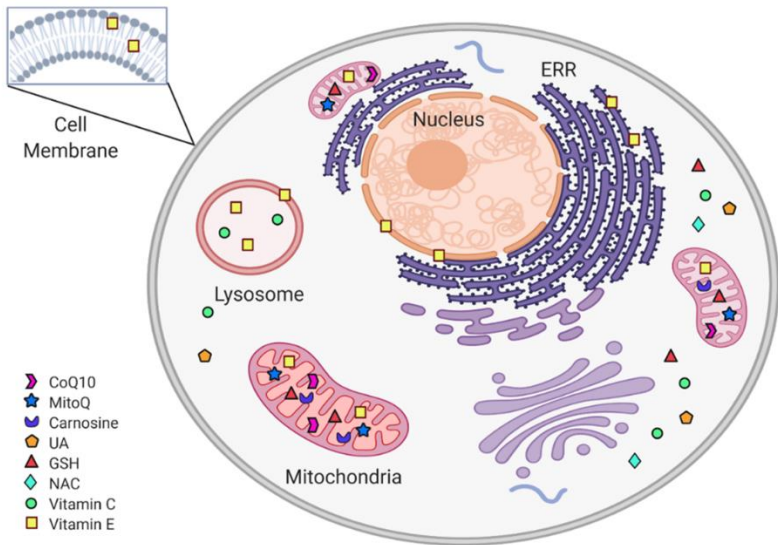


Fig. 12: Subcellular non-enzymatic antioxidants targets. Within the cell, non-enzymatic antioxidants are distributed according to their subcellular target. The mitochondria are protected from oxidative stress by CoQ10, MitoQ, carnosine, and Vit C. In the cytoplasm, the antioxidant system includes GSH, NAC, and UA. Vit E is found in cytoplasmic, ERR, and mitochondrial membranes, as well as in lysosomes. (Figure created in BioRender.com)

The second class is represented by antioxidant enzymes, including catalases (CATs), glutathione peroxidases (GPXs) and, principally, superoxide dismutases (SODs) which, cooperating in a chain

Chapter I

mechanism, destroy ROS. Specifically, these enzymes within cells remove superoxide and peroxides before they react with metal catalysts to form more reactive species.

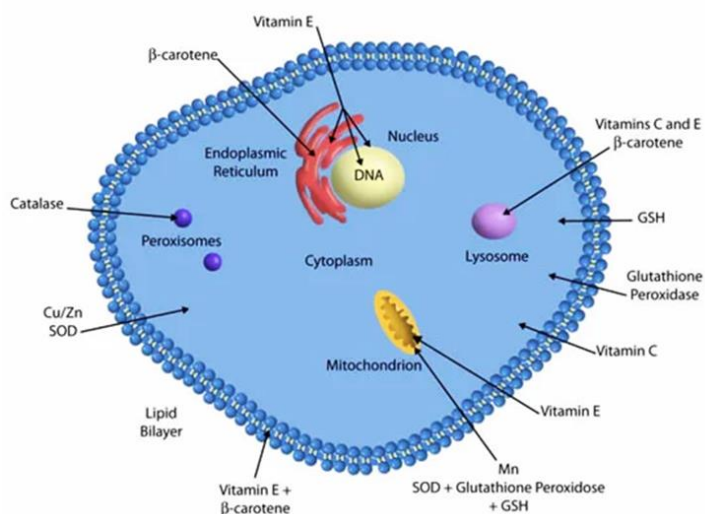


Fig. 13: Antioxidant enzyme systems. They catalyze reactions to neutralize free radicals and reactive oxygen species. These enzymes, including superoxide dismutase, glutathione peroxidase, glutathione reductase and catalases, metabolize oxidative toxic intermediates and represent the body's endogenous defence mechanisms to help protect against free radical-induced cell damage.

1.3.1. Superoxide dismutase enzymes

SODs (EC 1.15.1.1) are a group of metalloproteins, whose enzymatic activity was discovered by Irwin Fridovich and Joe McCord in 1968 [McCord, J.M. and Fridovich, I., 1969]. Specifically, SOD enzymes can destroy the highly reactive free radical superoxide, by converting

Chapter I

it to the less reactive peroxide H_2O_2 , which can in turn be transformed into H_2O and O_2 by the enzyme CAT (**Figure 14**).

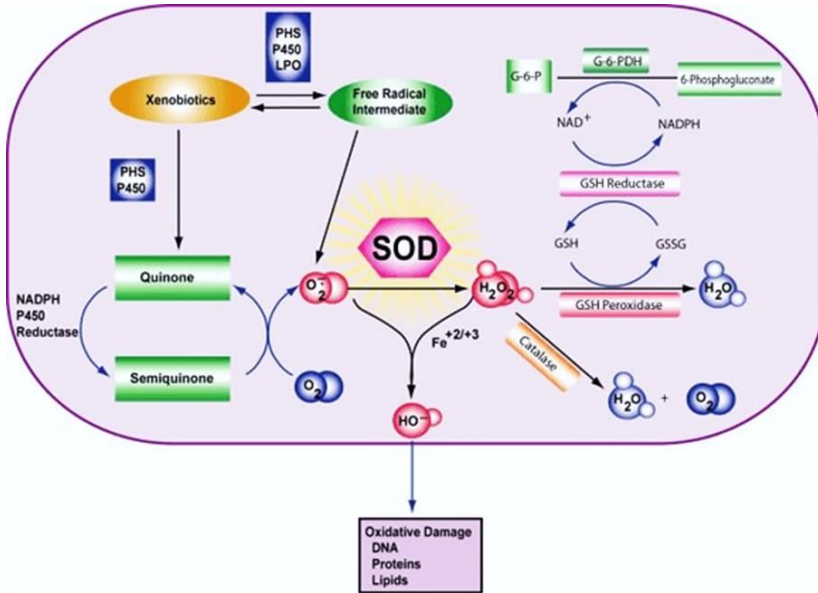
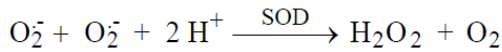


Fig. 14: Superoxide dismutase reaction

SODs are ubiquitous enzymes and they are classified in four classes, according to the type of metal ion associated to the catalytic site: Fe-SOD (found in prokaryotes and in some plant chloroplasts), Mn-SOD (in prokaryotes and in mitochondria), Cu/Zn-SOD (in all eukaryotes, including animals and plants) and Ni-SOD (found primarily in prokaryotes) (**Figure 15**) [Whittaker, M. and Whittaker, J. W., 1998].

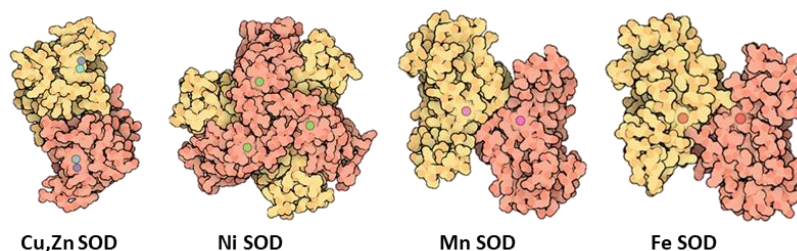


Fig. 15: Classes of Superoxide dismutase enzyme

Fe-SODs and Mn-SODs are highly homologous in sequence and three-dimensional structure, with identical metal chelating residues at the active site, while the other SODs are structurally unrelated [Majima, H., 1998].

Thanks to their versatile properties, these enzymes have been proposed for a wide range of industrial applications, but most of them belong to mesophilic organisms, thus they are characterized by low stability, and easily lose their antioxidant capacity when exposed to more extreme conditions [Padmapriya, V. and Anand, N., 2010]. For this reason, like most enzymes, their use is limited in food sector as many do not resist the industrial conditions and they require specific ranges of chemico-physical conditions to work properly and effectively. In this context, extremophile microorganisms, living in extreme habitats and conditions, can represent an interesting source of stable, highly active, and resistant SOD enzymes, able to work in harsh conditions such as high and low temperatures or pHs, elevated UV doses, and high levels of salt [Liu, J. *et al.*, 2011; Pinmanee, P. *et al.*, 2022; Stetter, K.O. *et al.*, 1990; Gogliettino, M. *et al.*, 2014; Guleria, S. *et al.*, 2021; Palmieri, G. *et al.*, 2019]. Therefore, SODs deriving

Chapter I

from extremophiles could be suitable for use in industrial biotechnology applications

1.3.2. Extremophilic organisms

An extremophile is an organism highly adapted to survive in extreme habitats, in which the environmental conditions are considered hostile or even lethal for other terrestrial life-forms (**Figure 16**).

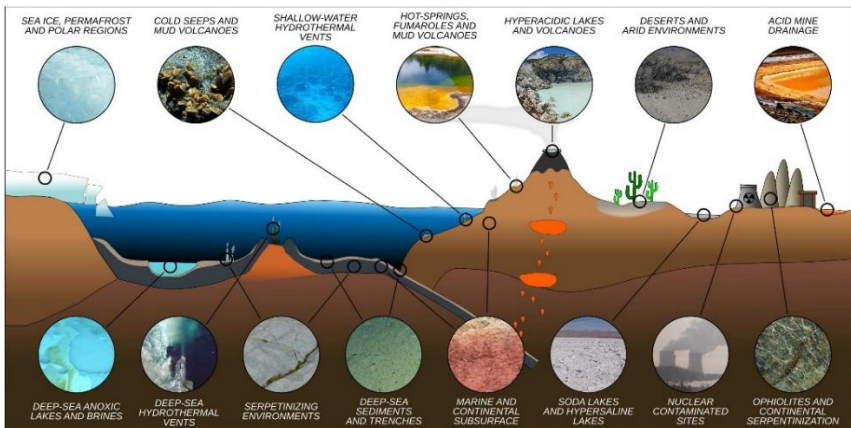


Fig. 16: Representative idealized cross section of Earth's crust showing the diversity of extreme environments and their approximate location. (Merino N. 2019)

Indeed, they grow and reproduce under high temperatures in hot springs or thermal vents, low temperatures in glaciers or the deep sea, acidic and basic pHs in industrial or mine wastewater effluents, high concentration of salts in salt lakes, and high levels of radiation and extreme desiccation in deserts among other physical or chemical

Chapter I

extreme conditions in various ecological niches. According to habitat, these organisms are classified as: thermophiles and hyperthermophiles (organisms growing at high or very high temperatures, respectively), psychrophiles (organisms that grow best at low temperatures), acidophiles and alkaliphiles (organisms optimally adapted to acidic or basic pH values, respectively), barophiles (organisms that grow best under pressure), and halophiles (organisms that require NaCl for growth) (**Figure 17**). Moreover, several organisms can be defined polyextremophiles, because they are able to live in habitats where various physicochemical parameters reach extreme values.



Fig. 17: A schematic diagram of extremophilic microorganisms which grow in reported extreme conditions.

Moreover, extremophiles can be divided into two wide categories: extremophilic organisms which require one or more extreme conditions in order to grow, and extremotolerant organisms which can tolerate extreme values of one or more physicochemical parameters though growing optimally at “normal” conditions. Extremophiles include members of all three domains of life, i.e., *Bacteria*, *Archaea*, and *Eukarya*. Specifically, *Archaea* represents the main group to

thrive in extreme environments and they are generally quite skilled in adapting to different extreme conditions, holding frequently extremophily records. Some archaea are among the most hyperthermophilic, acidophilic, alkaliphilic, and halophilic microorganisms known. In order to survive in hostile conditions, these organisms have established a diversity of molecular strategies which are of great interest from the biotechnological point of view, making them useful alternatives to labile mesophilic counterparts. Specifically, biocatalysts isolated by these organisms, termed extremozymes, remain catalytically active under extremes of temperature, salinity, pH, and solvent conditions, posing new opportunities for biocatalysis and biotransformations, as well as for the development of new line of research, through their application [Babu, P. *et al.*, 2015; Coker, J. A., 2016; Durvasula, R. and Rao, D. V. S., 2018; Rampelotto PH., 2013].

1.3.2.1. *Archaea*

Archaea is a domain constitute of single-celled organisms lacking nuclei and, therefore, are prokaryotes. Firstly, *Archaea* were classified as bacteria, with term “*Archaeobacteria*”, but it has fallen out of use [Pace, NR., 2006]. Then, they were classified separately from bacteria in 1977 by Carl Woese and George E. Fox, based on their ribosomal RNA (rRNA) genes [Woese, CR. and Fox, GE., 1977]. Archaeal cells have unique properties separating them from the other two domains, *Bacteria* and *Eukaryota*. According to

Chapter I

Woese, *Bacteria*, *Archaea*, and *Eukaryotes* represent separate lines of descent that diverged early on from an ancestral colony of organisms. Probably, this separation occurred before the evolution of cells, when the lack of a typical cell membrane allowed unrestricted lateral gene transfer, and the common ancestors of the three domains arose by fixation of specific subsets of genes (**Figure 18**) [Woese, C., 1998; Kandler, OT., 1998].

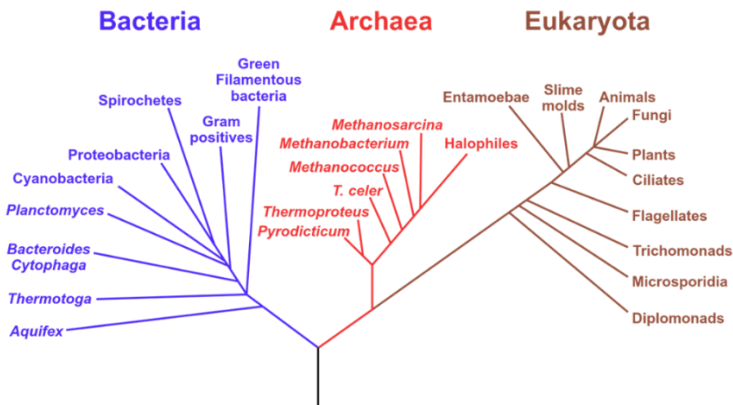


Fig. 18: A phylogenetic tree of living things, based on RNA data and proposed by Carl Woese, showing the separation of bacteria, archaea, and eukaryotes. By This vector version: Eric Gaba (Sting – fr: Sting) – NASA Astrobiology Institute, found in an article, Public Domain.

Even if Archaea are morphologically like Bacteria, the term prokaryote may suggest a false similarity between them. In fact, Archaea possess genes and several metabolic pathways that are more closely related to those of Eukaryotes, specifically for the enzymes involved in transcription and translation [Woese, CR., 1994].

Chapter I

The biochemistry and some of the structural features of Archaea are unique. They use different energy sources than eukaryotes, varying from organic compounds such as sugars, to ammonia, metal ions or even hydrogen gas [Valentine, DL., 2007]. Moreover, membranes are built with L-glycerol ether/ isoprenoid chains instead of D-glycerol fatty acid esters and cell walls lack peptidoglycan [Nkamga, VD. *et al.*, 2017] (**Table 2**).

Table 2: Comparison of structural and metabolic features in bacteria, eukaryotes, and Archaea. (Youssouf S. *et al.*, 2019).

Features	Bacteria	Eukaryote	Archaea
DNA separated from the cytoplasm by a membrane	No (except in Planctomycetes)	Yes (nuclear membrane)	No
Presence of intracellular organelles	No	Yes (mitochondria, chloroplasts)	Yes
Presence of a wall around the cells	Yes (with few exceptions), composed of peptidoglycans containing muramic acid	In some eukaryotes (plants, fungi, etc.), but never contains muramic acid	Yes (with a few exceptions), the composition varies according to the groups, but there is never muramic acid
Types of lipids present in the cytoplasmic membrane	Fatty acid chains linked to a glycerol-3-phosphate by ester bonds	Fatty acid chains linked to a glycerol-3-phosphate by ester bonds	Connected aliphatic chains connected to a glycerol-1-phosphate by ether bonds
Formation of gas vesicles	Yes	No	Yes
RNAi initiator of the translation	N-Formylmethionine	Methionine	Methionine
Polycistronic mRNAs	Yes	No	Yes
Maturation of mRNAs (de-stoning of introns, placement of a cap and a poly-A tail)	No	Yes	No
Ribosome type	70S	80S	70S
Reaction of elongation factor 2 with diphtheria toxin	No	Yes	Yes
Number of types of RNA polymerases	1	3	1
Type II promoters for RNA polymerase	Absent	Present	Present
Type of ATPase	A	B	B
Ability to produce methane	No	No	Yes, in some lineages
Ability to fix nitrogen	Yes	No	Yes
Photosynthesis based on chlorophyll	Yes	Yes	No
Ability to perform chemolithotrophy	Yes	No	Yes

Archaea exhibit higher morphological diversity compared to bacteria. Spherical, spiral, flat, square- or rod-shaped, and Gram-negative or Gram-positive Archaea live as isolated cells, aggregates,

Chapter I

or filaments and multiply by binary fusion, budding, or fragmentation [Krieg, N., 2005].

Archaea can be aerobic, optionally anaerobic, or strictly anaerobic and nutritionally extend from chemolithoautotrophic to organotrophic. Finally, some Archaea are mesophilic while others are able to thrive in hyperthermophilic environments [Garcia, JL. *et al.*, 2000]. In fact, they have been detected in different habitats spanning an array of sediments (salt and fresh water, hypersaline, marine, and geothermal marine sediments), together with hot springs, oil fields, rice paddies, anaerobic digesters, free unicellular eukaryota, and even in gastrointestinal tract of animals, such as rumen digesters [Liu, Y. and Whitman, WB., 2008; Balch, WE. *et al.*, 1979]. Furthermore, they are present within the human microbiome, specifically in the gut, to facilitate digestion, in the mouth, and on the skin [Chaban, B. *et al.*, 2006; Eckburg, PB. *et al.*, 2005; Samuel, BS. and Gordon, JL., 2006; Gophna, U. *et al.*, 2004]. Today, Archaea are a large and diverse group of organisms abundantly distributed throughout nature [Bang, C. and Schmitz, RA., 2015] and no clear examples of archaeal pathogens or parasites are known [Shiffman, ME. and Charalambous, BM., 2012; Moissl-Eichinger, C. *et al.*, 2018].

Their morphological, metabolic, and geographical diversity permits them to be used for biotechnological purposes. For instance, methanogens are involved in multiple ecological roles: carbon fixation, nitrogen cycling, organic compound turnover [DeLong, EF., 1998; Schiraldi, C. *et al.*, 2002] and in sewage treatment, being

part of the community of microorganisms that carry out anaerobic digestion and produce biogas [Norris, PR. *et al.*, 2020]. Additionally, methanogenic and acidophilic Archaea are used in mineral processing, showing display promise for the extraction of metals from ores, including gold, cobalt and copper [Breithaupt, H., 2001]. Nevertheless, the use of the organisms themselves in biotechnology is less developed compared to applications of estremozyms which are able to catalyse chemical reactions under harsh conditions, like those found in industrial processes, such as high temperatures and organic solvents [Egorova, K. and Antranikian, G., 2005; Synowiecki. J. *et al.*, 2006], allowing their use in environmentally friendly, efficient, and sustainable technologies.

1.3.2.1.1 *Aeropyrum pernix*

Aeropyrum pernix was the first strictly aerobic hyperthermophilic archaea to be discovered. It belongs to the phylum *Crenarchaeota* and it was originally isolated aerobically from heated marine sediments and venting water collected in 1996 from a solfataric vent at Kodakara-jima Island in Kyusyu, Japan. [Sako, Y., 1996]. The cells of *Aeropyrum pernix* are spherical in shape with $\sim 1 \mu\text{m}$ in diameter and are covered by an S-layer with hexagonal symmetry, consisting of proteins in a crystallized pattern which serves a way for cells to protect themselves (**Figure 19**).

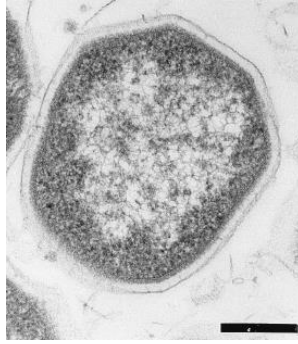


Fig. 19: Ultrathin section of *Aeropyrum pernix* K1. Bar, 0.2 μm .
(Sako Y. *et al.*,1996).

This organism grows between 70 and 100 °C (optimum 90-95 °C), at pH 5 to 9 (optimum, pH 7), and at 1.8 to 7.0 % salinity (optimum, 3.5 % salinity).

The ability to function in the extreme environment in which it thrives is given by the particularly thick cell membrane that acts as a protective barrier [Sako, Y., 1996].

An interesting feature of *Aeropyrum pernix* is that it does not require sulfur containing compounds for growth and so it does not generate any H_2S during growth. It is a heterotroph that uses aerobic degradation of complex proteinaceous substrates for energy and grow optimally at 95 °C. Transport systems, such as the dependent ATP-binding cassette (ABC) transporters, facilitate the uptake of essential nutrients to sustain growth [Palmieri, G., 2006].

Thanks to these characteristics, the halophilic-thermophilic enzymes of *Aeropyrum pernix* are employed in many biotechnological applications.

2 MATERIALS AND METHODS

2.1 Cloning of *Aeropyrum pernix* K1 Mn/Fe-SOD Coding DNA Sequences (CDS)

Genomic DNA from *Aeropyrum pernix* K1 (taxonomy ID: 272557) was isolated from frozen cells using the PureLink® Genomic DNA Mini Kit (Invitrogen/Thermo Fisher Scientific, Waltham, MA, USA). The CDS (coding DNA sequence) of the *sod* gene (locus SODF_AERPE), encoding the Mn/Fe-dependent SOD (UniProtKB accessions Q9Y8H8), was amplified by PCR. The amplification mix was as follows: 25 ng of genomic DNA as a template, 0.02 U/ μ L of Phusion Green HotStart II High-Fidelity DNA Polymerase (Thermo Fisher Scientific, USA), 0.5 μ M of each primer (**Table 3**), and 200 μ M of each dNTP. The PCR reaction was performed in a thermal cycler (Eppendorf srl, Milano, Italy) programmed as follows: denaturation at 98 °C for 30 s for one cycle, 30 cycles at 98 °C for 10 s, 58 °C for 30 s, and 72 °C for 45 s. A final extension cycle at 72 °C for 7 min concluded the reaction. The generated amplicons were confirmed by sequencing at Eurofins Genomics (Ebersberg, Germany). The 645 bp *sodAp* product was subcloned into the blunt end pSC-B-amp/kan vector using the StrataClone PCR Cloning Kit (Agilent Technologies, Santa Clara, CA, USA) and the final construct was verified by sequencing (**Figure 20**).

Table 3: Primer sequences used in this study

N.	Name	Sequence 5'-3'	Ta (°C)	Amplicon size
1	Sod _{Ap} for	ATGGTGAGCTTTAAGAGGTAC		
2	Sod _{Ap} rev	CTACTGGGGGAGCAGG		
			56	645 bp



Fig. 20: Coding DNA sequences (CDS) of SOD_{Ap} extremozyme inserted in the subcloning pSCB vector.

2.2 Cloning of SOD_{Ap} in Plant Expression Vectors

Sod coding sequence was cloned into pCK-EGFP vector [Reichel, C. *et al.* 1996] by replacing EGFP (enhanced green fluorescent protein) with the sod sequence. The construct was modified by the addition of four restriction sites (KpnI, SalI, SpeI, SmaI) at the 3' of the 35S terminator (terK3S). The Open Reading Frame (ORF) of sod_{Ap} was amplified by PCR from the pSCB-SOD_{Ap} cloning vector

Chapter I

using the primers SOD_{Ap}_NcoI_F and SOD_{Ap}_BX_R (**Table 4**) and the purified product was cloned into the NcoI-XbaI sites of pCK-EGFP.

Table 4: Primer sequences used in this study. Restriction sites are underlined.

N.	Name	Sequence 5'-3'	Ta (°C)	Amplicon size
1	EGFPseq-for	GAAGCGGATCACATGG		
2	35STer-KSSS-rev	<u>CCCGGGACTAGTGTGACCGGTACCTGTC</u> ACTGGATTTTGGTTTATAGG		
3	SOD _{Ap} -NcoI-for	GGGCC <u>ATGGT</u> GAGCTTTAAGAGGT		
4	SOD _{Ap} -BX-rev	CCCT <u>CTAGAGGATCC</u> CTACTGGGGGAGCAG		
			60	645 bp

The expression box of pCK vector included a tandem duplication of the 250 bp upstream sequences of the TATA elements of the CaMV 35S promoter which acted as a strong enhancer of protein expression. For in planta expression of sod_{Ap}, the binary plasmid pBI121 was modified by replacing the existing GUS expression cassette with those inserted in the previously described pCK-_{Ap}SODterK3S. The expression cassette for SOD_{Ap} under the control of the CaMV 35S promoter and terminator sequences (between HindIII and SmaI restriction sites) was briefly subcloned into pBI121 digested with HindIII and EcoRI (**Figure 21**). The accuracy of the subcloning procedures was controlled by nucleotide sequencing on the newly synthesized vectors.

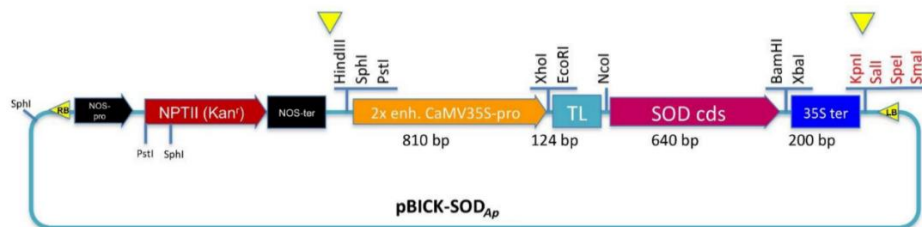


Fig. 21: Schematic representation of pBICK-SOD_{Ap}. The vector was assembled by introducing between the HindIII/EcoRI restriction sites of the original pBI121 binary vector the expression cassette from pCK expression vector encoding gene of interest (pCK-SOD_{Ap}terK3S described in Materials and Methods) under the control of double-enhancer 35S (2x) promoter and a transcription leader sequence (TL). Transcription stops thanks to the terminator of CaMV 35S. 2x enh. CaMV35S-pro: double-enhancer 35S (2x) promoter from Cauliflower mosaic virus 35S; 35Ster: Cauliflower mosaic virus 35S terminator; SOD_{Ap}: *Aeropyrum pernix* SuperOxide Dismutase; NPTII (kanr): neomycin phosphotransferase II gene for kanamycin resistance; NOS: nopaline synthase; RB: right border and LF: left border.

2.3 Genetic Transformation of Tomato Plants by *Agrobacterium Tumefaciens*

The sod_{Ap} gene, subcloned into the expression vector pBI121, was transferred to the plant cells via *Agrobacterium tumefaciens* transformation, according to the procedure reported as follows. One microgram of the plasmid (pBI121-SOD_{Ap}) was added to 0.1 mL of *Agrobacterium* cells (LBA4404). The cells were frozen in dry ice/ethanol for 5 min and then thawed at 37 °C for 10 min. Subsequently, 1 mL of YEP (Yeast Extract Peptone) medium was

Chapter I

added and the cells incubated for 3 h at 28 °C with gentle shaking. After incubation, the cells were spread on YEP agar medium with kanamycin (50 mg L⁻¹). *Agrobacterium* colonies, grown for 48 h, were verified by PCR using primers designed for the detection of *sod_{Ap}* gene on the binary vector. A small portion of the growing colony was picked up with a sterilized toothpick and suspended in the reaction mixture, containing the following constituents: 0.25 µl Wonder Taq, (Euroclone, Milan, Italy), 4 µl of Wonder Taq reaction buffer (5x), containing 5 mM dNTPs and 15 mM MgCl₂, 0.4 µM forward primers (5'-CTTGAGCCCCATATCGACGC-3') and 0.4 µM reverse primers (5'-CAGAAGGCGGCGAGGTAGTC-3'). The mixture was filled with sterilized water up to 20 µl and the reaction was performed as follows: initial denaturation (95 °C, 5 min), 35 cycles of denaturation (95 °C, 1 min), annealing (53 °C, 30 s) and extension (72 °C, 30 s), and additional extension (72 °C, 10 min). The amplification products were electrophoretically analysed on a 1.5% agarose gel, stained with 0.5 µg/mL ethidium bromide, and displayed with the Geliance 200 Imaging system (Perkin Elmer, MA, USA). The primers used to amplify the *sod_{Ap}* are reported in **Table 5**.

Table 5: Primer sequences used in this study to amplify the SOD_{Ap}

N.	Name	Sequence 5'-3'	Ta (°C)	Amplicon size
1	SOD _{Ap} for	CTTTAAGAGGTACGAGCTCC		
2	SOD _{Ap} rev	GTGCTCCCACACGTCAATAAC		
			53	498 bp

Chapter I

Solanum lycopersicum seeds (cv MicroTom) were surface-sterilised by immersion into 70% ethanol for 1 min and in a 2% (v/v) solution of sodium hypochlorite for 15 min, then rinsed four times in sterile distilled water. Afterwards, they were placed on 25 mL of half-strength MS (Murashige and Skoog) medium (pH 5.7), containing 15 g L^{-1} sucrose and 7 g L^{-1} agar, and they were incubated for 7–10 days at $27 \text{ }^{\circ}\text{C}$ for germination. Cotyledon pieces ($\sim 0.25 \text{ cm}^2$) were cut from tomato seedlings and soaked for 15 min with *Agrobacterium* cells ($\text{OD}_{600\text{nm}} = 0.5$) in the co-cultivation medium consisting of MS containing 30 g L^{-1} sucrose, 1 mM MES, 0.75 mg L^{-1} trans-zeatin, 1.0 mg L^{-1} IAA, and $200 \text{ }\mu\text{M}$ acetosyringone, pH 5.7, and incubated at $27 \text{ }^{\circ}\text{C}$ in the dark. After 2 days, the cotyledon pieces were transferred to the stem cell induction medium according to DSMZ recipe (DSMZ, Braunschweig, Germany) with some modifications: Gamborg B5 medium was supplemented with myo-inositol 100 mg L^{-1} , sucrose 40 g L^{-1} , nicotinic acid 1 mg L^{-1} , thiamine hydrochloride 10 mg L^{-1} , pyridoxal hydrochloride 1 mg L^{-1} , 2,4-Dichlorophenoxyacetic acid 1 mg L^{-1} , kinetin 0.45 mg L^{-1} , NAA 0.01 mg L^{-1} and phytoagar 8 g L^{-1} , in the presence of cefotaxime 250 mg L^{-1} and kanamycin sulfate 50 mg L^{-1} . After 4 weeks at $25 \text{ }^{\circ}\text{C}$, under a 16 h light photoperiod, the calli were separated from the plant tissue and placed onto fresh medium for further growth.

2.4 Molecular Analysis of the Tomato Transformed Lines

To verify the presence of the transgene in the transformed lines, total RNA was extracted from 50 mg of calli using DNeasy Plant Mini Kit (Qiagen, Hilden, Germany). To avoid the presence of any residual DNA, the RNA sample was treated with 5 U of Ambion™ RNase I (Thermo Fisher Scientific, MA, USA) for 30 min at 37 °C. The cDNA was synthesized using 1 µg of total RNA with RevertAid Reverse Transcriptase (Thermo Fisher Scientific, MA, USA) and all PCR reactions were carried out using the QuantumRNA™ Universal 18S Internal Standard as internal control for sample normalization. The primers and the conditions used for the RT-PCR reactions were identical to those described for the analysis of colony-PCR in *Agrobacterium*.

For Western Blot (WB) analysis, the total proteins were extracted from 100 mg of tomato calli ground in the extraction buffer consisting in 150 mM Tris-HCl, pH 7.4, 150 mM NaCl, 1.5 mM EDTA, 1.5% Triton X-100, and a mixture of protease inhibitors with a broad specificity for the inhibition of serine, cysteine, aspartic proteases, metalloproteases, and aminopeptidase (MERCK, Darmstadt, Germany). Hence, the homogenates were centrifugated at 15,000× g for 15 min at 4 °C to remove cellular debris, and the supernatants were used as crude cell extracts. The total protein content was determined by using the Bio-Rad protein assay kit (Bio-Rad, Hercules, CA, USA). The immuno-blot was performed as described below.

2.5 Production of Tomato Cell Extracts

Plant cell cultures were initiated suspending 50 mg of 30–35-day-old callus in 50 mL of tomato stem-cell induction medium (previously described) in absence of agar and the cultures were incubated at 25 °C with a photoperiod of 16 h light and 8 h dark, under constant orbital stirring (110 rpm). The calli gradually disintegrated and formed dense liquid cultures after 10 days. The suspensions were then transferred into larger volumes, in particular 50 mL of culture was used as starting material to inoculate 1 L of culture medium. After seven days, the cells were collected and filtered through a layer of Miracloth fabric (MERCK, Germany). The drained cells were then resuspended in 100 mL of PBS (136 mM NaCl, 2.7 mM KCl, 12 mM NaH₂PO₄ and 1.76 mM KH₂PO₄, pH 7.4) and homogenized in a mechanical grinder. The resulting lysate was centrifuged at 10,000 × g to precipitate the particulate fraction and isolate the soluble components. The supernatant was collected and lyophilized. The lyophilised powder was dissolved in water at a concentration of 10% w/v, and the protein concentration was measured by the Bradford assay [Bradford, M.M., 1976], using bovine serum albumin (BSA) as standard.

2.6 SOD and NBT Assays

SOD activity was measured spectrophotometrically based on the inhibition of the Nitro Blue Tetrazolium (NBT) reduction [3]. Briefly, the reaction mixture (1 mL), containing 2 μ g of the enzyme extracts obtained from non-transformed (WT, wild-type) or sod-transformed tomato cells, Tris-HCl 50 mM, pH 8.0, 0.1 M EDTA and 1.5 mM NBT was exposed to a light source for 8 min. Following the exposition, 0.12 mM riboflavin was added, and the solution was exposed to the light for an additional 12 min to initiate the photochemical reaction. The reaction was stopped by switching off the light source, and absorbance was measured at 560 nm using a Jasco 640-V spectrophotometer equipped with a temperature control unit. One unit of SOD activity was defined as the amount of enzyme required to produce a 50% inhibition of NBT reduction under assay conditions. Protein concentration was estimated by the Bradford method [Bradford, M.M., 1976], using BSA as the standard. The effect of ionic strength on the SOD_{Ap} activity was evaluated by incubating protein samples in 50 mM Tris-HCl, pH 8.0 for 15 min at 37 °C at different NaCl concentrations (0.5–1.5 M). The effect of temperature was measured by performing the SOD activity assay after incubation for 15 min at temperatures ranging from 60 to 90 °C. The SOD activity in all the experimental conditions was assayed as described above. Fold increase was calculated as a ratio between SOD activity in crude protein extracts of wild-type plants and SOD activity in crude protein extracts of transgenic plants, using the NBT

assay. The relative activity was expressed as a percentage of the corresponding maximal activities under the standard assay conditions. All experiments were performed in triplicate on three different protein preparations.

An in-gel SOD assay was performed as described in Beauchamp and Fridovich [Beauchamp, C. and Fridovich, I., 1971], with slight modifications. Specifically, an equal amount of each sample was separated by electrophoresis on 10% non-denaturing polyacrylamide gel (Native-PAGE). Then the gel was soaked in a 50 mM Tris-HCl buffer (pH 8.0) containing 0.305 mM of NBT and 0.275 mM of riboflavin for 15 min in the dark at room temperature, followed by incubation in 50 mM Tris-HCl buffer, pH 8.0, and 0.1% TEMED for an additional 15 min under the same conditions. The SOD bands were visualized as a clear white region in the purple formazan background after illumination with a fluorescent lamp.

2.7 Molecular Mass Determination

The SOD_{Ap} protein was partially purified from the transformed tomato cell extracts by two subsequent steps of ultrafiltration using molecular weight cut-off (MWCO) spin filters of 100-kDa and 30-kDa (Millipore, Burlington, MA, USA). The retentates were analyzed through the size exclusion chromatography, performed on a Superdex 200 column (Pharmacia Biotech, Milan, Italy) to estimate the native molecular mass of the partially purified SOD_{Ap}. The column was pre-equilibrated with 50 mM Tris-HCl buffer (pH

7.5) containing 50 mM NaCl. Standard protein markers (BioRad code 151–1901) were used to calibrate the gel filtration column.

2.8 SDS-PAGE and Western Blot Analyses

Thirty micrograms of the total proteins were loaded into 12% SDS-PAGE gel, and the immunoblotting was performed on polyvinylidene fluoride (PVDF) membrane (Millipore) by using the specific anti-SOD antibody, diluted 1:10,000 in TTBS buffer (Tris-buffered saline and 0.05% tween 20) containing 5% Blotting-Grade Blocker (BioRad, *Hercules, CA, USA*). A goat anti-rabbit antibody conjugated to *horseradish peroxidase* (HRP) was used as a secondary antibody (dilution 1:5000), and the membrane was developed by a Pierce TM 1-Step Ultra TMB blotting solution (Thermo-fisher, *Waltham, MA, USA*). The commercially available MnSOD_{Ec} from *E. coli* (SRP6107 MERCK, KGaA, Germany) was used as a control.

2.9 ORAC Assay

The spectrophotometric quantification of the inhibition of myoglobin (Mb) peroxidation was used to assess the antioxidant capacity of the tomato extract enriched in SOD_{Ap} by a high-throughput 96-well microplate assay. Specifically, the chemical damage to Mb by peroxy radicals generated by the thermal decomposition at 37 °C and pH 7.4 of the azo initiator AAPH was measured as a decrease in its intrinsic absorption at 409 nm. The

method was conducted in 50 mM phosphate buffer (pH 7.4) at 37 °C, where 100 µL of Trolox standard solutions (5-100 mM) or plant cell extracts (WT and SOD_{Ap}) and 100 µL of myoglobin (75 mg/mL) were mixed in each well. Then, the microplate was pre-incubated at 37 °C for 30 min. 100 µL of freshly prepared AAPH solution (180 mM) was added, and the absorbance at 409 nm was recorded every minute for 40 min. The antioxidant activity of the extracts was determined according to the method already described by Huang, D. *et al.* [2002]. Briefly, the net area under the curve (AUC) of the samples and standards, represented by different dilutions of Trolox, was calculated. The standard curve was obtained by plotting Trolox concentrations against the average net AUC of the two measurements for each concentration. Net AUC was obtained by subtracting the AUC of the blank from that of the sample or the standard. ORAC values of the samples were expressed as micromoles of Trolox equivalents per gram.

2.10 Sampling Preparation

Chilled yellowfin tuna (*Thunnus albacares*) and fresh bluefin tuna (*Thunnus thynnus*) fillets were purchased at local markets in Southern Italy. Bluefin tuna was filleted in the laboratory and each fillet was cut into portions of the equal size and weight (4516 ± 10.5 g). Experimental brines were inoculated by using a multi-needle industrial brine injector (Metalbud Nowicki MHM-39/156) (**Figure 22**) and manually adjusted as follows: brine pressure needle at 1.3

Chapter I

atm, the head speed at 30 cycles/minute, and conveyor belt speed at 75 mm/cycle.

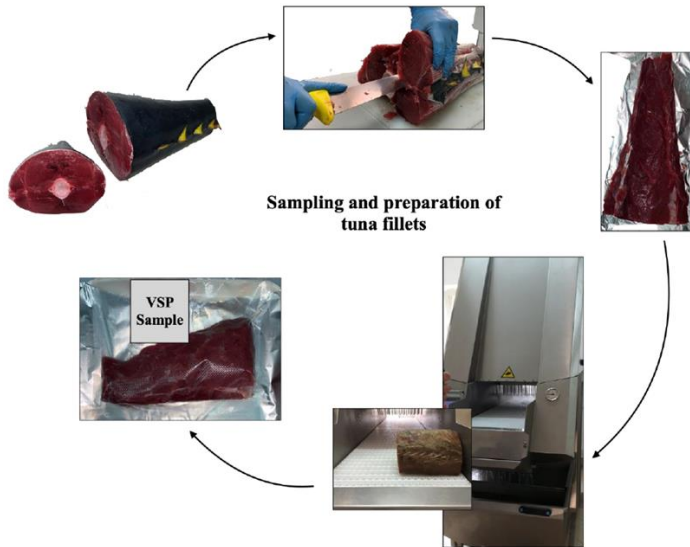


Fig. 22: Scheme of the experimental procedure for the sampling and preparation of tuna fillets (filleting, brine injection, and vacuum skin packaging-VSP)

The fillets, placed on a conveyor belt, were injected with different brines, while control samples (CTR) were injected with an aqueous solution. Once the weight was stable, each sample was packed under a vacuum and stored at refrigeration temperature (2 ± 1 °C) for 10 days. Several samples were created: yellowfin tuna fillets treated with the commercial brine solution (CM), a vegetable extract prepared by dissolving 7.5 g in 1 L of water, as recommended by the

manufacturer; yellowfin and bluefin tuna fillets treated with SOD_{Ap} and WT solutions. All analyses were performed on days 0, 6 and 10.

2.11 Colour Measurements

The changes in the colour of tuna fillets over time were followed by using the Konica Minolta CM-2500d colourimeter (Minolta Co., Ltd., Osaka, Japan) with observer 10° (CIE64) and illuminant D65 as the main measuring conditions set. The colour measurements were conducted, including a specular component (sci mode) and adopting the CIELAB colour space: lightness (L*), redness (a*), and yellowness (b*). Total colour difference (ΔE) and variation in a* (Δa^*) were calculated to better describe the colour changes that occur during the storage period as follows:

$$\Delta E = \sqrt{(L^*_1 - L^*_2)^2 + (a^*_1 - a^*_2)^2 + (b^*_1 - b^*_2)^2}$$

$$\Delta a^* = a^*_2 - a^*_1$$

where L*₂, a*₂, and b*₂ were the values recorded on a specific day during the storage; instead, L*₁, a*₁, and b*₁ were the values collected at day 0. For the colorimetric analysis of the fresh bluefin and thawed yellowfin tuna over the storage time, the evaluation of the inner surface was performed after 10 min of its exposure to air. To obtain representative results, four superficial measurements were carried out on the surface of tuna slices because the colour might not

be homogeneous over the entire surface. Specifically, imagining the major surface of a tuna slice as a triangular figure, the colour measurements were performed on areas corresponding to the three angles and the centre.

2.12 Histamine and Nitrate Determination in Tuna Fillets

The histamine content was measured using a commercial enzyme immunoassay test kit (RIDASCREEN[®] Histamine enzymatic, R-Biopharm, Darmstadt, Germany) following the manufacturer's instructions. The histamine concentration ($\mu\text{g}/\text{kg}$) was calculated with the RIDASOFT[®] Win.NET software.

The measurement of the nitrate levels in yellowfin tuna fillets was conducted according to Cortesi, ML. *et al.* [2015]. Briefly, 137.1 mg of pre-dried primary standard sodium nitrate (at 105 °C for 24 h) or 150.0 mg of primary standard sodium nitrite (at 110 °C for 1 h), were dissolved in distilled water and then diluted to 100 mL. Work solutions were prepared by diluting the nitrate or nitrite stocks (1 g L^{-1}) with distilled water. On each sample, the analyses were performed in triplicate the day after the injection of brines.

2.12.1 Color reagent

Color reagent was prepared according to the official method of AOAC International (993.03). 600 mg of sulfanilic acid ($\text{C}_6\text{H}_7\text{NO}_3\text{S}$) were dissolved in 50 mL hot water. After cool, add 20 mL glacial acetic acid and dilute to 100 mL with water.

20 mg of N-(1-naphthyl)-ethylenediamine dichloride ($C_{12}H_{16}Cl_2N_2 \cdot CH_3OH$) were dissolved in 20 mL glacial acetic acid and dilute to 100 mL with water. Mix equal volumes of sulfalinic acid solution and N-(1-naphthyl)-ethylenediamine dichloride reagent immediately before use. Discard any unused color reagent.

2.12.2 Reduction of nitrate to nitrite

For each sample, ca 600 mg Zn powder into separate 50 mL volumetric flasks were weighed and powder over bottom of flask was spreaded. Additional flask for standards were prepared. Carefully 4 mL of 10% (w/v) cadmium sulfate $3CdSO_4 \cdot (H_2O)$ solution was added to zinc powder in flask to obtain homogeneous mixture. The newly formed spongy metallic cadmium was let stand for 10 min without moving. 2 mL 25% NH_4OH and 10 mL sample solution were added to 1 flask. Standard nitrate concentrations (containing 0, 50, 100, 150 and 200 $\mu g NaNO_3$) were prepared adding 10 mL of each standard solution to separate volumetric flasks prepared with spongy cadmium. Flasks were shaken for exactly 1 min to loosen spongy cadmium and, after 10 min of stand, the solutions were diluted to volume with H_2O and filtered. After use, contents of volumetric flasks were poured into waste bottle. The possible residues in volumetric flasks were dissolved with concentrated HCl to another waste bottle. The waste from color reaction were

collected in another bottle, to arrange for proper disposal of waste bottles.

2.12.3 Nitrite determination

10 mL clear filtrates of samples and standard solutions (equivalent to 0, 10, 20, 30 and 40 $\mu\text{g NaNO}_2$) were pipetted to separate glass stoppered mixing cylinders. Then, 10 mL color reagent were added to each and mixed for 1 min by hand. Therefore, the absorbance at 530 nm and water blanks were recorded using a Spectrophotometer UV/VIS V-530 Jasco (Japan). Nitrate concentration was calculated using nitrate calibration curve.

2.13 Statistical Analysis

Experiments were performed in triplicate, and results were expressed as means \pm standard error. Data were statistically analysed with a generalised linear mixed model (GLMM) through SPSS version 27 (IBM Analytics, Armonk, NY, USA) with brine type and storage times as a fixed effect. Tukey's HSD post-hoc test was used to calculate the significant differences between means at a significance level of $p < 0.05$.

On each sample, the analyses were performed in triplicate the day after the injection of brines.

3. RESULTS AND DISCUSSION

3.1 Expression of SOD_{Ap} in Tomato Cell Cultures

Firstly, the gene coding SOD_{Ap} was cloned following the methods described in the Materials and Methods section (*paragraph 2.1*) and sequenced to confirm its identity. Therefore, to boost the gene expression of the extremozyme in the plant cells, the coding sequence was expressed under the control of a variant of the 35S promoter, which includes a TEV leader (TL) sequence and a duplication of 250 base pairs upstream the 35S TATA element [Reichel, C. *et al.*, 1996], to induce a ten-fold increase of the transcriptional activity and an enhancement of the translation efficiency [Restrepo, M.A. *et al.*, 1990].

Moreover, the sub-cloning of the full expression cassettes into the binary expression vector pBI121 was facilitated by the incorporation of additional unique sites at the end of the terminator. Cotyledonary leaves of tomato cv MicroTom were co-cultivated with *Agrobacterium tumefaciens* cultures carrying the binary vector pBICK-SOD_{Ap} for plant transformation (**Figure 21**).

After approximately four weeks, calli, originating on selective media from the explants, were transferred to specific media to allow their growth and to maintain the callus state (**Figure 23 A-D**).

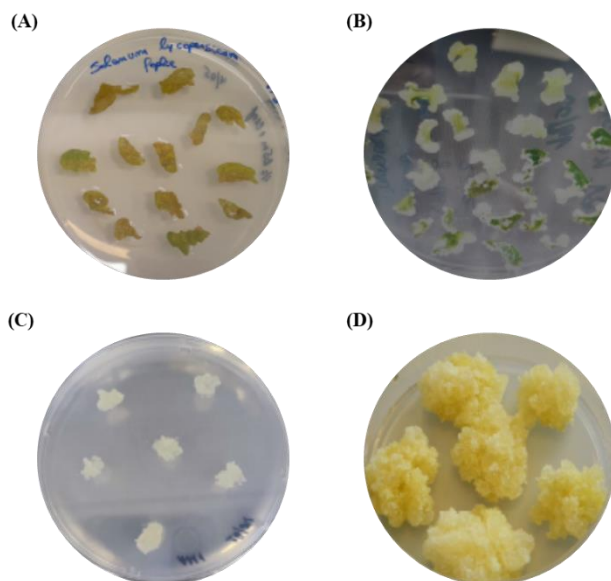


Fig. 23: Transgenic calli production from tomato cotyledones (cv *MicroTom*). (A) callus induction in leaf pieces; (B) callus formation from hypocotyls on MS medium containing NAA and kinetin; (C) callus lines regenerated; (D) transgenic clones characterized for the presence and the expression of etherologous SOD.

Hence, semi-quantitative RT-PCR was performed to detect the expression of the *sod* gene in the different transgenic lines. The presence of an amplification band corresponding to transgenic *sod_{Ap}* (**Figure 24**) gene was evidenced in all the analysed cell lines, differently from the untransformed tomato cells (WT).

Therefore, the transformed callus lines were sub-cultured and the total proteins were extracted.

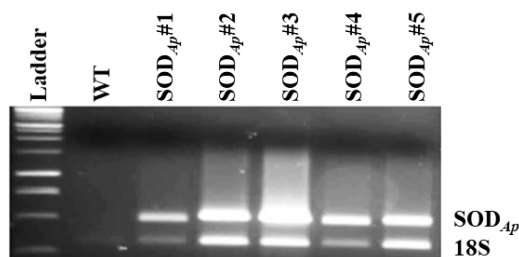


Fig. 24: Semi quantitative RT-PCR analysis of transgenic SOD_{Ap} gene. Ladder: 1 Kb DNA ladder (Promega); WT: untransformed tomato calluses; 18S: amplification product of 18S gene (internal standard).

Then, the crude extracts were analysed by SDS-PAGE, NBT-PAGE and western blotting, to confirm the presence of the expressed protein (**Figure 25**). As shown in **Figure 25 A**, the SDS-PAGE analysis revealed the presence of an extra protein band with the expected molecular mass of 24.5 kDa in all the analysed SOD_{Ap} transgenic samples, compared to the protein profile of the wild-type. This band was also positive for Native-PAGE followed by in-gel SOD activity (**Figure 25 B**) and Western Blot analysis by using the specific anti-SOD antibody (**Figure 25 C**), thus confirming the presence and the nature of the recombinant protein in the plant transgenic extracts.

In order to estimate the percentage of transgenic SOD_{Ap} in the total soluble proteins (TSP) of tomato cells, the iBriqTM software was

Chapter I

used for the densitometric analysis and SOD_{Ap} was quantified by using the commercially available SOD from *Escherichia coli* at known concentrations as reference (**Figure 25 A, C**). It should be noted that it was not possible to perform the same analysis by Western blot as exogenous and endogenous SOD isoforms were undistinguishable with the anti-SOD Ab.

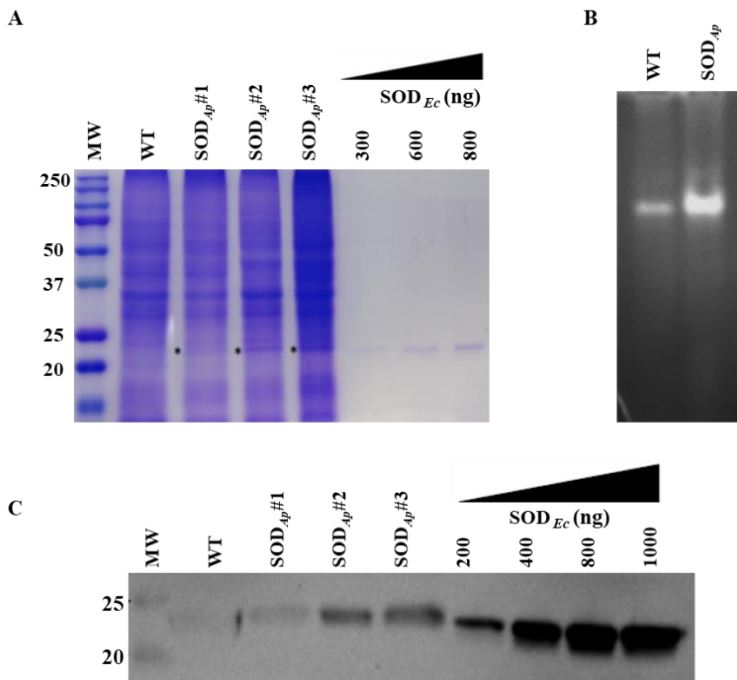


Fig. 25: SDS-PAGE, NBT-PAGE and western blot analyses of total protein extracts from transgenic tomato cell lines. (A) Total protein extracts (30 μ g) were electrophoresed on 12% SDS-polyacrylamide gel and detected with Coomassie blue staining. **(B)** Total protein extracts (15 μ g) obtained from tomato cell lines untransformed (WT) or transformed with SOD_{Ap} gene, were electrophoresed on Native-PAGE (10%). Following Native-PAGE,

Chapter I

protein bands were detected by in-gel SOD activity staining using the Riboflavin-NBT assay. The results are representative of three independent experiments on three different proteins.

(C) Total proteins were extracted from the tomato cell lines, separated by SDS-PAGE and transferred to PVDF membrane. WT: untransformed tomato cells; SOD_{Ap}#1, SOD_{Ap}#2 and SOD_{Ap}#3: callus lines transformed with SOD_{Ap} gene. SOD_{EC}: purified SOD used for comparative quantification of the relative intensity of band of interest (indicated with *).

Following this analysis, the percentage of SOD_{Ap} accumulated in transgenic tomato cells was estimated to be around 1.2-1.5% (w/w). Finally, the molecular mass of partially purified SOD_{Ap} was also determined under native conditions by gel-filtration chromatography, using a Superdex 200 column calibrated with proteins of known molecular size. As shown in **Figure 26**, SOD_{Ap} eluted as single symmetric peak with an apparent Mr of ~52 kDa, according to the calibration curve and to the electrophoretic analyses followed by enzyme activity staining (**Figure 27**).

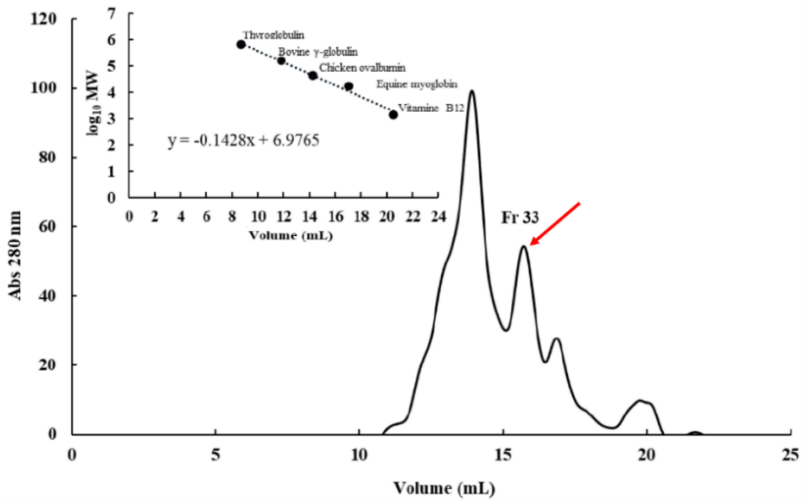


Fig. 26: Gel filtration chromatography of partially purified SOD_{Ap}. Size-exclusion chromatogram of partially purified SOD_{Ap} on Superdex 200 column in 50 mM Tris-HCl buffer pH 7.5 containing 50 mM NaCl. The absorbance was measured at 280 nm. Insert: calibration curve of Superdex 200 column using protein standards of known molecular masses: Thyroglobulin (670 kDa), Bovine γ -globulin (158 kDa), Chicken ovalbumin (44 kDa), Equine myoglobin (17 kDa), Vitamine B12 (1.35 kDa).

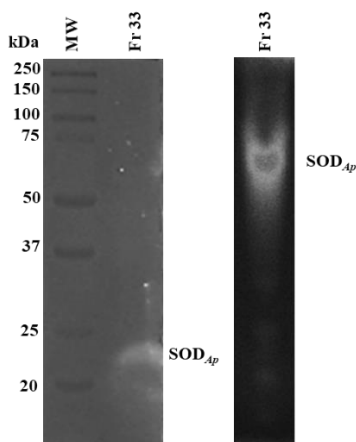


Fig. 27: Electrophoretic analyses followed by enzyme activity staining. SDS-PAGE (10%) (left) and Native-PAGE (10%) (right) analyses of SOD_{Ap} fraction obtained after gel filtration chromatography. MW: molecular markers. Following electrophoretic analyses, protein bands were detected by in-gel SOD activity staining using the Riboflavin-NBT method. The results are representative of three independent experiments on three different protein preparations.

This value approached the theoretical mass of a homodimer, thus confirming that the extremophilic enzyme had a structural organization consisting of two identical subunits of approximately 24 kDa when expressed in tomato cells.

3.2. Biochemical characterization of SOD_{Ap}

To evaluate the potential applications of the extremozyme in industry, the effects of diverse physicochemical effectors such as temperature, pH and saline concentration on SOD activity were examined in the transgenic protein extracts in comparison with those evaluated in untransformed extracts (WT), using the

Chapter I

Riboflavin-NBT assay. As shown in **Figure 28**, SOD activity in transgenic extracts was 10.4- to 12.4-fold greater than that in the WT in the temperature range from 70 °C to 90 °C (**Figure 28 A**), with the maximum registered at 80 °C. Moreover, the enzymatic activity in transgenic protein samples was 0.5- to 2.3-fold higher than that in WT under the tested NaCl concentrations (**Figure 28 B**). Therefore, these results suggested that the overexpression of the extremophilic SOD conferred to the transgenic cell extracts the resistance to adverse environmental conditions compared to non-transgenic ones, in accordance with the hyperthermo-halophilic nature of SOD_{Ap}.

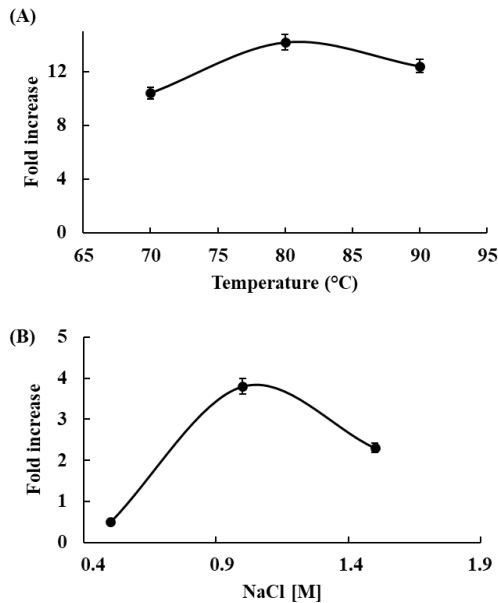


Fig. 28: Biochemical analysis of transgenic extracts: Effects of (A) temperature and (B) NaCl on SOD_{Ap} activity. Fold increase was calculated as ratio between SOD activity in crude protein extracts from wild-type plants/SOD

Chapter I

activity in crude protein extracts from transgenic plants, using the NBT assay. All experiments were performed in triplicate on three different protein preparations. Data were expressed as means \pm standard deviation. Standard deviation values lower than 5% were not shown.

Moreover, the characterization of the biochemical properties of the SOD_{Ap} was carried out under the specific environmental conditions in which its organism thrives. The obtained results revealed that recombinant SOD showed the optimum activity at 80°C, in agreement with its hyperthermophilic origin (**Figure 29 A**), but it still kept more than 80% of activity at 90°C, with a linear reduction observed between 60 °C and 70 °C.

Finally, the influence of saline concentration was investigated, showing that SOD_{Ap} activity increased concomitantly with salinity, reaching its optimum at 1.5 M NaCl concentration, thus reflecting its marine source (**Figure 29 B**).

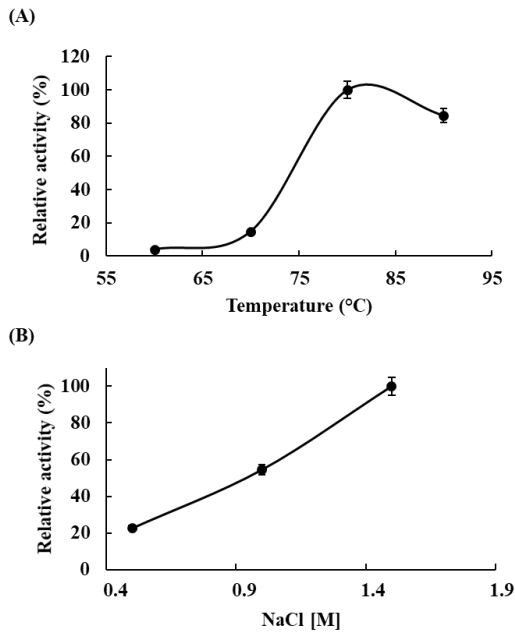


Fig. 29: Biochemical properties of SOD_{Ap}: Effect of (A) temperature and (B) NaCl on SOD_{Ap} activity. The activity at the optimal temperature or NaCl concentration was defined as 100%. The SOD activity was measured using the NBT assay and all experiments were performed in triplicate on three different protein preparations. Data were expressed as means \pm standard deviation. Standard deviation values lower than 5% were not shown.

3.3. Activity of SOD_{Ap}-tomato cell extracts on tuna slices

The consumption of tuna fish is widespread all over the world because it is an extremely protein-rich food and it is considered a commercially valuable species of fish.

In fact, the global tuna fish market size was USD 40.12 billion in 2021 and it is expected to surge from USD 41.06 billion in 2022 to USD 49.70 billion in 2029, propelling industry growth [Fortune Business. 2022].

Chapter I

However, consumers' trust is sometimes challenged by the illegal use of additives or unknown substances capable of masking the state of freshness of tuna and preserving its red colour [Sáez-Hernández, R. *et al.* 2022]. Lately, tuna adulteration has been detected in the European Union. Targeting to hinder the labour of the inspectors, some manufacturers and dealers adopted strategies aimed at arresting the undesirable changes occurring during processing and storage, especially the loss of the appreciated red colour. It is well known that the bright red colour of tuna is considered the main sensory parameter that determines its acceptability in the market and guides the consumers' choices, acquiring the role of the most economically important factor. In the last years, stakeholders have been using substances able to stabilize the colour of tuna meat, such as nitrate and/or nitrite salts, carbon monoxide, or vegetable extracts with high nitrate concentration, which could mask the degradation progress of tuna and, therefore, its histamine content [Djenane, D. and Roncales, P., 2018; Howes, B.D. *et al.*, 2019]. Indeed, this important biogenic amine continuously accumulates during storage and for this reason its concentration is adopted as indirect method to discover the day of life of histidine-rich fish fillets and slices and to detect fraud.

However, European Commission regulated these treatments forbidding the addition of such components [Regulation 1333/2008 of the European Parliament and of the Council of 16 December 2008 on Food Additives], due to the possible economic fraud and the potential health problems associated with sophisticated tuna

consumption [Al-Bulushi, I. *et al.*, 2009; Alexander, J. *et al.*, 2009]. In this scenario, novel strategies are necessary both to ensure consumer safety and to provide stakeholders with natural and permitted substances that allow them to achieve their goals without neglecting public health risks.

To date the only additives allowed for this type of products are the antioxidants (ascorbic acid, sodium ascorbate, calcium ascorbate) whose use has been limited at 300 mg/kg by the current European Commission rules.

In this study, to test the preservation capacity of fish meat, the natural extracts obtained from tomato cell lines transformed with SOD_{Ap} were tested on fillets of thawed yellowfin tuna (*Thunnus albacares*) and fresh bluefin tuna (*Thunnus thynnus*), by evaluating their influence on the fish colour and monitoring the histamine content during the storage period.

Regarding the analyses on the thawed yellowfin tuna fillets, an increasing value of the total colour difference (ΔE) over time was detected, because of the colour deterioration that normally occurs. Indeed, the ΔE value is strictly connected to the changes in the pigmentations of tissue and, therefore, to all the coordinates of CIElab colour space (L^* , a^* and b^*). Specifically, the highest values of ΔE were reached by the WT samples (extracts from non-transformed cell lines) followed by the control ones (CTR, injection of only water). Differently, the CM (commercial brine) and SOD_{Ap}-tuna samples exhibited the lowest grade of browning (**Figure 30 A**),

confirming the differences on the general colour appearance of the brines employed in this study.

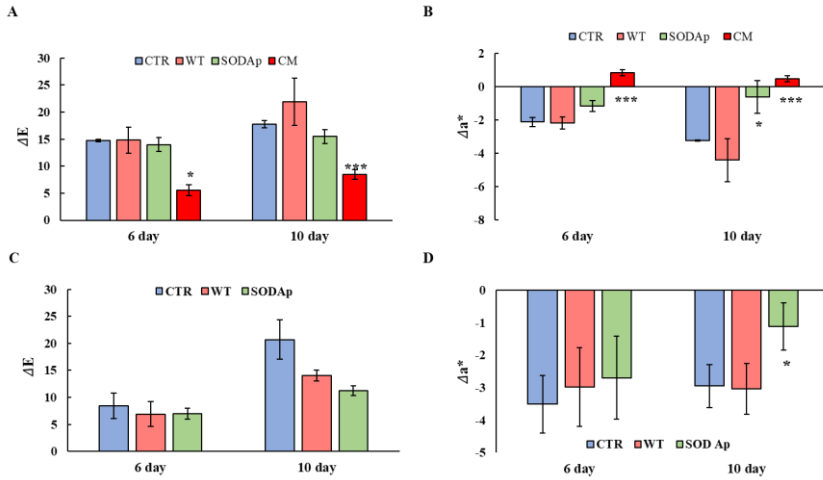


Fig. 30: Analyses of total color difference (ΔE) and variation in a^* (Δa^*) in *Thunnus albacares* and *Thunnus thynnus* fillets during the storage (4 ± 1 °C) for 10 days. (A) ΔE and (B) Δa^* values in *Thunnus albacares* fillets injected with aqueous solutions containing: water only (CTR: blue); extracts from tomato cell lines non-transformed with sodAp (WT: light red); extracts from tomato cell lines transformed with sodAp (SOD_{Ap}: green); commercial brine (CM: red). (C) ΔE and (D) Δa^* values of *Thunnus thynnus* fillets injected with aqueous solutions containing: water only (CTR: blue); extracts from tomato cell lines non-transformed with sodAp (WT: light red); extracts from tomato cell lines transformed with sodAp (SOD_{Ap}: green). The measurements were carried out on the inner surface of the tuna fillets after 10 minutes of exposure to air. Results are means of three independent experiments and error bars represent the standard error (sem). *Significant difference ($p < 0.05$) between the treated and the control samples. * Significant difference ($p < 0.001$) between the treated and the control samples.**

Chapter I

Nevertheless, a more specific sensory parameter for describing the changes in acceptability of tuna fillets is the redness value, which is closely related to the content and status of oxidation of myoglobin and haemoglobin. Indeed, when the red meat is exposed to air, myoglobin evolves from an intense red colour (due to oxymyoglobin, Fe (II), to a brown tone due to formation of deoxymyoglobin, and metamyoglobin Fe (III) [Chaijan, M., 2011]. As reported in **Figure 30 B**, the values of Δa^* (variations in redness) suggested an important activity of the commercial brine to significantly enhance the red colour of fillets. This result highlights its alarming ability to mask the natural degradation of the tuna, which retains its freshness properties even when the legislative limit for histamine could be exceeded. Indeed, although the sensory properties were preserved only in CM samples on the 12th day of storage (data not shown), the analysis of histamine showed higher concentrations (124.2 ± 2.6 mg/kg) compared to the minimum limit set at 100 mg/kg by the Reg. (CE) no. 2073/2005. This commercial powder, which is probably a plant extract of beet, is recognized for its natural high content in nitrates, which could act in the food matrix as chemical additives. Concerning the level of nitrate detected in the samples under study, none of them exceeded the concentration of 7 mg/kg, with the CM samples showing the highest concentration (5.33 ± 1.16 mg/Kg), which was very close to the average amount of nitrate detectable in fish (5 mg/kg) [Sáez-Hernández, R. *et al.*, 2022; Hambridge, T., 2003]. In this regard, it is interesting to note that the use of low concentration of this

commercial powder is dangerous not for their nitrate content but for their ability to stabilize the colour over time, adulterating the tuna and hiding its real state of conservation. Therefore, the tomato cell lines transformed with sod_{Ap} (SOD_{Ap}) can be considered a promising tool that could guarantee the preservation of red colour without representing a problem for public human health (**Figure 30 B**). Indeed, our results demonstrated that the efficiency of SOD_{Ap} brine in improving the tuna colour up to the 10th day of storage, when the histamine values were found below to the legislative limits, was due to the presence of the extremophilic SOD enzyme, as the WT samples had no effect (**Figure 30**).

Another set of experiments was conducted to investigate on the antioxidant potential of SOD_{Ap} extracts in bluefin tuna (*T. thynnus*), which is richer in slow fibers and myoglobin compared to *T. albacares* [Blank, J.M. *et al* 2007]. To this aim, WT and SOD_{Ap} extracts were injected in fresh bluefin tuna fillets using the water only as control (CTR) and the colour evolution was followed up to the 10th day of storage. As reported in **Figure 31**, although slight colour differences among samples were detectable already after 6 days of storage at refrigeration temperature, a notable effect of SOD_{Ap} brines was observed on the fillets after 10 days. Specifically, the values of colour differences (ΔE) and the redness variations (Δa^*) clarify the potential effects of SOD_{Ap} brine in slowing down the deterioration processes which affect the general appearance of fresh tuna fillets (**Figure 30 C**). Taking into account the colour evolution (ΔE) that considers the initial state of tuna fillets

pigmentation, significant differences between the colour of each sample were found. Indeed, the ΔE values in samples injected with the SOD_{Ap} brine were lower than those recorded for the other samples (**Figure 30 C**).

However, although a weak effect of the tomato extract alone on the general appearance of the product was observed, the values of Δa^* referred to WT samples made evident that the decreased ΔE did not contribute to the conservation of red colour.

Instead, significant differences ($p < 0.05$) were found comparing the Δa^* values of SOD_{Ap} -tuna samples with those of control and WT-treated fillets over 10 days of storage (**Figure 30 D**).

In conclusion, the injection of SOD extremozymes in tuna fillets, both fresh and thawed, could guarantee an extension of the shelf-life of the products, without resorting to the use of illicit substances.

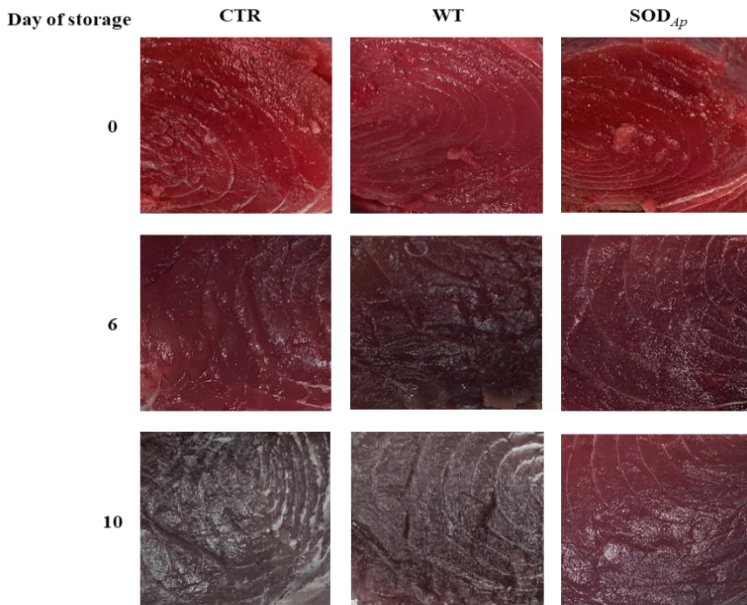


Fig. 31: Appearance of *Thunnus thynnus* slices stored for 10 days at refrigerated temperature (4 ± 1 °C). The samples were injected with aqueous solutions containing water only (CTR); extracts from tomato cell lines non-transformed with sodAp (WT); extracts from tomato cell lines transformed with sodAp (SODAp).

3.4. Activity of SOD_{Ap}-tomato cell extracts on myoglobin oxidation

As the loss of the red colour in fish meat is mainly linked to the oxidation of oxymyoglobin (OxyMb), an ORAC assay was performed to assess the ability of SOD_{Ap}-containing extracts to protect myoglobin from oxidation, using the compound 2,2'-Azobis(2-amidinopropane) dihydrochloride (AAPH) as oxidant [Marques, S.S. *et al.* 2015]. Therefore, scalar dilutions of WT and transgenic SOD_{Ap} tomato extracts were incubated with myoglobin

Chapter I

in the presence of AAPH and the absorbance decay, due to the oxidation of the heme group of the protein caused by the oxidant, was measured at 409 nm. The values of antioxidant capacity, expressed as micromole of Trolox equivalents per gram, were calculated as explained in the Materials and Methods section and resulted as $388 \pm 24 \mu\text{mol Trolox eq}\cdot\text{g}^{-1}$ for the SOD_{Ap} extract, and $195 \pm 21 \mu\text{mol Trolox eq}\cdot\text{g}^{-1}$ for the WT sample, indicating that the presence of the enzyme in the tomato cell extract significantly increased the myoglobin protection against oxidation and confirming the results on the redness preservation of fish slices showed above.

4. CONCLUSIONS

In addition to microbial spoilage, oxidation is considered another of the major processes responsible for the gradual reduction and deterioration of sensory and nutritional quality of foods such as meat [Min B., D.U., 2005], dairy products [Collomb, M. and Spahni M., 1996], fruits and vegetables and seafood products [Secci, G. and Parisi, G., 2016], affecting the consumer acceptance. Therefore, the control, or at least minimization, of the oxidation processes is of great interest to the food industry. In the nutrition technology, the enrichment of various foodstuffs with synthetic compounds such as t-Butyl-4-HydroxyAnisole (BHA) or other typology of antioxidants (e.g. vitamins, carotenoids, polyphenols) is a frequently adopted method to counteract the oxidation phenomena, working as "scavenger". Nevertheless, many of these additives cannot be used in large quantities as they can be health hazards and can cause serious side effects, while vitamins are not stable over time and are subjected to hydrolytic processes mostly caused by high temperatures or high salt concentrations [Poljsak, B. *et al.*, 2021]. Therefore, the food industry currently faces the challenge of which processing techniques and storage methods should be used to minimize their impact on food quality and safety, also due to the increased consumers' perception and awareness. In this scenario, extremophilic microorganisms represent an underutilized and innovative source of novel enzymes, having developed unique mechanisms to survive under a wide range of extreme and

Chapter I

inhospitable environmental conditions in terms of temperature, pH, or salinity, among others. As consequence, the extremophile-derived enzymes, or extremozymes, offer new alternatives for biotechnological applications [Sarmiento, F. *et al.*, 2015], being able to perform reactions under harsh conditions, like those found in several industrial processes.

In this thesis, protein extracts enriched with a SOD enzyme isolated from an extremophilic organism, was heterologously expressed in tomato cell lines, using *Agrobacterium tumefaciens*-mediated genetic transformation and biochemically characterized. This innovative approach, which combines the advantage of using plant cells as a bio-factory of recombinant proteins with the extraordinary catalytic properties of extremozymes, could represent the cornerstone for the development of environmentally friendly, efficient, and sustainable food technologies with positive impacts on human health.

5. REFERENCES

- ACSA. (2013). Informe sobre la evaluación del riesgo para la utilización de nitritos y nitros en productos de la pesca frescos.
- AESAN. (2019). Uso de extractos vegetales en pescado y productos de la pesca.
- Akovou E, Kourti M. A Comprehensive Overview of the Complex Role of Oxidative Stress in Aging, The Contributing Environmental Stressors and Emerging Antioxidant Therapeutic Interventions. *Front Aging Neurosci.* 2022 Jun 13;14:827900. doi: 10.3389/fnagi.2022.827900. PMID: 35769600; PMCID: PMC9234325.
- Al-Bulushi, I., Poole, S., Deeth, H. C., & Dykes, G. A. (2009). Biogenic Amines in Fish: Roles in Intoxication, Spoilage, and Nitrosamine Formation—A Review. *Critical Reviews in Food Science and Nutrition*, 49(4), 369–377.
- Alexander, J., Benford, D., Cockburn, A., Cravedi, J.-P., Dogliotti, E., Domenico, A. Di, Luisa Fernandez-Cruz, M., Fürst, P., Fink-Gremmels, J., Corrado, L., Galli, P., Grandjean, J., Gzyl, G., Heinemeyer, N., Johansson, A., Mutti, J., Schlatter, R., Van Leeuwen, C. Van, & Peteghem, P. V. (2009). Nitrite as undesirable substances in animal feed. Scientific Opinion of the Panel on Contaminants in the Food Chain. In *The EFSA Journal* (Vol. 1017).
- Babu, P., Chandel, A. K., and Singh, O. V. (2015). Extremophiles and Their Applications in Medical Processes. Berlin: Springer. doi: 10.1007/978-3-319-12808-5.
- Bahorun T., Soobrattee M. A., Luximon-Ramma V., Aruoma O. I. Free radicals and antioxidants in cardiovascular health and disease. *Internet Journal of Medical Update.* 2006.
- Balch WE, Fox GE, Magrum LJ, Woese CR, Wolfe RS (1979) Methanogenic Archaea: reevaluation of a unique biological group. *Microbiol Rev* 43:260–296.
- Bang C, Schmitz RA (September 2015). "Archaea associated with human surfaces: not to be underestimated". *FEMS Microbiology Reviews.* 39 (5): 631–48.
- Beauchamp, C.; Fridovich, I. Superoxide dismutase: Improved assays and an assay applicable to acrylamide gels. *Anal. Biochem.* 1971, 44, 276–287.
- Blank, J.M.; Farwell, C.J.; Morrissette, J.M.; Schallert, R.J.; Block, B.A. Influence of swimming speed on metabolic rates of juvenile Pacific bluefin tuna and yellowfin tuna. *Physiol. Biochem. Zool.* 2007, 80, 167–177.
- Bradford, M.M. A rapid and sensitive method for the quantitation of microgram quantities of protein utilizing the principle of protein-dye binding. *Anal. Biochem.* 1976, 72, 248–254.
- Breithaupt H (November 2001). "The hunt for living gold. The search for organisms in extreme environments yields useful enzymes for industry". *EMBO Reports.* 2 (11): 968–71.
- Burton, G. W., Joyce, A. & Ingold, K. U. (1983) *Arch. Biochem. Biophys.* 221, 281–290.
- Butterfield D. A. Amyloid beta-peptide (1-42)-induced oxidative stress and neurotoxicity: implications for neurodegeneration in Alzheimer's disease brain. A review. *Free Radical Research.* 2002;36:1307–1313.
- C. L. Hawkins, M. J. Davies, *Biochim. Biophys. Acta Bioenerg.* 2001, 1504, 196–219.
- Caimi, G., Carollo, C. and Presti, R.L. (2004). Chronic renal failure: Oxidative stress, endothelial dysfunction and wine. *Clin. Nephrol.*, 62: 331-335.
- Caramori G., Papi A. Oxidants and asthma. *Thorax.* 2004;59:170–173.
- Ceriello A. Possible role of oxidative stress in the pathogenesis of hypertension. *Diabetes Care.* 2008;31(Supplement 2):S181–S184. doi: 10.2337/dc08-s245.
- Chaban B, Ng SY, Jarrell KF (February 2006). "Archaeal habitats--from the extreme to the ordinary". *Canadian Journal of Microbiology.* 52 (2): 73–116.

Chapter I

- Chaijan, M. Physicochemical changes of tilapia (*Oreochromis niloticus*) muscle during salting. *Food Chem.* 2011, 129, 1201–1210.
- Chambers, E., IV. Analysis of Sensory Properties in Foods: A Special Issue. *Foods* 2019, 8, 291.
- Coker, J. A. (2016). Extremophiles and biotechnology: current uses and prospects. *F1000Res.* 5:F1000 Faculty Rev-396. doi: 10.12688/f1000research.7432.1.
- Cortesi, M.L.; Vollano, L.; Peruzy, M.F.; Marrone, R.; Mercogliano, R. Determination of nitrate and nitrite levels in infant foods marketed in Southern Italy. *CyTA-J. Food* 2015, 13, 629–634.
- D.M. Smith. Functional and biochemical changes in deboned turkey due to frozen storage and lipid oxidation. *Journal of Food Science*, 52 (1987), pp. 22-26.
- DeLong EF (December 1998). "Everything in moderation: archaea as 'non-extremophiles'". *Current Opinion in Genetics & Development.* 8 (6): 649–54.
- Diplock, A.T., Charleux, J.L., Crozier-Willi, G Kok, F.J., Rice-Evans, C., Roberfroid, M., Stah, W. and Viiia-Ribes, J. (1998). Functional food science and defence against reactive oxidative species. *British Journal of Nutrition*, 80(1): 77-112.
- Djenane, D.; Roncales, P. Carbon monoxide in meat and fish packaging: Advantages and limits. *Foods* 2018, 7, 12.
- Droge W. Free radicals in the physiological control of cell function. *Physiological Reviews.* 2002;82:47–95. doi: 10.1152/physrev.00018.2001.
- Durvasula, R., and Rao, D. V. S. (eds). (2018). "Extremophiles: from Biology to Biotechnology," in *Extremophiles* (Boca Raton: Taylor & Francis, a CRC title, part of the Taylor & Francis imprint, a member of the Taylor & Francis Group, the academic division of T&F Informa plc, 2018 (Boca Raton, FL: CRC Press), 1–18.
- E.A. Decker, R.J. Elias, D.J. McClements (Eds.), *Oxidation in Foods and Beverages and Antioxidant Applications*, Woodhead Pub, Philadelphia, 2010.
- Eckburg PB, Bik EM, Bernstein CN, Purdom E, Dethlefsen L, Sargent M, *et al.* (June 2005). "Diversity of the human intestinal microbial flora". *Science.* 308 (5728): 1635–38.
- Egorova K, Antranikian G (December 2005). "Industrial relevance of thermophilic Archaea". *Current Opinion in Microbiology.* 8 (6): 649–55.
- F. Shahidi, Zhong Y. *Lipid oxidation: Measurement methods* (6th ed.)F. Shahidi (Ed.), Bailey's industrial oil and fat products, Vol. 1, John Wiley & Sons, Inc., Hoboken, NJ (2005), pp. 357-386.
- F. Shahidi. Antioxidants in foods and food antioxidants *Die Nahrung*, 44 (2000).
- Foote, C. S. & Denny, R. W. (1968) *J. Am. Chem. Soc.* 90, 6233-6235.
- Fortune Business, (2022). <https://www.fortunebusinessinsights.com/industry-reports/tuna-fish-market-100744>, access on 20 October 2022.
- Foyer, C.H. and Noctor, G. (2002). Oxygen processing in photosynthesis: regulation and signaling. *New Phytol.*, 146: 359-388.
- Frei B. *Reactive Oxygen Species and Antioxidant Vitamins*. Oregon State University: Linus Pauling Institute; 1997.
- G. Liu, Y.L. Xiong. Electrophoretic pattern, thermal denaturation, and in vitro digestibility of oxidized myosin. *Journal of Agricultural and Food Chemistry*, 48 (2000), pp. 624-630.
- G. Scott. *Antioxidants: In science, technology, medicine and nutrition* Albion Publishing, Chichester, UK (1997), pp. 36-79.
- Garcia JL, Patel BK, Ollivier B (2000) Taxonomic, phylogenetic, and ecological diversity of methanogenic archaea. *Anaerobe* 6:205–226.
- Gogliettino, M.; Riccio, A.; Cocca, E.; Rossi, M.; Palmieri, G.; Balestrieri, M. A new pepstatin-insensitive thermopsin-like protease overproduced in peptide-rich cultures of *Sulfolobus solfataricus*. *Int. J. Mol. Sci.* 2014, 15, 3204–3219.
- Gomberg M. An instance of trivalent carbon: Triphenylmethyl. *J Am Chem Soc.* 1900;22:757–71
- Gophna U, Charlebois RL, Doolittle WF (May 2004). "Have archaeal genes contributed to bacterial virulence?". *Trends in Microbiology.* 12 (5): 213–219.

Chapter I

- Guleria, S.; Jain, R.; Singh, D.; Kumar, S. A thermostable Fe/Mn SOD of *Geobacillus* sp. PCH100 isolated from glacial soil of Indian trans-Himalaya exhibits activity in the presence of common inhibitors. *Int. J. Biol. Macromol.* 2021, 179, 576–585.
- Halliwell B. Biochemistry of oxidative stress. *Biochemical Society Transactions.* 2007;35:1147–1150. doi: 10.1042/BST0351147.
- Halliwell B. Free Radicals and other reactive species in disease. *Nature Encyclopedia of life sciences.* 2001. p. 1–7.
- Halliwell B. Role of free radicals in neurodegenerative diseases: therapeutic implications for antioxidant treatment. *Drugs & Aging.* 2001;18:685–716.
- Halliwell, B. & Gutteridge, J. M. C. (1989) *Free radicals in biology and medicine* (2nd edn) Clarendon Press, Oxford.
- Hambridge, T. Nitrate and nitrite: Intake assessment. *WHO Food Addit. Ser.* 2003, 50, 1053–1071.
- Howes, B.D.; Milazzo, L.; Droghetti, E.; Nocentini, M.; Smulevich, G. Addition of sodium ascorbate to extend the shelf-life of tuna meat fish: A risk or a benefit for consumers? *J. Inorg. Biochem.* 2019, 200, 110813.
- Huang, D.; Ou, B.; Hampsch-Woodill, M.; Flanagan, J.A.; Prior, R.L. High-throughput assay of oxygen radical absorbance capacity (ORAC) using a multichannel liquid handling system coupled with a microplate fluorescence reader in 96-well format. *J. Agric. Food Chem.* 2002, 50, 4437–4444.
- Iannario, Maria & Manisera, Marica & Piccolo, Domenico & Zuccolotto, Paola. (2012). Sensory analysis in the food industry as tool for marketing decisions. *Advances in Data Analysis and Classification.* 6. 10.1007/s11634-012-0120-4
- J.R. Vercellotti, A.J. St. Angelo, A.M. Spanier. Lipid oxidation in foods: An overview A.J. St. Angelo (Ed.), *Lipid oxidation in food*, American Chemical Society, Washington, DC (1992), pp. 1-11.
- K. Schaich in *Lipid Oxidation Pathways*, Vol. 2 (Eds.: A. Kamal-Eldin, A. D. Min), AOCS Press, Urbana, 2008, pp. 183–274.
- Kandler OT (August 1998). "The early diversification of life and the origin of the three domains: a proposal." In Wiegel J, Adams WW (eds.). *Thermophiles: the keys to molecular evolution and the origin of life.* Athens: Taylor and Francis. p. 19-31. ISBN 978-1-4822-7304-5.
- Kanner J. Dietary advanced lipid oxidation endproducts are risk factors to human health. *Mol Nutr Food Res.* 2007 Sep;51(9):1094-101. doi: 10.1002/mnfr.200600303. PMID: 17854006.
- Krieg N (2005). *Bergey's Manual of Systematic Bacteriology.* US: Springer. pp. 21–26.
- L. Lyras, N.J. Cairns, A. Jenner, P. Jenner An assessment of oxidative damage to proteins, lipids, and DNA in brain from patients with Alzheimer's disease *Neurochemistry*, 68 (1997), pp. 2061-2069.
- L.J. Rowe, K.R. Maddock, S.M. Lonergan, E. Huff-Lonergan. Oxidative environments decrease tenderization of beef steaks through inactivation of μ -calpain. *Journal of Animal Science*, 82 (2004), pp. 3254-3266.
- Lindley, M.G. The impact of food processing on antioxidants in vegetable oils, fruits and vegetables. *Trends Food Sci. Technol.* 1998, 9, 336–340.
- Liu Y, Whitman WB (2008) Metabolic, phylogenetic, and ecological diversity of the methanogenic archaea. *Ann N Y Acad Sci* 1125:171–189.
- Liu, J.; Yin, M.; Zhu, H.; Lu, J.; Cui, Z. Purification and characterization of a hyperthermostable Mn-superoxide dismutase from *Thermus thermophilus* HB27. *Extremophiles* 2011, 15, 221–226.
- Lushchak VI, Storey KB. Oxidative stress concept updated: Definitions, classifications, and regulatory pathways implicated. *EXCLI J.* 2021 May 26;20:956-967. doi: 10.17179/excli2021-3596. PMID: 34267608; PMCID: PMC8278216.
- M. Collomb, M. Spahni. Review of the methods for determining lipid oxidation products, in particular lipids from milk products. *Schweizerische Milchwirtschaftliche Forschung*, 25 (1996), pp. 3-24.

Chapter I

- M. Estévez, C. Luna, Crit. Rev. Food Sci. Nutr. 2017, 57, 3781 – 3793.
- M. Hellwig, K. Löbmann, T. Orywol, A. Voigt, J. Agric. Food Chem. 2014, 62, 4425–4433.
- M. J. Davies, Biochem. J. 2016, 473, 805–825.
- M. Renner, F. Dumont, P. Gatellier. Antioxidant enzyme activities in beef in relation to oxidation of lipid and myoglobin. Meat Science, 43 (1996), pp. 111-121.
- MacNee W. Oxidative stress and lung inflammation in airways disease. European Journal of Pharmacology. 2001;429:195–207.
- Mahajan A., Tandon V. R. Antioxidants and rheumatoid arthritis. Journal of Indian Rheumatology Association. 2004;12:139–142.
- Majima H, T. D. Oberley, K. Furukawa, M. P. Mattson, H. C. Yen, L. I. Szewda & D. K. St. Clair: Prevention of Mitochondrial Injury by Manganese Superoxide Dismutase Reveals a Primary Mechanism for Alkaline-induced Cell Death. J Biol Chem 273, 8217-8224 (1998).
- Marques, S.S.; Magalhaes, L.M.; Mota, A.I.P.; Soares, T.R.P.; Korsak, B.; Reis, S.; Segundo, M.A. Myoglobin microplate assay to evaluate prevention of protein peroxidation. J. Pharm Biomed. Anal. 2015, 114, 305–311.
- Matés JM, Sánchez-Jiménez F. Antioxidant enzymes and their implications in pathophysiologic processes. Front Biosci. 1999 Mar 15;4:D339-45. doi: 10.2741/mates. PMID: 10077544.
- McCord JM, Fridovich I (November 1969). "Superoxide dismutase. An enzymic function for erythrocyte (hemocuprein)". The Journal of Biological Chemistry. 244 (22): 6049–6055.
- Merino N, Aronson HS, Bojanova DP, Feyhl-Buska J, Wong ML, Zhang S, Giovannelli D. Living at the Extremes: Extremophiles and the Limits of Life in a Planetary Context. Front Microbiol. 2019 Apr 15; 10:780. Erratum in: Front Microbiol. 2019 Aug 13;10:1785. PMID: 31037068; PMCID: PMC6476344.
- Min B., D.U. Ahn. Mechanism of lipid peroxidation in meat and meat products—A review Food Science and Biotechnology, 14 (2005), pp. 152-163.
- Moissl-Eichinger C, Pausan M, Taffner J, Berg G, Bang C, Schmitz RA (January 2018). "Archaea Are Interactive Components of Complex Microbiomes". Trends in Microbiology. 26 (1): 70–85.
- Morzell, M., Gatellier, Ph., Sayd, T., Renner, M., Laville, E., Chemical oxidation decreases proteolytic susceptibility of skeletal muscle myofibrillar proteins. Meat Sci. 2006, 73, 536–543.
- Mukherji SM, Singh SP. Reaction mechanism in organic chemistry. Madras: Macmillan India Press; 1986.
- N. Kamin-Belsky, A.A. Brillon, R. Arav, N. Shalkai. Degradation of myosin by enzymes of the digestive system: comparison between native and oxidatively cross-linked protein. Journal of Agricultural and Food Chemistry, 44 (1996), pp. 1641-1646.
- Nkamga VD, Henrissat B, Drancourt M (2017) Archaea: essential inhabitants of the human digestive microbiota. Hum Microbiome J 3:1–8.
- Norris PR, Burton NP, Foulis NA (April 2000). "Acidophiles in bioreactor mineral processing". Extremophiles. 4 (2): 71–76.
- P. Nagy, A. J. Kettle, C. C. Winterbourn, J. Biol. Chem. 2009, 284, 14723–14733.
- Pace NR (May 2006). "Time for a change". Nature. 441 (7091): 289. Bibcode:2006 Natur. 441..289P. PMID 16710401. S2CID 4431143
- Pacher P., Beckman J. S., Liaudet L. Nitric oxide and peroxynitrite in health and disease. Physiological Reviews. 2007;87:315–424. doi: 10.1152/physrev.00029.2006.
- Padmapriya, V.; Anand, N. Purification and characterization of iron-containing superoxide dismutase from *Anabaena variabilis* Kutz ex Born. et Flah. Biomed. Pharmacol. J. 2010, 3, 349–356.
- Palmieri G, Casbarra A, Fiume I, Catara G, Capasso A, Marino G, Onesti S, Rossi M. "Identification of the first archaeal oligopeptide-binding protein from the hyperthermophile *Aeropyrum pernix*." Extremophiles: life under extreme conditions. 2006 Oct;10(5):393-402. Epub 2006 Apr 25.
- Palmieri, G.; Arciello, S.; Bimonte, M.; Carola, A.; Tito, A.; Gogliettino, M.; Cocca, E.; Fusco, C.; Balestrieri, M.; Colucci, M.G.; *et al.* The extraordinary resistance to UV radiations of a

Chapter I

- manganese superoxide dismutase of *Deinococcus radiodurans* offers promising potentialities in skin care applications. *J. Biotechnol.* 2019, 302, 101–111.
- Phaniendra, A., Jestadi, D. B., and Periyasamy, L. (2015). Free radicals: properties, sources, targets and their implication in various diseases. *Indian J. Clin. Biochem.* 30, 11–26. doi: 10.1007/s12291-014-0446-0.
- Pinmanee, P.; Sompinit, K.; Arnthong, J.; Suwannarangsee, S.; Jantimaporn, A.; Khongkow, M.; Nimchua, T.; Sukyai, P. Enhancing the productivity and stability of superoxide dismutase from *Saccharomyces cerevisiae* TBRC657 and its application as a free radical scavenger. *Fermentation* 2022, 8, 169.
- Pizzino G, Irrera N, Cucinotta M, Pallio G, Mannino F, Arcoraci V, Squadrito F, Altavilla D, Bitto A. Oxidative Stress: Harms and Benefits for Human Health. *Oxid Med Cell Longev.* 2017;2017:8416763. doi: 10.1155/2017/8416763. Epub 2017 Jul 27. PMID: 28819546; PMCID: PMC5551541.
- Poljsak, B.; Kovač, V.; Milisav, I. Antioxidants, Food Processing and Health. *Antioxidants (Basel)* 2021, 10, 433.
- Rahman MS (eds). Handbook of food preservation. 2nd ed. Food science and technology. Boca Raton: CRC Press; 2007.
- Rahman, T., Hosen, I., Islam, M.M.T. and Shekhar, H.U. (2012). Oxidative stress and human health. *Advances in Bioscience and Biotechnology*, 3: 997-1019.
- Rampelotto PH. Extremophiles and extreme environments. *Life (Basel)*. 2013 Aug 7;3(3):482-5. doi: 10.3390/life3030482. PMID: 25369817; PMCID: PMC4187170.
- Regulation (EC) No 1333/2008 of the European Parliament and of the Council of 16 December 2008 on food additives (Text with EEA relevance), 16 (2008) (testimony of European
- Reichel, C.; Mathur, J.; Ecker, P.; Langenkemper, K.; Koncz, C.; Schell, J.; Reiss, B.; Maas, C. Enhanced green fluorescence by the expression of an *aequorea victoria* green fluorescent protein mutant in mono- and dicotyledonous plant cells. *Proc. Natl. Acad. Sci. USA* 1996, 93, 5888–5893.
- Restrepo, M.A.; Freed, D.D.; Carrington, J.C. Nuclear transport of plant potyviral proteins. *Plant Cell* 1990, 2, 987-998.
- S. Robinson, R. Bevan, J. Lunec, H. Griffiths, *FEBS Lett.* 1998, 430, 297–300.
- S.S. Seehafer, D.A. Pearce. You say lipofuscin, we say ceroid: defining autofluorescent storage material. *Neurobiology of Aging*, 27 (2006), pp. 576-582.
- Sáez-Hernández, R.; Antela, K.U.; Mauri-Aucejo, A.R.; Morales-Rubio, A.; Cervera, M.L. Smartphone-based colorimetric study of adulterated tuna samples. *Food Chem.* 2022, 389, 133063.
- Sako Y, Nomura N, Uchida A, et al (1996). "*Aeropyrum pernix* gen. nov., sp. nov., a novel aerobic hyperthermophilic archaeon growing at temperatures up to 100 degrees C". *Int. J. Syst. Bacteriol.* 46 (4): 1070–7.
- Samuel BS, Gordon JI (June 2006). "A humanized gnotobiotic mouse model of host-archaeal-bacterial mutualism". *Proceedings of the National Academy of Sciences of the United States of America.* 103 (26): 10011–16.
- Sarmiento, F.; Peralta, R.; Blamey, J.M. Cold and Hot Extremozymes: Industrial Relevance and Current Trends. *Front. Bioeng. Biotechnol.* 2015, 20, 148.
- Schiraldi C, Giuliano M, De Rosa M (September 2002). "Perspectives on biotechnological applications of archaea". *Archaea.* 1 (2): 75–86.
- Secci G, Parisi G. 2016. From farm to fork: lipid oxidation in fish products. A review. *Ital J Anim Sci.* 15:124–36.
- Shiffman ME, Charalambous BM (2012). "The search for archaeal pathogens". *Reviews in Medical Microbiology.* 23 (3): 45–51.
- Sies H. Oxidative stress: Introductory remarks. In: Sies H, editor. *Oxidative stress.* London: Academic Press; 1985. pp. 1–8.
- Sies H. Oxidative stress: Oxidants and antioxidants. *Exp Physiol.* 1997;82:291–5.

Chapter I

- Sies, H. (1993), Strategies of antioxidant defense. *European Journal of Biochemistry*, 215: 213-219.
- Stetter, K.O.; Fiala, G.; Huber, G.; Huber, R.; Seegerer, A. Hyperthermophilic microorganisms. *FEMS Microbiol. Lett.* 1990, 75, 117–124.
- Synowiecki J, Grzybowska B, Zdzieblo A (2006). "Sources, properties and suitability of new thermostable enzymes in food processing". *Critical Reviews in Food Science and Nutrition*. 46 (3): 197–205.
- T. Grune, T. Jung, K. Merker, K.J.A. Davies. Decreased proteolysis caused by protein aggregates, inclusion bodies, plaques, lipofuscin, ceroid, and aggresomes during oxidative stress, aging, and disease. *The International Journal of Biochemistry & Cell Biology*, 36 (2004), pp. 2519-2530.
- V.E. Kagan. *Lipid Peroxidation in Biomembranes*, CRC Press, Boca Raton, FL (1988), p. 29.
- Valentine DL (April 2007). "Adaptations to energy stress dictate the ecology and evolution of the Archaea". *Nature Reviews. Microbiology*. 5 (4): 316–23.
- Valko M., Leibfritz D., Moncola J., Cronin M. D., Mazur M., Telser J. Free radicals and antioxidants in normal physiological functions and human disease. *The International Journal of Biochemistry & Cell Biology*. 2007;39:44–84.
- Walston J., Xue Q., Semba R. D., *et al.* Serum antioxidants, inflammation, and total mortality in older women. *American Journal of Epidemiology*. 2006;163:18–26. doi: 10.1093/aje/kwj007.
- Whittaker M & J. W. Whittaker: A glutamate bridge is essential for dimer stability and metal selectivity in manganese superoxide dismutase. *J Biol Chem* 273, 22188-22193 (1998).
- Woese C (June 1998). "The universal ancestor". *Proceedings of the National Academy of Sciences of the United States of America*. 95 (12): 6854–59.
- Woese CR (March 1994). "There must be a prokaryote somewhere: microbiology's search for itself". *Microbiological Reviews*. 58 (1): 1–9.
- Woese CR, Fox GE (November 1977). "Phylogenetic structure of the prokaryotic domain: the primary kingdoms". *Proceedings of the National Academy of Sciences of the United States of America*. 74 (11): 5088–90.
- Wolff, S. P., Dean, R. T., Fragmentation of proteins by free radicals and its effect on their susceptibility to enzyme hydrolysis. *Biochem. J.* 1986, 234, 399–403.
- Young I., Woodside J. Antioxidants in health and disease. *Journal of Clinical Pathology*. 2001;54:176–186.
- Youssef Sereme, Soraya Mezouar, Ghiles Grine, Jean-Louis Mege, Michel Drancourt, et al.. Methanogenic Archaea: Emerging Partners in the Field of Allergic Diseases. *Clinical Reviews in Allergy and Immunology*, 2019, 57 (3), pp.456-466.

CHAPTER II

1. INTRODUCTION

Food sector contributes significantly to the financial statements of the European Union (EU), generating more than 750.000.000.000 euros per year [EU, 2020], despite the foods losses, which in the last decades have been reaching very high figures. Among the main food losses there is the food waste, understood as “food appropriate for human consumption being discarded, whether or not after it is kept beyond its expiry date or left to spoil” [FAO, 2013]. In 2011, the Food & Agriculture Organization (FAO) estimated that around 1.3 billion tons of food never reached the tables of consumers, resulting in the loss of one-third of all foods produced for human consumption [FAO, 2019] and scientists stated that the global trend was set to grow in the near future [Lemaire, A. and Limbourg, S., 2019]. At the same time, there is a growing consumer awareness about the nature and the origin of all ingredients that reach his table, demanding for fresh, minimally processed and “natural” food products, together with the requirements for maintenance and improvement of safety, quality and shelf-life [Barreiro, M. *et al.*, 2014; Carochó, M. *et al.*, 2015].



1.1 Food safety and Food security

The issue of food safety has gained the attention of consumers and institutions in recent years. In this context, it is necessary to introduce two different but complementary concepts: food safety and food security.

Specifically, food security refers to the economic and social aspects, that is the universal possibility of access to a quantity of food sufficient to lead a dignified, healthy and active life. Indeed, malnutrition is a widespread phenomenon, which does not only affect the least developed countries and it is estimated to increase by 60% until 2050. On the other hand, food safety concerns the hygiene and wholesomeness of a food, including a set of rules designed to protect human health. These guidelines indicate how to manage food at all stages of the production process, from preparation and storage, transport and distribution to the general public. In fact, it is known that the quality level of a food especially depends on the production conditions, which must be such as to guarantee products with high and constant quality starting from the first stages of selection of raw materials. Hence, from this point of view, the safety of a food must be guaranteed along the entire food chain, reducing or eliminating microbiological hazards and events capable of determining potential contaminations.

Therefore, the increase interest in food safety has led the European Commission to consider the achievement of the highest possible standards of food safety as a priority, identifying and characterizing

all the factors that reduce the health risk present from production to consumption of food.

Moreover, consumer requests are increasingly oriented towards high quality foods, both in terms of safety and for their sensory and nutritional characteristics, with the expectation that this level will be maintained from the moment of purchase of the product until consumption. This has caused, also at an international level, the raised need to orientate the choices in terms of food safety on a more general and global level, which allows not only to prevent epidemic episodes, but also to estimate, in a realistic manner, the probability and the severity of the impact of foodborne diseases on consumers and their effects.

1.2 Food spoilage

Generally, food spoilage may be considered as ecological phenomenon where a food product becomes unsuitable to ingest by the consumer, as it may cause changes in the available nutrients, alteration of organoleptic properties and food poisoning. Every year, one-third of the world's food produced for the consumption of humans is lost due to spoilage [Garcha, S., 2018]. This process includes physical damage and chemical changes, such as lipid oxidation and colour changes, or the appearance of off-flavors and off-odors resulting from microbial growth and the product's associated metabolism [Zheng, A. *et al.*, 2013]. The food spoilage may be caused by many outside factors, such as mechanical, physical, chemical, and microbial effects, as well as how the

Chapter II

product is packaged and stored. In fact, damages could occur during harvesting, processing, and distribution of food, leading to ultimate reduction of shelf-life. For example, during the multiple phases of distribution and storage, the products undergo complex environmental conditions of temperature, light, oxygen, humidity, which trigger physico-chemical and microbiological reactions leading to their rapid and natural degradation.

The direct consequence of such phenomena is usually manifested by chemical and microbial deterioration and the alteration of the sensory characteristics of the products (appearance, smell, taste) (**Figure 1**).



Fig. 1: Examples of contaminated foods: fruit, meat and bread.

1.2.1 Microbial food spoilage

Microbial growth represents one of the main causes of food spoilage, leading the development of undesirable sensory characteristics, and making the food unsafe for consumption. It has been estimated that approximately 25% of all foods produced are lost due to microbial spoilage (**Figure 2**) [Petruzzi, L. *et al.*, 2017].

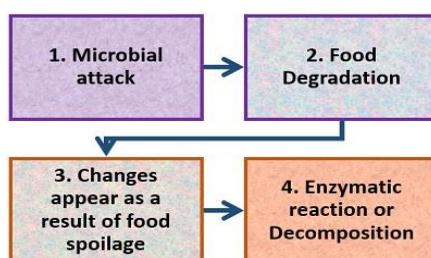


Fig. 2: Representative scheme of food spoilage caused by microbial agents. The enzymes of microorganisms growing on foods, lead to by-products formation which are responsible of the spoilage and alteration of organoleptic characteristics.

Foods are derived from other living organisms and during their development and preparation they are continuously exposed to microbial contamination. Prior to harvest, fruits and vegetables generally have good defence mechanisms against microbial attack, but, after separation from the plant, they can easily succumb to microbial proliferation. Similarly, meat upon slaughter is unable to resist to rapidly growing microbes [Singh, R. P., 1994].

Chapter II

The dominance of a specific microbial process on food depends upon factors, which persist during processing, transportation and storage. It is very important to consider that under ideal conditions microorganisms can grow very rapidly, being able to double in number in a short period of time. A variation in the optimum environmental conditions is selective for growth of different types and species of microorganisms, which can be categorized into broad groups such as aerobes and anaerobes based on their tolerance and use of oxygen and psychrophiles, mesophiles, and thermophiles based on their growth temperatures.

Moreover, several microorganisms are pathogens and represent a major safety concern in the processing and handling of foods. In fact, they produce by-products that are toxic to humans, causing a wide variety of infections and intoxications responsible of illness and/or even death. In agreement with the latest data provided by the World Health Organization (WHO) in 2015, the estimated number of cases of foodborne illness and deaths annually were around 600.000.000 and 420.000, respectively [WHO, 2015]. All this despite the fact that European Union (UE) since 2005 had already defined how to declare food poisoning events and made outbreak communication mandatory for Member States (MS). Indeed, in agreement with Directive 2003/99/EC, each MS submitted data on zoonoses, antimicrobial resistance and food-borne outbreaks which were examined by the European Food Safety Authority

Chapter II

(EFSA). In collaboration with the European Centre for Disease Control (ECDC), collected data were used to compose the annual Community Summary Report. The latest scientific Zoonoses Report of EFSA and ECDC (2021) reconfirmed campylobacteriosis and salmonellosis as the first and second most reported zoonoses in humans, with 220.682 and 87.923 confirmed cases, respectively (**Figure 3**), followed by the Shiga-toxin producing *Escherichia coli* (STEC), with a high rate of hospitalization (50 cases in 2019). However, *Listeria monocytogenes*, even if with only 2621 confirmed human cases in 2019, boasted to be one of the most serious foodborne diseases because of the high percentage of case fatality (17.6%).

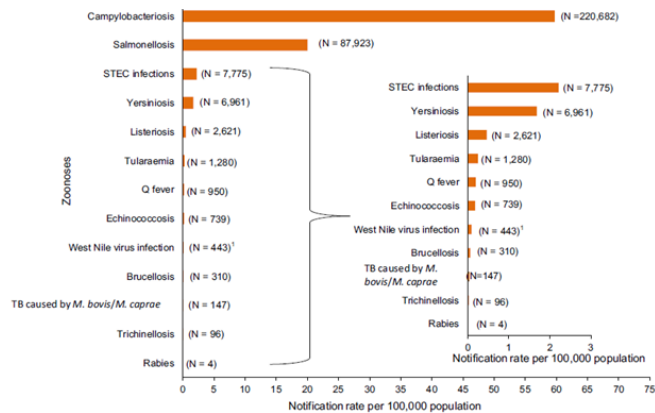


Fig. 3: Notification rates and reported numbers of confirmed human cases of zoonoses in the EU, 2019 (EFSA and ECDC, 2021).

Note: the total number of confirmed cases is indicated between parentheses at the end of each bar.

¹Exception: West Nile virus infection for which the total number of cases was used.

As reported, many significant problems in the food industry derive mainly by *Escherichia coli*, *Listeria monocytogenes*, *Salmonella* spp., *Shigella* spp., *Staphylococcus aureus*, *Vibrio cholerae*, *Yersinia enterocolitica*, *Campylobacter* and many others, which are among the principal spoilage microorganisms that could cause safety problem for consumers.

1.2.1.1 *Listeria monocytogenes*

Listeria monocytogenes (**Figure 4**) is an opportunistic Gram-positive bacterium and its widespread presence in the environment together with its ability to grow at low temperatures make it a pathogen of special concern. In industrialized countries, it is considered one of the main contaminants in the food chain and it can be found in smoked fish, raw meat, cheese, vegetables.

In fact, it is a psychrotrophic bacterium and therefore, the refrigeration of food can slow down its multiplication, but not completely inhibit it. Due to its remarkable resistance to conditions that are adverse for other bacteria, and thanks to its survival mechanisms, such as the formation of biofilms, *L. monocytogenes* can persist for a long time in food processing environments that can be sources of food contamination.

It can cause mild infections or severe invasive forms in human, mostly in pregnant women, kids, the elderly and immunocompromised patients, which may develop the disease, known as listeriosis, because of the consumption of

contaminated food, also with low levels of bacterial load [Palmieri, G. *et al.*, 2018]. Symptoms include fever, muscle aches, headache, stiff neck, confusion, loss of balance, and convulsions [Listeriosi - Relazione epidemiologica annuale 2017 (europa.eu)].

The number of cases of listeriosis confirmed in EU countries from 2013 to 2021 shows a statistically significant upward trend, and in 2022, more than 70 cases of listeriosis were recorded in Italy [*Listeria Monocytogenes* | Servizio di ispezione e sicurezza alimentare (usda.gov); Listeriosi - Relazione epidemiologica annuale 2017 (europa.eu)]



Fig. 4: Image of *Listeria monocytogenes* produced by microscope.

1.2.1.2 *Salmonella* spp.

Salmonella (**Figure 5**) is a genus of rod-shaped (bacillus) Gram-negative bacteria belonging to the family *Enterobacteriaceae*.

Salmonella species are non-spore-forming, facultative anaerobes and predominantly motile enterobacteria, able to obtain their energy from oxidation and reduction reactions,

Chapter II

using organic sources. *Salmonella* species are intracellular pathogens, of which certain serotypes cause illness, such as typhoid fever that can lead to life-threatening hypovolemic shock and septic shock. Most infections are due to ingestion of food contaminated by both animal or by human feces. [Goldrick, B., 2003]

This microorganism is mostly associated with animals and birds and it is only present on vegetables through cross-contamination. The majority of *Salmonella* species are mesophilic bacteria, but many isolates are able to survive well during storage at 5 °C. According to the Istituto Superiore di Sanità (ISS) in 2021, *salmonellosis* was confirmed as the most frequently reported zoonotic disease with more than 2600 cases.

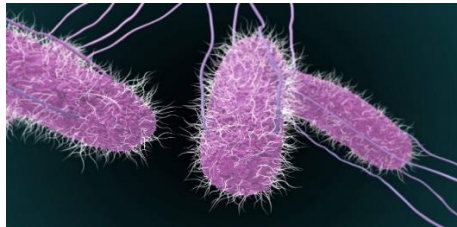


Fig. 5: Image of *Salmonella* produced by microscope.

1.2.1.3 *Staphylococcus aureus*

Staphylococcus aureus (**Figure 6**) is a Gram-positive spherically shaped bacterium and it is a usual member of the microbiota of the human body. It is a facultative anaerobe that can grow in the absence of oxygen [Masalha, M. *et al.*, 2001]

Chapter II

but does not grow well under chill conditions. Although *S. aureus* usually acts as a commensal of the human microbiota, it can also become an opportunistic pathogen, causing skin infections, respiratory infections and food poisoning. Moreover, this microorganism can be transmitted to food via meat grinder knives and food handlers [Arun, K., 2018] but it can be also transmitted by the consumption of creamy foods prepared with dairy products. Finally, *S. aureus* has been found on fresh products and ready-to-eat vegetable salads, shellfish, fish, meats and hams.

The food poisoning caused by *S. aureus* is one of the most reported foodborne illnesses worldwide. Indeed, *S. aureus* have caused nearly one-third of all food poisoning cases recorded during the 1970s and 1980s in the United States, even if a marked decrease over the past two decades was recorded. Moreover, *S. aureus* is one of the leading pathogens for deaths associated with antimicrobial resistance and the emergence of antibiotic-resistant strains, such as methicillin-resistant *S. aureus* (MRSA), represents a worldwide problem in clinical medicine. Unfortunately, vaccine development efforts against *S. aureus* have failed so far.

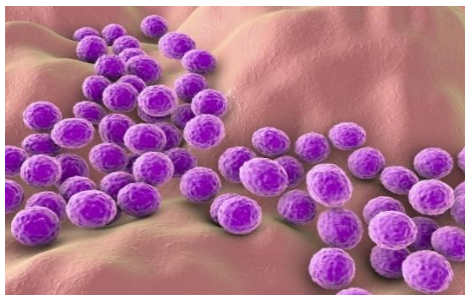


Fig. 6: Image of *Staphylococcus aureus* produced by microscope.

1.2.1.4 Escherichia coli

Another important cause of morbidity and mortality worldwide is ascribable to the pathogenic variants of *Escherichia coli* (**Figure 7**). This is a Gram-negative rod-shaped bacterium which may or may not be motile depending on whether it has a flagellum or not. Most strains of *E. coli* are non-pathogenic and only a small subset have pathogenic characteristics that make them responsible for a variety of diseases. In recent years, an increasing number of foodborne outbreaks caused by pathogenic *E. coli* have been observed in industrialized countries, mainly due to the consumption of contaminated meat, fruit and vegetables. The spread of this bacterium in the environment occurs through faecal material, which through the contamination of drinking water, irrigation water and soil, can contaminate fresh fruit and vegetables. Some *E. coli* pathotypes such as *E. enterohemorrhagic coli* (EHEC) can be transferred through meat (especially ground

Chapter II

beef), but some outbreaks have been associated with dairy products, mayonnaise, apple cider, sprouts, lettuce, and spinach. EHEC is a subset of *E. coli* capable of producing *Shiga* toxin (STEC). The natural reservoir of STEC is represented by cattle, but these bacteria have also been isolated from the faeces of chickens, goats, sheep, pigs, dogs, cats and seagulls [Arun, K. 2018].



Fig. 7: Image of *Escherichia coli* produced by microscope.

1.2.1.5 *Campylobacter* spp.

Campylobacter spp. (**Figure 8**) are small spiral-shaped Gram-negative bacteria and they are microaerophiles. Human pathogenic species are classified as thermophilic *Campylobacter*, having a narrow temperature range for growth, ranging from a minimum of 30 °C to a maximum of about 46 °C [Humphrey, T. *et al.*, 2007]. Even if mammals and birds are considered the main reservoirs of *Campylobacter*, this microorganism can also infect rabbits, sheep, horses, cows, pigs, poultry and even domestic animals,

Chapter II

constituting the cause of 80% of all cases of human campylobacteriosis. In addition to the meat products, also the intake of vegetables, shellfish and contaminated water has been associated with *Campylobacter's* poisoning. Worldwide, the emergence of antibiotic resistance in *Campylobacter*, especially in the two most representative species (*C. jejuni* and *C. coli*) is causing great concern [Arun, K. 2018].

According to the WHO, approximately 1% of the population of Western Europe is infected each year with *Campylobacter jejuni*, which is one of the most common bacterial enteric pathogen associated with diarrhea and enterocolitis, belonging to the family of *Campylobacteriaceae*,



Fig. 8: Image of *Campylobacter* produced by microscope.

1.2.1.6 Yeasts and moulds

Yeasts and moulds are organisms belonging to the kingdom of mushrooms and they are widely spread in nature. Their presence is also known in food, in which they can provoke spoilage. Yeasts are unicellular eukaryotic microfungi of

Chapter II

which about 1000 species are known and they can have both beneficial, such as in fermentation processes, or harmful effects causing food spoilage.

Yeasts (**Figure 9 A**) are able to infect many types of foods and, generally the factors influencing microbial growth are pH and water activity. For instance, the high concentration of sugars and the acidic pH, together with the high-water activity, make the fruits ideal substrates for the growth of yeasts. The vegetables are in contact with the soil and, so, they are an easy target of infections during production [Sathe, S. J. *et al.*, 2007]. Moreover, yeasts contamination, especially by *Candida* spp., can also affect dairy products such as yogurt, butter and cheese. Specifically, the milk is a perfect substrate, and yeasts thrive without any competition from bacteria, growing to 10^8 - 10^9 CFU/mL [Roostita, R., and Fleet, G. H., 1996]. Further food spoilage of fungal origin is caused by moulds (**Figure 9 B**), multicellular microorganisms that are able to grow and survive on a wide variety of products and in conditions that would be prohibitive for any other life forms, such as acidity, dry conditions and low temperatures. They can have both beneficial and detrimental effects depending on the type of mould, growing medium and environmental conditions [Gourama, H., *et al.*, 2015]. Generally, the moulds affect plant products and they can also represent a risk factor for human health by triggering allergic reactions or in even more serious cases carcinogenesis, teratogenesis, skin

Chapter II

irritation, neurotoxicity or death, due to the effect of their mycotoxins.

The main moulds known for the production of mycotoxins are *Aspergillus*, *Penicillium* and *Fusarium* [Arun, K., 2018].

Specifically, the major producer of aflatoxins is *Aspergillus flavus* and it is responsible for the spoilage of various products (fruit and vegetables, spices, cereals, bread, walnuts, peanuts, almonds and pistachios), influencing also the chains of food and feed supplies, including crop producers, animal producers and consumers. About 25 - 50% of food products, especially those based on grains and nuts, are presumed to be contaminated with mycotoxins, which can lead to toxic effects to human health, resulting in a reduced yields and a lower profit and to damages to animal health that can take contaminated feed and to humans.

In fact, according to the FAO, 25% of the world's crops are contaminated by moulds every year, causing losses reaching around 1 billion cans of food.

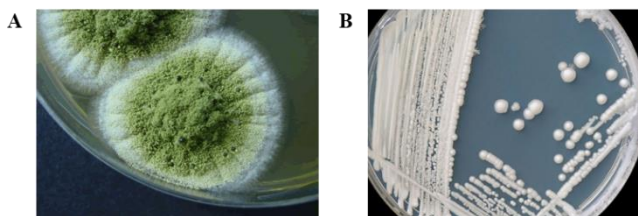


Fig. 9: Representative plates of the (A) mould *Aspergillus Flavus* and (B) yeast *Candida*.

1.3 Food preservation

All foods, both vegetable or animal origin, consist mainly of water, proteins, lipids, carbohydrates and minerals and they can undergo a process of deterioration caused both by microbial agents and by chemical or physical substances [Rahman, T. *et al.*, 2012].

Several foods are a suitable substrate for bacterial replication, especially high perishable ones such as fish and fishery products, dairy products, and meat and derivate products. Therefore, food preservation, which aims to preserve their quality, and extend their shelf-life, is becoming more and more important.

Specifically, food preservation includes several procedures or techniques, able to control internal and external factors responsible of foods alteration.

Conventional techniques including drying, freezing, refrigeration, pasteurization and chemical preservation are used all over the world today. Moreover, another strategy used to preserve and hinder the growth of harmful microorganisms in food products, involves the addition of several substances such as nitrites and nitrates. Specifically, they are added in meat and its derivate products (cured meats and sausages) to preserve their integrity, maintain their color and improve their taste. These substances play a major role in inhibiting the growth of foodborne pathogens, including *Clostridium botulinum* (*C. botulinum*), the bacterium responsible for botulism.

Nevertheless, these substances contained in food can be rapidly absorbed by the body. Part of them is excreted as nitrates, but

another part is recirculated by the salivary glands and partially converted into nitrites by the bacteria present in the oral cavity. Excessive amounts of nitrites can provoke toxic effects, such as the oxidation of haemoglobin into methaemoglobin, resulting in a reduced ability of red blood cells to bind and transport oxygen in the body. Moreover, another consequence may also be the formation of nitrosamines in the stomach, recognized as potent carcinogens.

The Acceptable Daily Intakes (ADI) for nitrite, established by the European Commission's Scientific Committee for Food (SCF) (in 1997) and the Joint FAO-WHO Committee on Food Additives (JECFA) in 2002, are respectively 0.06 and 0.07 milligrams per kilogram of body weight per day (mg/kg bw/day), while both institutions set the ADI at 3.7 mg/kg bw/day for nitrate.

In this scenario, scientific progress is making a great contribution to the evolution of existing technologies and to the development of new ones to render conservation procedures increasingly efficient, without producing toxic effects for human health.

1.3.1 Active packaging

One of the primary purposes of food packaging, is to protect food from unintentional contamination and undesirable chemical reactions, preserving the food integrity and allowing a safely consume, as well as to provide a physical protection.

However, the need to develop new cutting-edge technologies has revolutionized the packaging idea, introducing an innovative concept: the active packaging.

This can be defined as the result of the interaction between packaging, product and environment, in order to extend the food shelf-life, to increase its safety or improve its sensory properties, without affecting its quality.

1.3.1.1 Antimicrobial packaging

Among the different kinds of active food-packages (**Figure 10**), antimicrobial packaging is one of the most promising innovations of packaging techniques [Floros, J.D. *et al.*, 1997], aiming to provide fresher, safer, and higher quality food products, concerning foodborne pathogenic and spoilage microorganisms, resulting in an increase of their shelf-life. [Han, J.H., 2000].

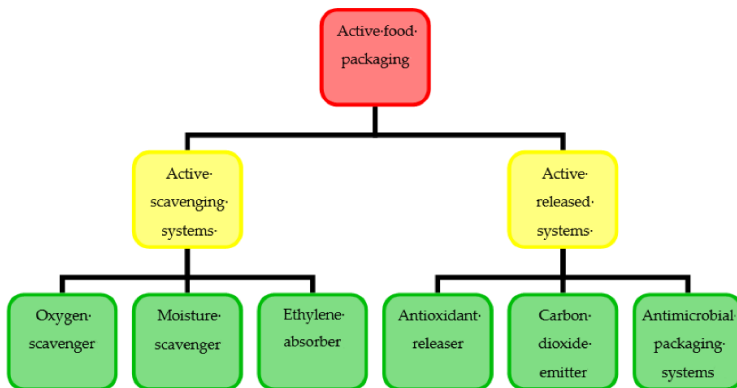


Fig. 10: Classification of active packages

Chapter II

Antimicrobial packaging can take several forms including incorporation of antimicrobial agents directly into polymers, coating or adsorbing antimicrobials onto polymer surfaces, immobilization of antimicrobials to polymers by ion or covalent linkages or use of polymers that are inherently antimicrobial (**Figure 11**) [Weng, Y. *et al.*, 1999]

The research on antimicrobial packaging generally started with the development of antimicrobial packaging materials containing chemicals in their macromolecular structures.

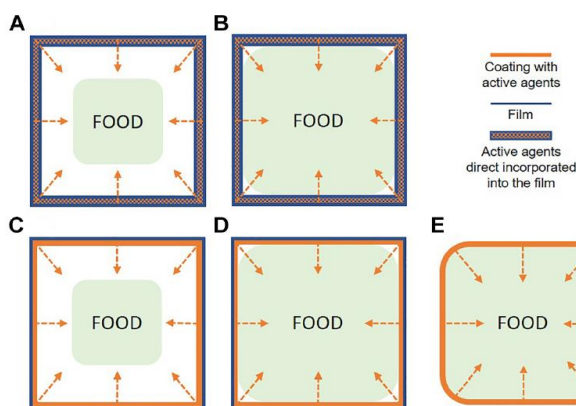


Fig. 11: Different strategies of incorporation to the polymeric film and mode of release of antimicrobial agents in foods: (A) inclusion of the bioactive molecule in the polymer before extrusion and release from the material with gradual diffusion from the material into the headspace; **(B)** incorporation into the plastic film prior to extrusion and gradual diffusion from the material into the food by direct contact; **(C)** surface coating on the film and release into the headspace by gradual diffusion; **(D)** surface coating on the

Chapter II

film and gradual diffusion from the material into the food by direct contact; **(E)** edible film and gradual diffusion from the material into the food by direct contact.

Nevertheless, the use of some chemical preservatives may cause adverse effects on human health and on the nutrition level of food. Moreover, it was observed that an excessive use of chemical preservatives, induces resistance phenomena in bacteria. Consequently, consumers require food with fewer chemical preservatives and minimal processing. Hence, there is a pressing need to search new natural molecules for the preservation of food and to solve food contamination in industries. About that, a new approach is to use antimicrobial peptides (AMPs) for improving the quality and security foods, extending their shelf-life. They can also be used in the packaging system, as antimicrobials, bio-preservatives and anti-biofilm agents, thanks to their versatile characteristics. Many researchers pointed out that antimicrobial peptides demonstrated activity against several food-borne pathogens, and therefore, can help in the food preservation [Hintz, T. *et al.*, 2015;]. Even if nowadays there is a limited number of AMPs used as food preservatives, this approach represents a promising strategy in food industry to preserve the food without changing its quality and inducing harmful effects for human health.

1.4 Antimicrobial peptides

Antimicrobial peptides are a class of natural molecules produced as a first line of defence by a wide variety of organisms. AMPs are also known as Host Defense Peptides (HDPs) and represent integral and natural components of innate immune system, which is the first part of the body to detect invaders such as viruses, bacteria, parasites and toxins, or to sense wounds or trauma. The AMPs can be considered a skilled class of new antibiotics, due to their broad-spectrum and potent antimicrobial efficacy against Gram-negative and Gram-positive bacteria, fungi, viruses and protozoa [Guzmán-Rodríguez J.J. *et al.*, 2015; Agrillo, B. *et al.*, 2020]

In recent decades, growing interest in antimicrobial peptides for their applications as bactericidal agents in different fields has been observed and many efforts have been made to discover new AMPs with improved performances, i.e., high antimicrobial activity, low cytotoxicity against human cells, high stability against proteolytic degradation and low costs of production. Moreover, the increased bacterial resistance due to the uncontrolled use of antibiotics has raised significant concerns in medicine, encouraging research into novel molecules to replace or supplement conventional antibiotics against multidrug-resistant pathogenic microorganisms. It was observed that most AMPs are able to interact with the biological membranes, leading to pore formation that destroys the membrane integrity and causes cell deaths. Consequently, their non-specific mode of action significantly prevents resistance phenomena, as it

Chapter II

is metabolically costly for most microbes to mutate or repair membrane component [Agrillo, B. *et al.*, 2020].

A total of 3,257 AMPs has been reported in the Antimicrobial Peptide Database (APD3) updated on October 26, 2022.

1.4.1 Classification

Plant and animal antimicrobial peptides are typically composed of 10 -50 amino acid residues and, generally, they have a cationic character due to the abundance in cationic residues like lysine, arginine and histidine in their sequences [Hancock, R. E. W. and Scott, M. G., 2000].

Generally, AMPs are classified based on source, activity, structural characteristics and amino acid-rich species (**Figure 12**) [Huan, Y., *et al.*, 2020].

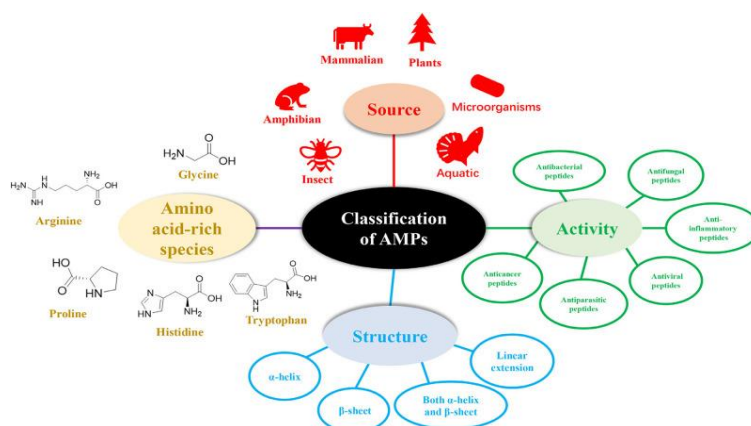


Fig. 12: Classification of AMPs

Chapter II

- *Classification based on sources*

The sources of AMPs can be divided into mammals (human host defence peptides account for a large proportion), amphibians, microorganisms, plants and insects.

The mammalian AMPs are found in humans, sheep, cattle, and other vertebrates. Cathelicidins and defensins are the main families of AMPs. In addition to antimicrobial activity, cathelicidins and defensins, also affect immune regulation, apoptosis, and wound healing [Huan, Y., *et al.*, 2020].

The amphibians AMPs are produced mainly by frogs and the most famous is magainin. AMPs are mainly synthesized in fat bodies and blood cells of insects, which is one of the main reasons for insects' strong adaptability to survival.

AMPs can be obtained from microorganisms like bacteria and fungi, and some well-known peptides are nisin and gramicidin from *Lactococcus lactis*, *Bacillus subtilis*, and *Bacillus brevis* [Huan, Y., *et al.*, 2020].

- *Classification based on activity*

The activity of AMPs can be divided into 18 categories that can be summarized as antibacterial, antiviral, antifungal, antiparasitic, anti-human immunodeficiency virus (HIV), and anti-tumor peptides [Huan, Y., *et al.*, 2020]. In this context, antibacterial peptides account for a large part of AMPs and have a broad inhibitory effect on common Gram-positive and Gram-negative

pathogenic bacteria, such as *S. aureus*, *Listeria monocytogenes*, *Salmonella* and *E. coli*.

- *Classification based on Amino Acid-Rich Species*

Proline-Rich Peptides (PrAMPs): proline is a typical non-polar amino acid. PrAMPs behave differently from other AMPs, as they enter bacterial cytoplasm by an inner membrane transporter instead of killing bacteria through membrane destruction. They mainly kill Gram-positive bacteria. Besides, some researches have shown that PrAMPs have immunostimulation activity [Huan, Y., *et al.*, 2020].

Tryptophan and Arginine-Rich Antimicrobial Peptides: Tryptophan, as a non-polar amino acid, has a remarkable effect on the interface region of the lipid bilayer, whereas the basic amino acid Arginine, confers peptide charge and hydrogen bond interactions, which are essential properties to combine with the bacterial membrane's abundant anionic component [Huan, Y., *et al.*, 2020].

Histidine-Rich Peptides: Histidine is a common basic amino acid, and histidine-rich AMPs show good membrane permeation activity [Huan, Y., *et al.*, 2020].

Glycine-Rich Antimicrobial Peptides: The R group of glycine is generally classified as a non-polar amino acid in biology. The presence of these residues has an important effect on the tertiary structure of the peptide chain [Huan, Y., *et al.*, 2020].

- *Classification based on structure characteristics*

The structural organization/arrangement of antimicrobial molecules is crucial to understanding their mechanisms of action and the way they interact with biological targets. AMPs can be divided into four categories according to their secondary structure (**Figure 13**) [Huan, Y., *et al.*, 2020].

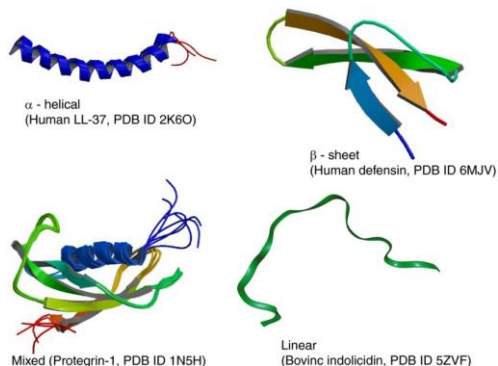


Fig. 13: Different structures of AMPs.

α -helix conformation: One of the largest and best-studied classes of AMPs is composed of cationic peptides with amphipathic α -helix conformation [Huan, Y., *et al.*, 2020]. However, there are also anionic α -helix peptides with hydrophobic properties, but these have shown to have less selectivity towards microorganisms than mammalian cells. In the α -helix conformation, each amino acid residue has a rotation of about 100° in the helical structure (the helix has 3.6 residues per revolution) and a translation of 1.5

Chapter II

Å (0.15 nm) along the helix axis [Bahar, A.A. and Ren, D., 2013]. The presence of α -helix motives is a key factor that promotes peptide interactions with target membranes and allows subsequent rupture. Therefore, when the α -helix structure is interrupted by substitution of amino acids, the antibacterial activity decreases significantly [Tossi, A. *et al.*, 1994]. In addition, the amphipathic conformation of the α -helix structure, in which the cationic and hydrophobic domains are arranged on opposite sides of the helix, represents an additional property that facilitates interaction between AMPs and cell membranes. Although the helical structure significantly affects antimicrobial potency of these peptides, it is also associated with hemolytic activity and toxicity to mammalian cells [Chen, Y. *et al.*, 2005; Zhu, X. *et al.*, 2015]. One of the most studied amphipathic helical cationic peptides is magainin, a peptide of 23 amino acids isolated from the epidermis of the African clawed frog, *Xenopus laevis*, which shows antimicrobial activity towards various microorganisms (Gram-positive and Gram-negative bacteria, fungi and protozoa) [Zaslhoff, M., 1987].

β -sheet conformation: This class of AMPs consist of at least one pair of two β strands arranged side by side and connected to each other through different hydrogen bonds and/or disulfide bonds [Huan, Y., *et al.*, 2020]. The presence of disulfide bridges is necessary for the stabilization of the structure. Because β -leaflet AMPs have a more stable structure, they do not undergo essential

conformational changes when interacting with phospholipid membranes. Leaflet- β AMPs include β -hairpin peptides and cyclic α -, β - and θ -defensins. β -hairpin antimicrobial peptides are characterized by antiparallel β leaflets that constitute a hairpin form stabilized by interstrand disulfide bridges [Edward, I.A. *et al.*, 2016]. Defensins represent one of the best-described groups of AMPs with a broad spectrum of antimicrobial activity against bacteria, fungi and viruses [Huan, Y., *et al.*, 2020].

Mixed α -helix/ β -sheet structure: this structure is stabilized by three or four disulphide bridges. Specifically, this cysteine (CS $\alpha\beta$)-stabilized α/β structural motif, which is composed of a single α -helix and a β -sheet consisting of two or three antiparallel strands, was first recognized in defensins and neurotoxins from insects. [Bontems, F. *et al.*, 1991; Zhu, S. and Gao, B., 2005]. CS $\alpha\beta$ -containing defensins are commonly found in plants and insects and have mainly shown antimicrobial activity against fungi and bacteria, respectively [De Oliveira D., R. and Franco, O.L., 2015].

Cyclic peptides: this class has been widely studied only in recent decades. The cyclization process is responsible for a strengthening of fundamental characteristics for such molecules as effectiveness, specificity and safety. From the conformational point of view, the cyclization reduces alternative conformations and non-specific bonds, making the peptide chain more stable and then, increasing

the specificity and the binding affinity with the target protein [Sohrabi, C., *et al.*, 2020].

Moreover, the reduced conformational flexibility causes an improvement in terms of resistance to the action of proteases, as it reduces the possibility of insertion into the catalytic site of these enzymes [Craik D. J., 2006]. Finally, cyclization also increases the effectiveness of peptide chains as it generates a larger area of protein-protein interaction [Angelini, A. *et al.*, 2012]. In addition, cyclization improves not only the structural properties of peptide chains, but also the pharmacokinetic properties for the absorption and permeability of the biological membrane, necessary to reach protein targets [Apostolopoulos, V. *et al.*, 2021 Bockus A. T. *et al.*, 2013].

1.4.2 Mechanism of action

AMPs exhibit several structural characteristics that are essential for their activity. First, most AMPs show a right balance of positive charge and hydrophobicity to interact with and penetrate bacterial membranes. Indeed, the net positive charge enables electrostatic attractions between AMPs and the negatively charged bacterial membranes. At the same time, the hydrophobicity of AMPs allows them to penetrate cells, inducing membrane lysis [Falcigno, L. *et al.*, 2021].

The negatively charged lipids, such as phosphatidylglycerol (PG), cardiolipin (CL), and the zwitterionic phosphatidylethanolamine (PE), are the main components of the bacterial cell membranes.

Chapter II

Gram-negative bacteria contain lipopolysaccharides (LPS) on their outer membrane, while the cell wall of Gram-positive bacteria is enriched in teichoic and teichuronic acids [Isabel, M. *et al.*, 2017].

Those molecules that confer a negative charge to the bacterial surface were selected as targets for cationic AMPs. Phosphatidylglycerol and cardiolipin are among the main responsible for the selectivity with which the bacterial membrane responds to specific peptide sequences, an effect that does not occur on eukaryotic cells in which lipids without charge prevail [Huan, Y., *et al.*, 2020].

Instead, Phosphatidylcholine (PC), phosphatidylinositol (PI), phosphatidylethanolamine, and phosphatidic acid (PA) are the main glycerophospholipids in fungal cell membranes [Ejising, C.S. *et al.*, 2009; Singh, A. and Prasad, S.M., 2011] which are more anionic than mammalian cell membranes and have higher PC content [Huan, Y., *et al.*, 2020].

The mechanisms by which AMPs can traverse microbial membranes are not common to all peptides and seem to depend on the molecular properties of peptide and lipid membrane composition. Several membrane defects can be induced by AMPs, among them we can highlight formation of pores, phase separation, and promotion of non-lamellar lipid structure or disruption of the membrane bilayer. Some models that may explain the membrane-targeting mechanisms of AMPs, have been proposed such as barrel-stave, toroidal, and carpet models.

Chapter II

Barrel-stave model: In this model, AMP binds to the membrane surface as a monomer, followed by their oligomerization and pore formation [Ehrenstein, G. and Lecar, H., 1977]. The recruitment of additional monomers can increase the pore size, allowing cytoplasmic content leaking with subsequent cell death. In this mechanism, peptide secondary structures, such as hydrophobic α -helix and/or β -sheet, are essential to pore formation [Breukink, E. and de Kruijff, B., 1999]. Indeed, these regions interact with the membrane lipids, while the hydrophilic portions form the lumen of the channel (**Figure 14**). [Broden, 2005].

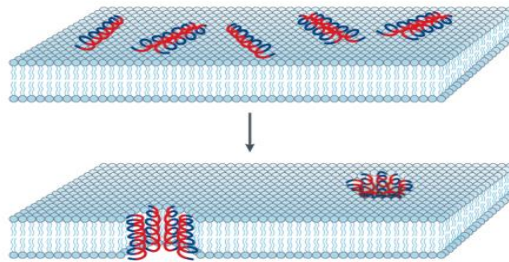


Fig. 14: Schematic representation of the "barrel-stave" model.

Hydrophilic and hydrophobic portions of peptides are represented in blue and red respectively.

Toroidal model: it involves an interaction of the hydrophilic portion of peptide molecules with the polar portion of phospholipids of the bacterial membrane. Subsequently, when peptides meet the hydrophobic component of membrane

Chapter II

phospholipids, they undergo a conformational change and helical structures are formed. In the initial phase, the helices remain parallel to the bacterial membrane, but when the concentration of the peptides reaches a certain threshold value, membrane-bound AMPs reorient and penetrate or insert into the hydrophobic core of bilayer with the formation of transmembrane pores. After the development of sufficient stress by antimicrobial peptides, a thinning and destabilization of the membrane occurs, resulting in its rupture (**Figure 15**) [Yeaman, M.R. and Yount, N.Y., 2003].

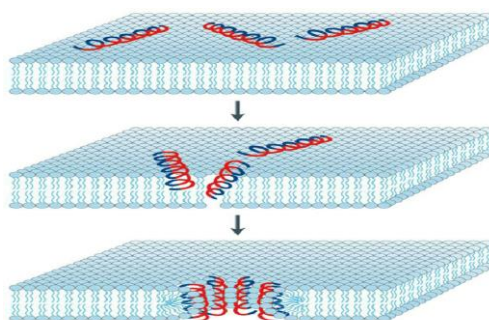


Fig. 15: Schematic representation of the "toroidal" model. The hydrophilic and hydrophobic portions of the peptide molecules are represented in blue and red respectively.

Carpet model: AMPs cover the membrane surface affecting its architecture. Their interaction is first driven by electrical attraction and, when the number of AMPs on the membrane surface reaches a threshold concentration, the membrane disintegrates, leading to

Chapter II

cell lysis and subsequent formation of micelles with a hydrophobic nucleus (**Figure 16**) [Oren, Z. and Shai, Y., 1998].

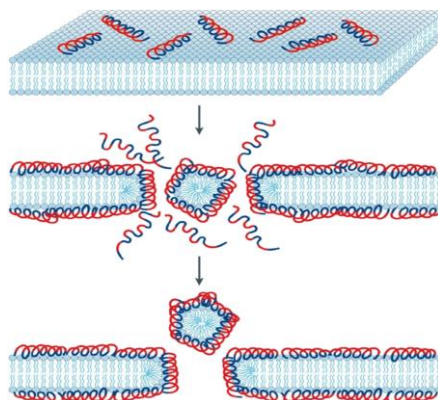


Figure 16: Schematic representation of the "carpet" model.

The hydrophilic and hydrophobic portions of the peptide molecules are represented in blue and red respectively.

Although most AMPs interact directly with cell membrane lipids, it was reported that some peptides might require a bacterial receptor [Casteels, P. and Tempst, P., 1994; Bulet, P. *et al.*, 1996]. Furthermore, it has already been shown that several AMPs have intracellular targets and exert their effects by inhibiting processes such as protein and cell wall synthesis. Among these, the proline-rich peptides have shown intracellular activity by inhibiting bacterial protein synthesis as they interact with the ribosome and inhibit translation, causing a block between the initiation and the elongation phase (**Figure 17**).

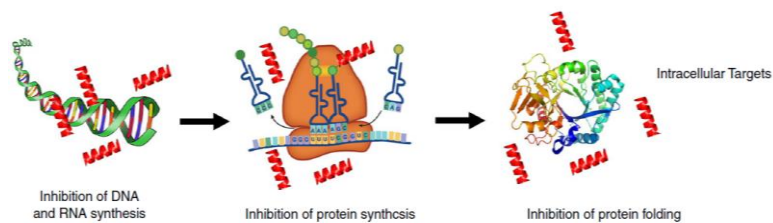


Fig. 17: Representative scheme of AMPs action mechanisms involving interaction with intracellular targets.

Another known mechanism is that PrAMPs act at the level of chaperone proteins, which guide the proper folding and assembly of newly synthesized proteins. They appear to be able to block protein folding [Gagnon, M.G. *et al.*, 2016; Mardirossian, M., *et al.*, 2018].

Due to the complexity of peptide-membrane interaction, the hydrophilicity/hydrophobicity properties must be finely balanced to optimize the activity and selectivity of AMPs avoiding cytotoxicity. In this regard, the conformational features of AMPs play a key role.

Peptides show different conformations and aggregations states in free or in membrane-bound form. Such items deeply influence the efficacy and selectivity of AMPs and it has been pointed out that the antibacterial activity of some of them is greatly attenuated by certain physical parameters such as pH, high salt, and high temperature.

1.4.3 AMPs applications and future perspectives

Since AMPs are small bioactive molecules enough versatile, produced both naturally and synthetically, they find application in different fields such as food industry, agriculture, and medicine.

Among AMPs widely used in food industry, there is nisin, that is the only bacteriocin legally approved as biopreservative in the dairy industry to control contamination from *Listeria* strains [Soltani, S. *et al.*, 2021].

In recent years, several strategies have been developed to produce innovative active packaging based on AMPs to deliver safer and high-quality food products.

Many studies conducted on the AMPs functions have suggested that AMPs play many roles in all stages of the plant life cycle, but especially antimicrobial role [Stotz H.U. *et al.*, 2009; Marshall, E. *et al.*, 2011]. For this reason, in the few last decades, AMPs are using in agriculture in order to cope with plant diseases and insect pests and to improve crop yields, in substitution to several chemical pesticides, which cause the harm effects on humans and animals.

In recent years, the alarming development and rapid spread of antibiotic resistance among pathogenic microbes has emerged as the major cause of the reduced effectiveness of antimicrobial therapies, thereby representing a huge challenge for modern medicine and a very large public health threat. According to WHO (World Health Organization), without urgent action, we are

heading for a post-antibiotic era, in which common infections and minor injuries can once again kill. In order to cope this phenomenon, AMPs are used on the basis of their antimicrobial properties, their safety and their ability to prevent the multidrug resistance phenomena.

Despite the useful and numerous applications in several fields of AMPs, until now, some AMPs have failed in clinical trials because of several drawbacks that strongly limit their applicability, such as proteolytic degradation and cytotoxicity. To overcome the limitations of native peptides, *in silico* tools have recently become an inevitable approach for the design and optimization of new AMPs with the desired characteristics. The rational design of antibacterial peptides should focus on the following aspects: chain length, secondary structure, net charge, hydrophobicity, and amphiphilicity. There are several specific methods for the AMPs designing, such as Site-Direct Mutation, which redesigns existing natural antimicrobial peptides by adding, deleting or replacing one or more amino acid residues, and *de novo* design, that projects molecules with predetermined structures and desired functions.

2. RESULTS OF THE RESEARCH GROUP

Antimicrobial peptides (AMPs) have received great attention for their potential benefits in the food industry sector, considering the strong impact of foodborne diseases on human health and the growing consumer's attention on the use of chemical agents.

Chapter II

In this context, my thesis work is integrated into an extensive and ongoing project developed by the research group led by Dr. G. Palmieri and focused on the design and functional/structural characterization of new antimicrobial peptides aimed at increasing the safety and extending the shelf-life of food products. The first peptide projected by the research group, was identified starting from the innate defense regulator 1018 (IDR-1018), a synthetic 12-amino acid (VRLIVAVRIWRR-NH₂) derivative of bactenecin. This compound is a well-known broad-spectrum antibiofilm peptide that acts by binding to the intracellular alarmone nucleotides (p)ppGpp [de la Fuente-Núñez *et al.*, 2012, 2014a; Reffuveille, F. *et al.*, 2014].

Specifically, by using an optimized *in silico* strategy, a panel of a single amino acid mutations were projected starting from the IDR-1018 sequence and the resulting peptides were functional characterized. Among all compounds, the peptide named IDR-1018K6, in which the alanine in position 6 was replaced with a lysine (A6 → K6 mutation) was chosen for further analyses. Indeed, the K residue substitution increases the positive charge, which is considered one of the most critical factors for improving the potential interaction of antimicrobial agents with the outer membrane of bacteria. Characterization studies of 1018-K6, conducted by using CD and fluorescence spectroscopy techniques, demonstrated a faster folding kinetic and an improved structural stability under different environmental conditions, compared to its progenitor IDR-1018. Moreover, 1018-K6 evidenced a significant antibiofilm/bactericidal efficiency towards Gram-Positive and Gram-Negative pathogens and specifically against *Listeria monocytogenes*

Chapter II

strains isolated from food-products and food processing environments, representing an excellent candidate for the development of alternative disinfection strategies in the food industry [Palmieri, G. *et al.*, 2018]. Moreover, preliminary studies on peptide functionalization of packaging materials and nanoparticles were also performed [Agrillo, B. *et al.*, 2019; [Palmieri, G. *et al.*, 2018], revealing the ability of 1018-K6 to preserve its excellent antimicrobial and anti-biofilm activity upon surface immobilization.

In order to identify a new generation of AMPs with high efficacy at lower dosages, few side effects, and, low production costs, a set of second generation of ten-amino acids short peptides was generated starting from the 1018-K6 sequence. Firstly, the removal of two residues and the subsequence single point substitutions were planned in the N-terminal region of 1018-K6 sequence, as it was reported that the substitution of any residues at the positions Val7 (V)-Arg12 (R) in the parent peptide (NH₂-VRLIVKVRIWRR-CONH₂) substantially reduced the antimicrobial activity and were mostly not favorable [Haney, E.F. *et al.*, 2018; Kalafatovic, D. *et al.*, 2017;]. To this aim, the following criteria were adopted: I) deletion of a Val residue, as the analysis of amino acid frequency in the AMPs available at Collection of Anti-Microbial Peptides (CAMP) database revealed that this amino acid was less often encountered [Suryawanshi, S.K. *et al.*, 2016]; II) deletion of a further neutral amino acid between Iso (I) or Leu (L) to conserve unaltered the net positive charge, since this aspect is essential for the interactions with the negatively charged membranes of bacteria; III) replacement of one neutral amino acid with Trp (W) residue to

Chapter II

enhance the total Trp ratio and the hydrophobicity, which represent key physicochemical parameters influencing the ability of several AMPs to adopt an amphipathic conformation upon binding to the bacterial membrane [Bi, X. *et al.*, 2014; Spohn, R. *et al.*, 2019]; IV) conservation of at least an Arg (R) residue, as it has been observed that this amino acid strongly improves the antibacterial activity, due to its enhanced membrane permeability with respect to Lys (K) [Yang, C. *et al.*, 2018]. Therefore, the following web server and software were used for determining the main peptide features such as the reliability, stability, half-life *in vivo*, and all the relevant physicochemical properties that are necessary to explicate the antimicrobial activity (Boman index, total net charge, GRAVY index, hydrophobicity, amphipathicity, hydrophobicity, aliphatic index, and instability index): PlifePred (PPred) [Mathur, D. *et al.*, 2018], PEPLife [Mathur, D. *et al.*, 2016], Antimicrobial Peptide Database3 (APD3) [Wang, G. *et al.*, 2016], and (CAMP) [Waghu, F.H. *et al.*, 2016].

Based on these *in silico* analyses, a new 10-mer peptide, named RiLK1, showing the same net cationic charge (+ 5) but higher half-life, hydrophobicity, total Trp ratio, amphipathicity, hydrophobicity, and Boman index, with respect to the parent 1018-K6, was selected for further biophysical examinations as well as *in vitro* antimicrobial tests (**Table 1**).

This background provided the context and purpose of the second part (Chapter II) of my thesis project focused on further studies on these peptides.

Chapter II

Table 1: List of the physicochemical properties calculated and predicted for the designed peptide RiLK1 in comparison with those of the parent AMP 1018-K6.

PARAMETERS	RiLK1 RLKW VRIWRR ^a	1018 K6VRLIVK VRIWRR
<i>Mol weight (Da)</i>	1468.96	1594.02
<i>Boman Index (kcal/mol)</i>	4.70	3.00
<i>Total net charge</i>	+5	+5
<i>Half-life (sec)</i>	855.71	835.61
<i>Hydrophobicity</i>	-0.56	-0.35
<i>Hydrophaticity</i>	-1.12	0.22
<i>Amphipathicity</i>	1.35	1.12
<i>Hydrophilicity</i>	0.31	0.14
<i>Total Trp ratio (%)</i>	20	8

The conserved amino acid residues of the parent peptide 1018-K6 are highlighted in red.

3. MATERIALS AND METHODS

3.1 ANTIMICROBIAL PEPTIDE 1018K6

3.1.1 Production of 1018K6

The peptide 1018K6 (VRLIVKVRIWRR-NH₂) was purchased from GenScript Biotech (Leiden, Netherlands). It was stored as a lyophilized powder at 20 °C. Analysis by mass spectrometry confirmed the identity of peptide.

3.1.2 *Atmospheric Plasma Treatment and 1018K6 Immobilization on Polymer Surfaces*

Openair-Plasma® Technology was used as plasma treatment to modify the surfaces of commercial polypropylene (PP). They were cut into square-shaped pieces (4.0×4.0 cm dimension), which were cleaned with ethanol prior to use and then were placed on the plate at 3 cm to the nozzle. In all the treatments, air was used as the processing gas with a power of 440 watts and a speed of 10 mm/sec. The effect of plasma treatment on the polymer surfaces was evaluated by using the test Ink (Plasmatrete) to assess the wettability of the material.

The PP surfaces pre-activated by atmospheric plasma treatment were incubated into solutions (3 mL) of 1018K6 prepared in distilled water at three concentrations (50, 100 and 200 μM) for about 4 h at 70 °C to totally remove the water. After drying, the functionalized PPs were immersed in a volume of distilled water equal to that evaporated for 16 h at room temperature in agitation, then they were sonicated for 20 min and the recovered solutions analyzed by Reverse-Phase High-Performance Liquid Chromatography (RP-HPLC) to indirectly estimate the immobilization yield. For these analyses, 200 μL of the samples were injected on a $\mu\text{Bondapak C18}$ reverse-phase column (3.9 mm x 300 mm, Waters Corp., Milford, MA, USA) connected to a HPLC system (Shimadzu, Milan, Italy), using a linear gradient of 5%-95% 0.1% TFA (Trifluoroacetic acid) in acetonitrile, at a flow rate of 1 mL/min. A reference solution was prepared with the initial peptide

concentration used in the coupling reaction and was run in parallel. Therefore, by knowing the added peptide concentration (reference solution), the amount of peptide not covalently attached on the polymer surface was calculated by comparing the peak area and expressed as a percentage. A calibration curve of the C18 column using different 1018K6 concentrations was built. All measurements were performed in triplicate on three different preparations.

3.1.3 *1018K6 release test*

To determine the stability of the 1018K6 on the functionalized polymers, a release assay was performed by RP-HPLC using a linear gradient of 5–95% 0.1% TFA in acetonitrile, at a flow rate of 1 mL/min. A volume of 1 mL of pure water or NaCl 1 M was poured onto the functionalized polymers, which were incubated for 7 days at 4 °C, sonicated for 20 min and then the recovered solutions were loaded on RP-HPLC column. The solutions in contact with the functionalized polymers at time $t = 0$ were used as control samples and were run in parallel. All measurements were performed in triplicate on three different preparations.

3.1.4 *Sample preparation*

Raw salmon (*Salmo salar*, Linnaeus 1758) from different batches were freshly purchased from a local fishery industry (Naples, Italy). Specifically, two samples were prepared under aseptic conditions

from each fillet that was sliced into pieces of approximately 50 g. The samples were separated in two groups: the control group (CTR-PP), including salmon fillets packaged in pre-activated PPs films not-functionalized with 1018K6 and the treated group, including salmon fillets packaged in PPs films functionalized with 1018K6 (1018K6-PP). Both 1018K6-PPs and non-functionalized PPs squares (4x4 cm) were placed on Petri dishes (both lid and base) to ensure constant contact between the pieces of salmon and the PPs. Subsequently, the packaged samples were refrigerated at 4 ± 1 °C for 7 days. The microbiological, physico-chemical properties and quality aspects of samples were analyzed at days 0, 4, and 7. Fish burgers of Atlantic bonito (*Sarda sarda*, Bloch 1793) were bought from a fishing industry in Naples (Italy). A total of 21 burgers (200 g) were included in the experimental design. The samples were randomly divided into CTR-PP and 1018K6-PP groups and prepared as described above for the salmon samples. Once the fish burgers were packaged, the samples were stored at refrigeration temperature (4 ± 1 °C) and sampled at day 0, 3, 5 and 7 to carry out the same analyses as for salmon fillets.

The same analyses were performed also on fish samples packaged in PP films that were not subjected to any surface modification.

3.1.5 *pH and water activity measurements*

The pH measurements were conducted with a digital pH meter (Crison-Micro TT 2022, Crison Instruments, Barcelona). Water

activity (aw) was measured with Aqualab 4 TE (Decagon Devices Inc., USA).

3.1.6 Microbiological analyses

Ten grams of each sample were added to 90 mL (1:10 w/v) of sterilized Peptone Water (PW, Oxoid, Madrid, Spain) in a sterile stomacher bag to be homogenized for three minutes at 230 rpm using a peristaltic homogenizer (BagMixer®400 P, Interscience, Saint Nom, France). Ten-fold serial dilutions of each homogenate were prepared. In order to better describe the microbial profile of samples and follow the growth trend of each bacterium responsible for the food alteration, the viable counts of various microorganisms were carried out. Total aerobic bacterial counts (TAB), both mesophilic and psychophilic, were performed on Plate Count Agar (PCA, Oxoid, Madrid, Spain) incubated at 30 °C for 48/72 h and 7 °C for 10 days, respectively (ISO 4833-1:2013 and ISO 17410:2019); Total Coliforms on Violet Red Bile Lactose Agar (VRBL, Oxoid, Madrid, Spain) incubated at 37 °C for 48 h (ISO 4831:2006); *Enterobacteriaceae* on Violet Red Bile Glucose Agar (VRBG, Oxoid, Madrid, Spain) incubated at 37 °C for 48 h (ISO 21528-2:2017); Lactic Acid Bacteria (LAB) on MRS agar with Tween 80 (Oxoid, Madrid, Spain), incubated at 30 °C for 72 h (ISO 15214:2015); *Pseudomonas* spp. on Pseudomonas Agar Base with CFC supplement (Oxoid, Madrid, Spain) incubated at 25 °C for 48 h (ISO 13720:2010); β -glucuronidase-positive *Escherichia coli* (ISO 16649-1:2018) on Triptone Bile X-glucuronide Agar (TBX,

Oxoid, Madrid, Spain) at 44 °C for 24 h; *Brochothrix thermosphacta* on STAA (streptomycin thallos acetate actidione agar, Oxoid, Madrid, Spain) at 37 °C for 48 h; *Enterococcus faecalis* on KAA (Kanamycin Aesculin Azide, Oxoid, Madrid, Spain) at 37 °C for 48 h; coagulase positive *staphylococci* on Baird-Parker Agar (Oxoid, Madrid, Spain) at 37 °C for 24/48 h (ISO 6888-1:1999). After counting, the data were expressed as logarithms of the number of colony forming units (CFU/g) and means and standard error were calculated.

3.1.7 Challenge test

Four fillets of approximately 150 g and from different batches were used to evaluate the inter-batch variability. All of them were tested in agreement with the AFNOR-BRD 07/10-04/05-Real Time PCR method to evaluate the absence of *L. monocytogenes* contamination. Three strains of *L. monocytogenes* isolated from fish samples were selected, following ISO 11290-1, to perform these analyses and stored in the Zooprofilactic Experimental Institute of Mezzogiorno biobank. All strains were re-suspended in diluent at 0.5 Mcfarland concentration, then a series of 10 times gradient dilution of *L. monocytogenes* was performed until to reach a concentration of 150 CFU/ml. All fillets were contaminated at surface to mimic contamination during the slicing, using one fillet not contaminated as a control. After artificial contamination, the samples were packed between two functionalized films and stored at 5 °C until 96 h. The enumeration of *L. monocytogenes* was

performed according to Annex 1 of Reg (CE) 2073/2005 [Commission Regulation, 2015] at 24 h, 48 h, 72 h, and 96 h, in agreement with the reference methods EN ISO 11290-2.

3.1.8 Colourimetric analyses

Colourimetric measurements of the surface appearance of salmon fillets and bonito fish burgers were performed using a Konica Minolta CR 300 colourimeter (Minolta, Osaka, Japan). The data were analysed in the CIELAB colour space, organizing in three orthogonal axes in a Cartesian coordinate system: Lightness (L^*), redness (a^*) and yellowness (b^*). Additionally, the angular coordinates of Hue angle [$h_{ab} = \text{ArcTan}(b^*/a^*)$], and Chroma [$C_{ab} = (a^{*2} + b^{*2})^{1/2}$] were calculate. Total colour difference (ΔE), variation in a^* (Δa^*), and in b^* (Δb^*) were calculated as:

$$\Delta E = \sqrt{(L^*_1 - L^*_2)^2 + (a^*_1 - a^*_2)^2 + (b^*_1 - b^*_2)^2}$$

$$\Delta a^* = a^*_2 - a^*_1$$

$$\Delta b^* = b^*_2 - b^*_1$$

where L^*_2 , a^*_2 , and b^*_2 are the values recorded at a specific day during the storage; instead, L^*_1 , a^*_1 , and b^*_1 are values collected at day 0.

ΔE represents the result of changes in lightness (ΔL^*), redness (Δa^*), and yellowness (Δb^*), which do not always change in parallel. For this reason, Δa^* and Δb^* were considered. Since the

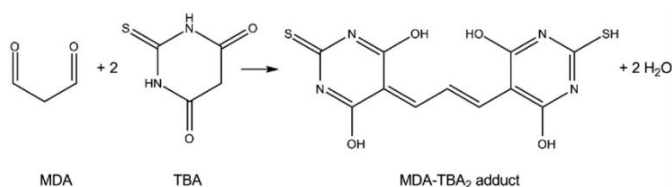
Chapter II

colour may not be homogeneous over the entire surface of fillets and burgers, five superficial measurements were performed for each sample to obtain representative results.

3.1.9 TBARS, Total volatile basic nitrogen and trimethylamine analyses

The TBARS assay (thiobarbituric acid reactive substance) involves the reaction of lipid peroxidation products, primarily malondialdehyde (MDA), with thiobarbituric acid (TBA) ($C_4H_4N_2O_2S$), leading to the formation of MDA-TBA₂ adducts called TBARS.

TBARS yields a red-pink color that can be measured spectrophotometrically at 532 nm.



Specifically, 10 g of fish samples were blended with 50 mL of distilled water in a Waring Blendor for 2 min and, then, the mixture was transferred quantitatively into a Kjehlahl flask by washing with an additional 47.5 mL of distilled water. Then, 2.5 mL of HCl solution were added to bring the pH to 1.5. A small amount of Dow antifoam A onto the lower neck of the flask was placed, and a few saddle stones to prevent bumping was added. Apparatus and heat

Chapter II

flasks at the highest heat obtainable on the Kjeldahl distillation apparatus were assembled. Approximately 10 min from the moment boiling begins were required to collect 50 mL of the distillate. The distillate was mixed, pipetting 5 mL into a 50 mL glass-stoppered tube, and 5 mL of TBA reagent were added. The tubes were stoppered and the mixed contents was immersed in a boiling water bath for 35 min. A distilled water-TBA reagent blank should be prepared and treated like the samples. After heating, cooling in tap water for 10 min was needed and, then, a portion was transferred into a cuvette and the optical density of the sample against the blank at a wavelength of 538 nm was read (A Jasco 640-V spectrophotometer was used).

Calibration curve was constructed using MDA at known concentrations as standard protein.

The Total volatile basic nitrogen (TVB-N) and trimethylamine (TMA) content for salmon and fish burger samples was estimated according to Conway's micro-diffusion method [Conway, E. *et al.* 1933].

Specifically, 100g of fish muscle was weighed and blended with 50 mL of 20% trichloroacetic acid (TCA). Therefore, 50 mL of water were added and the blend was then centrifugated at 2000 rpm for five minutes to obtain clear extract. The supernatant was filtered and the microdiffusion analysis was performed in Conway's apparatus. 1.5ml of distilled water and 1ml of sample were placed into outer ring while 1 ml of 1% boric acid was pipetted in the central chamber, prepared as follows: 10 g of boric acid were dissolved in

200 ml of 95% ethyl alcohol and 700 ml of water; 10ml of a mixture of 0.033% bromocresol green and 0.066% methylene red were added (16.5mg of bromocresol green and 33mg of methylene red in 50ml of 95% ethyl alcohol); the solution was made up to 1 liter and the pH was adjusted to 5.

1 ml of saturated potassium carbonate solution was quickly placed in the outer ring and the unit was immediately closed .

The content was mixed with a rotational movement and incubated at 35 °C for two hours, or at room temperature for one night. The inner ring solution was titrated against 0.01N HCl using a micro-burette until green colour turns pink.

The Total volatile basic nitrogen (TVB-N) is equal to ml of hydrochloric acid used, multiplied by 27.67mg of nitrogen per 100g of fish.

The same method was used also for dosage of TMA, with the only difference that 1 mL of filtrate, 1 mL of distilled water and 0.5 mL of neutralizing formalin were placed in the external corolla.

The results were expressed as mg TVB-N or TMA-N per 100 g of sample.

3.1.10 Sensory testing

Sensory testing of salmon fillets and bonito fish burgers was undertaken by a panel consisting of 5 trained panelists. The judge's acceptability study was assessed through a sensory evaluation, considering odour, colour, and general acceptability.

Appropriate attributes have been fixed to minimize individual differences and ensure results' repeatability. Sensory assessments were performed under controlled humidity, light, and temperature. A Likert scale (9-point) was used to assess each attribute; in the scale, 9 corresponded to excellent, 8 to very good, 7 to good, 6 to reasonable, 5 to not good (acceptable limit), 4 to disliked, 3 to bad, 2 to very bad, and 1 to completely unacceptable [Angiolillo, L. *et al.* 2018]. Coded samples were randomly and simultaneously distributed to each panelist.

3.1.11 Statistical analyses

Physicochemical and microbiological data were statistically analysed with generalized linear mixed model of SPSS version 26 (IBM Analytics, Armonk, NY, USA). Analysis of variance was performed to study parameters of salmon fillets and bonito fish burgers at each sampling time, including the fixed effect of packaging used and storage times. An a posteriori contrast analysis was carried out using the Tukey test, considering a p value of <0.05 as statistically significant.

3.2 ANTIMICROBIAL PEPTIDE RiLK1

3.2.1 *Production of RiLK1*

The peptide RiLK1 (RLKWVRIWRR-NH₂) was purchased from GenScript Biotech (Leiden, Netherlands). It was stored as a lyophilized powder at 20 °C. Analysis by mass spectrometry confirmed the identity of peptide.

3.2.2 *Circular Dichroism and Fluorescence Spectroscopies of RiLK1*

The secondary structure of RiLK1 was investigated by Circular Dichroism (CD) spectroscopy. All spectra were recorded on JASCO J-810 spectropolarimeter (JASCO, Tokyo, Japan) equipped with a temperature control unit using a 0.1-cm path-length quartz cell (Hellma Analytics, Milan, Italy) in the 195 nm–250 nm wavelength range at 20 nm/min scanning speed by averaging 5 scans. The CD spectra of the peptide (0.1 g/L) were acquired in different environments in the presence of 3 mM SDS, mimicking the biological membrane, and recorded after 24 h incubation. The effect of pH on the secondary structure of the peptide was evaluated by dissolving the sample in different buffer solutions at 10 mM concentration: glycine-HCl, pH 2.0; sodium acetate, pH 4.0; Tris-HCl, pH 7.0; glycine-NaOH, pH 9.0 and 11.0. Structural changes upon temperature were also recorded in 10 mM Tris-HCl buffer pH 7.0 and 3 mM SDS at three different temperatures: 4 °C, 25 °C, and 90 °C. The folding kinetic measurements of the peptide were carried out in 10 mM Tris-HCl buffer, pH 7.0, in the presence of SDS (3

mM) over 24 h incubations. A blank spectrum of a sample containing all components except the peptide was acquired to baseline-correct the CD spectra of the peptide. After noise correction, ellipticities were converted to mean residue molar ellipticities $[\theta]$ in units of $\text{deg cm}^2 \text{ dmol}^{-1}$. Secondary structure content was estimated by BeStSel web server [Micsonai, A. *et al*; 2018] and DichroWeb software using CONTIN-LL algorithm [Whitmore, L. *et al*; 2004].

The fluorescence emission spectra of the Trp residue in the RiLK1 sequence (0.1 mg/mL) were monitored in 10 mM sodium acetate buffer pH 4.0 in the presence of 3 mM SDS over 24 h incubation at 25 °C by using a Shimadzu RF-6000 spectrofluorometer (Kyoto, Japan). Fluorescence was measured at an excitation wavelength of 280 nm and an emission wavelength ranging from 300 to 400 nm, setting the slit widths at 5 nm.

3.2.3 *Effect of Ionic Strength on RiLK1 Stability*

The effect of ionic strength on the RiLK1 stability was examined by reverse-phase (RP) High-Performance Liquid Chromatography (HPLC) analysis. The antimicrobial compound at a final concentration of 50 μM was incubated in a water solution containing 1 M sodium chloride until 9 days at 25 °C. For the analyses, 200 μL of the sample solution were recovered at different times and loaded onto a $\mu\text{Bondapak C18}$ reverse-phase column (3.9 mm \times 300 mm, Waters Corp., Milford, MA, USA) connected to a HPLC system (Shimadzu, Milan, Italy) using a linear gradient of

0.1% trifluoroacetic acid (TFA) in acetonitrile from 5 to 95%. A reference solution at time 0 ($t = 0$) was prepared under the same reaction conditions and run in parallel. The peptide stability in saline solution was evaluated by comparing the peak area of the peptide at the different incubation times, with that of the peptide at $t = 0$.

3.2.4 Antimicrobial assays

Escherichia coli, *Salmonella* Typhimurium, *Listeria monocytogenes* LM3 (serotype 4b), and *Staphylococcus aureus* were isolated from food products. They were detected in the Laboratory of Microbiological Food Control—Department of Food Microbiology of the Istituto Zooprofilattico Sperimentale del Mezzogiorno in Portici (Naples, Italy) in raw and processed foodstuffs of animal origin. *S. Typhimurium* was isolated from chicken according to UNI EN ISO 6579-1, and it was serotyped according to ISO/TR 6579-3:2014 by agglutination with specific anti-sera for O (State Serum Institute—DK) and H antigens (Difco, Franklin Lakes, NJ, USA), using two strains of *Salmonella enterica* (*S. Typhimurium* and *S. Blockley*), which were kindly provided by the National Reference Laboratory for *Salmonella* (Istituto Zooprofilattico Sperimentale delle Venezie, Padova, Italy) as quality control. *L. monocytogenes* was isolated from fish according to UNI EN ISO 11290-1, *E. coli* was isolated from mussels

Chapter II

according to UNI EN ISO 16649-3, and *S. aureus* was isolated from pastry product according to UNI EN ISO 6888-2.

Salmonella strains of human origin were collected from hospitals located in Campania region by the Centro Tipizzazione Salmonelle—Department of Food Microbiology of the Istituto Zooprofilattico Sperimentale del Mezzogiorno in Portici (Naples, Italy), which is the local reference laboratory for *Salmonella* serotyping [Capuano F. et al; 2013]. The strains were isolated from stools of patients with gastroenteritis. The antimicrobial susceptibility was performed by the disk-diffusion method, following the Clinical and Laboratory Standards Institute (CLSI) recommendations. The following antibiotics (Oxoid, Basingstoke, England, and Becton Dickinson, Mississauga, ON, Canada) were used: nalidixic acid (NAL, 30 µg), ampicillin (AMP, 10 µg), chloramphenicol (CHL, 30 µg), gentamicin (GEN, 10 µg), tetracycline (TET, 30 µg), trimethoprim-sulfamethoxazole (SXT, 25 µg), ciprofloxacin (CIP, 5 µg), colistin sulfate (CST, 10 µg), ceftazidime (CAZ, 10 µg), and cefotaxime (CTX, 30 µg). A quality-control strain (*Escherichia coli* ATCC 25922) was included in the test. The antibiotic resistance or susceptibility interpretation was performed according to the CLSI standards. Specifically, the strains displaying intermediate resistance were evaluated as resistant, while those resistant to at least three antibiotic classes were considered multidrug resistant (MDR).

The Minimum Bactericidal Concentration (MBC) was determined by the standard broth microdilution method in accordance with the

Chapter II

Clinical & Laboratory Standards Institute guidelines (CLSI, 2015). For microbroth dilution assay, *L. monocytogenes*, *E. coli*, *S. aureus* and *S. Typhimurium* were grown in BPW (Thermo Fisher, Milan, —Italiay). Bacterial cells were cultured at 37 °C in the appropriate culture media until collection and then diluted in fresh broth to final concentration of 1.0×10^3 CFU/mL (CFU, colony forming units). Thereafter, serial dilutions of RiLK1 in the suitable medium (ranging from 1 to 100 μ M), prepared starting from a stock solution in Dimethyl-sulfoxide (DMSO), were added to each bacterial suspension and incubated at 37 °C for 6 h. Samples containing only cell suspension and DMSO were used as controls. MIC is defined as the lowest peptide concentration, which inhibits the visible growth of bacteria. The MBCs were determined by transferring onto selective agar plates (*L. monocytogenes*, Agar Listeria acc. to Ottaviani & Agosti (ALOA) —Biolife Italiana; *S. Typhimurium*, Salmonella Chromogenic agar—Oxoid UK; *S. aureus*, Baird Parker agar base—Biolife Italiana; *E. coli*, TBX agar—Biolife Italiana) 50 μ L of the bacterial cell suspensions, taken based on the MICs and incubated 24/48 h at 37 °C for *L. monocytogenes*, *S. Typhimurium* and *S. aureus* while *E.coli* was incubated overnight at 44 °C. MBC is defined as the lowest concentration of peptide at which more than 99.9% of the bacterial cells are killed. IC50 is defined as the concentration of a compound that inhibits 50% growth of bacterial cultures relative to control. IC50 and MBC values were assessed by GraphPad Prism version 6.00 (Graph-Pad Software, La Jolla, CA,

USA). All values were calculated as mean of three independent experiments conducted in triplicate.

3.2.5 *Antifungal assays*

Fungal strains were purchased from the American Type Culture Collection (ATCC, Manassas, VA, USA) as follows: *Aspergillus brasiliensis* ATCC 9341 and *Candida albicans* ATCC 14053 strains. Briefly, for both fungal species, the cell suspension was adjusted to 1.0×10^5 CFU/mL in buffered peptone water (BPW) (bioMerieux, Florence, —Italy). Peptide stock solution in DMSO was added to the fungal suspension at a final concentration of 25 μ M and 50 μ M and incubated for 6 h at 37 °C. The minimum fungicidal concentration (MFC) was determined by plating 100 μ L cultures on DG18 plates (Dichloran 18% Glycerol Agar—ISO 21527-2) for CFU counting. After incubation at 25 °C for 7 days, the Minimum Fungicidal Concentration (MFC) was defined as the lowest peptide concentration that resulted in 99.9% killing compared with the drug - free group. The analyses were performed in triplicate on three different experiments.

3.2.6 *Evaluation of Cell Morphology and In Vitro Cytotoxicity Assays*

The *in vitro* effect of RiLK1 on the morphology of eukaryotic cells was evaluated against the human keratinocytes (HaCAT), fetal (WI-38) and adult (TIG-3) lung fibroblast-like cell lines purchased from the American Type Culture Collection (ATCC). The human cells were grown in Dulbecco's modified Eagle's medium (DMEM)

Chapter II

(DIFCO) supplemented with 1% L-glutamine and 10% fetal calf serum (FCS, DIFCO). Cells were seeded in six-well plates (5×10^4 cell/well) and incubated for 16 h at 37 °C in a humidified atmosphere of 5% CO₂. Then, the cells were treated with different concentrations of peptide (ranging from 1 to 10 μM) for 24 h. Untreated cells were used as negative controls. After 24 h treatment, the cells were washed with Phosphate-Buffered Saline (PBS) buffer, fixed with 4% paraformaldehyde (PFA) for 30 minutes and visualized by phase-contrast microscopy using the DMI6000B inverted fully automated microscope with DFC420 RGB camera (Leica Microsystems, Wetzlar, Germany). Leica LASV5.4 software was utilized for the image acquisition/elaboration (contrast/γ adjusting).

Toxicity of RiLK1 on mammalian fibroblasts BALB 3T3 clone A31 (ATCC CCL-163), at increasing peptide concentrations, was determined using the Neutral Red Uptake (NRU) assay. BALB 3T3 clone A31 (ATCC CCL-163) cells were cultivated in Dulbecco's Modified Eagle's Medium (DMEM) supplemented with 10 % Newborn Calf Serum and 4 mM Glutamine. For the NRU assay, the cells were seeded in 96-well microtiter plate (Thermo Fisher Scientific, Milan, Italy) and incubated for 24 h at 37 °C and 5% CO₂ in a humidified environment allowing cell sedimentation and the constitution of a subconfluent monolayer prior to treatment with RiLK1. Therefore, cells were exposed at increasing concentrations of RiLK1 (10, 25, and 50 μM) for 24 h at 37 °C. Following treatment, each well was rinsed with 150 μL of D-PBS with

$\text{Ca}^{2+}/\text{Mg}^{2+}$ and treated with 50 $\mu\text{g}/\text{mL}$ Neutral Red (NR) dye solution for 3 h at 37 °C. Afterwards, each well was again rinsed with 150 μL of D-PBS with $\text{Ca}^{2+}/\text{Mg}^{2+}$ and 150 μL of NR desorb solution (49 % ddH₂O, 50 % ethanol, 1 % acetic acid) were added. Plates were placed under gentle agitation in darkness for 10 min and the Optical Density of the NR extract at 540 nm was measured by using spectrophotometer. Cell viability was expressed as percentage of BALB 3T3 clone A31 cells grown in the treatment medium (DMEM with 5 % NCS, 4 mM Glutamine, 0.1% DMSO, and RiLK1), with respect to the control group represented by the cells grown in DMEM with 5 % NCS, 4 mM Glutamine and 0.1% DMSO (viability control cells = 100 %).

$$(\text{OD treated cells} - \text{OD blank}) / (\text{OD Control Cells} - \text{OD blank}) \times 100$$

Interpretation of the data was performed according to ISO 10993-5:2009: the compound was considered cytotoxic if the relative cell viability of the sample was <70 % of the control group, while it was considered non-cytotoxic if cell viability of the sample was ≥ 70 % of the control group.

3.2.7 Preparation of Model Membranes: Multilamellar Vesicles (MLVs)

Model membranes (liposomes) were made using lipid stock solutions (10 mM) in chloroform:methanol (2:1, v/v) of 1-palmitoyl-2-oleoyl-sn-glycero-3-phosphoethanolamine (POPE) (Avanti Polar Lipids, Alabaster, United States), 1,2-dioleoyl-sn-glycero-3-phosphoethanolamine (DOPE) (Avanti Polar Lipids,

Chapter II

Alabaster, United States), L- α -lysophosphatidylcholine (Egg Lecithin, PC) (Avanti Polar Lipids, Alabaster, United States), N-Acyl-D-sphingosine-1-phosphocholine (chicken egg yolk, SM) (Sigma-Aldrich, St. Louis, MO, USA), phosphatidyl serine (PS) (Avanti Polar Lipids, Alabaster, United States), 1',3'-bis [1,2-dioleoyl-sn-glycero-3-phospho]-glycerol (Cardiolipin 18:1, CL) (Avanti Polar Lipids, Alabaster, United States) and 1-palmitoyl-2-oleoyl-sn-glycero-3-phosphatidylglycerol (POPG) (Larodan AB, Sweden). Lipid films were prepared in glass tubes by mixing an appropriate volume of phospholipids to achieve the desired molar ratio (**Table 2**). Subsequently, the solutions were dried under argon flow and then subjected to a vacuum for at least 3 h to remove traces of the solvent. A sufficient volume of binding buffer composed of 4-(2-Hydroxyethyl) piperazine-1-ethanesulfonic acid 10 mM (HEPES, Sigma-Aldrich) and NaCl 100 mM (Sigma-Aldrich), pH 7.2 was used to resuspend the lipidic film, yielding 2 mM lipid phosphorus. Fresh lipid suspensions were prepared before each experiment.

Table 2: Membrane lipid composition in eukaryotic and prokaryotic organisms (% mol).

Membrane	PC	SM	PS	DOPE	POPE	POPG	CL
Eukaryotic membrane ¹	40	15	5		40		
Zwitterionic membrane	100						
<i>Salmonella</i> Typhimurium ^{2, GN}				78		18	4
<i>Staphylococcus aureus</i> ^{3, GP}						58	42

PC, phosphatidylcholine; SM, sphingomyelin; PS, phosphatidylserine; DOPE, dioleoyl-phosphatidylethanolamine; POPE, palmitoyl-oleoyl-phosphatidylethanolamine; POPG, palmitoyl-oleoyl-phosphatidylglycerol; CL, cardiolipin. GN, Gram-negative bacteria; GP, Gram-positive bacteria.

¹ [Casares, D *et al*; 2019]; ² [Barbosa, S.C *et al*; 2019]; ³ [Epanand, R.M. and Epanand, R.F.; 2011].

3.2.8 Lipid Binding Assay

To assess the extent of the peptide-MLV interactions, reaction mixtures were prepared in Eppendorf tubes combining each lipid solution (at the fixed molar concentration of 1800 μM) with pre-formed liposomes containing different amounts of peptide, ranging from 20 to 120 μM (when saturation did not occur, higher peptide concentrations were tested). The solutions were vortexed vigorously and incubated at room temperature for 30 min to allow binding. As negative controls, analogous samples were made using the buffer solution vehicle rather than the stock peptide solution. At the end of the incubation period, the solutions were carefully transferred to polycarbonate centrifuge tubes (1 mL, 8 \times 51 mm: Beckman Coulter, USA) and centrifuged at ca. 60,000 \times g (20,000 rpm, outer row) for 1 h at 20 $^{\circ}\text{C}$ (Beckman LE-80 Ultracentrifuge; rotor type 25). After centrifugation, the supernatant was removed and the pellet was washed and resuspended with binding buffer containing Sodium Dodecyl Sulfate (SDS, Thermo Fischer, Germany) at a final concentration of 1%. The binding of the peptide to the model membranes was assessed by quantifying the amount of

RiLK1 in the pellet and supernatant using calibration curves generated by adding known amounts of peptide to control supernatants or pellets of vesicles prepared in the absence of the peptide. Peptide binding to multilamellar vesicles (MLVs) was measured by fluorescence spectroscopy taking advantage of the presence of the tryptophan residues in RiLK1.

3.2.9 *Steady-State Tryptophan Fluorescence*

Tryptophan (Trp) fluorescence spectra were recorded for each supernatant and pellet sample after 30 min of stirring at 900 rpm in a Thermo-Shaker (TS-100: Biosan) at room temperature. The variation in Trp emission was recorded between 300 and 450 nm excitation, at $\lambda_{\text{ex}} = 280$ nm, using a Cary Eclipse Fluorescence spectrophotometer (Varian, Sydney, Australia). Slit widths were 2.5 nm for excitation and 5 nm for emission, and each spectrum was corrected by subtracting the liposome background.

3.2.10 *Statistical Analysis*

Statistical analysis was performed using GraphPad Prism®, version 8.0.1 (GraphPad, San Diego, CA, USA). All experiments were performed at least three times and the data were presented as the mean (M) \pm standard error (SE). GraphPad Prism® was used to perform Scatchard analyses and the student's t-test ($p < 0.05$).

4 RESULTS AND DISCUSSION

4.1 ANTIMICROBIAL PEPTIDE 1018K6

4.1.1 1018K6 Immobilization on PP Surface

Following confirmation of the excellent antimicrobial properties preserved by 1018K6 even after bonding on different materials such as Polyethylene terephthalate (PET) and nanoparticles [Agrillo B. *et al.*, 2019; Palmieri G. *et al.*, 2018], the peptide was immobilized on a further plastic polymer commonly used in food packaging such as Polypropylene (PP).

To this aim, commercial PP slides were exposed to plasma treatment to activate the inert polymeric surfaces with reactive -COOH* functional groups that are available to interact with the amine moieties of 1018K6 forming an amide bond [Baniya, H.B *et al.*, 2020].

In order to develop an antimicrobial packaging more adequate for food application, the conditions applied in our previously studies to functionalize the polymeric materials, were modified. Specifically, the covalent attachment of 1018K6 on the pre-activated PP polymers was executed by a one-step immobilization process involving the immersion of the polymeric surfaces in a water solution containing the peptide at different concentrations. Therefore, the slides were kept at 70 °C for about 4 h to completely

remove the water and to drive the coupling reaction. To validate the successful of our immobilization procedure, the test ink was carried out confirming the increase in the surface hydrophilicity of the AMP-functionalized PP slides following the immobilization procedure due to the introduction of polar groups on the hydrophobic polymer. Moreover, Reverse-Phase High-Precision Liquid Chromatography (RP-HPLC) analysis was performed to quantify the amount of 1018K6 immobilized on PP surfaces. For this investigation, 1018K6-PP slides after the coupling reactions were immersed in distilled water and incubated for 16 h at room temperature under agitation. Then, the polymers were subjected to sonication for 20 min at room temperature and the recovered solutions loaded on RP-C18 column. By knowing the initial peptide concentrations that were used in the conjugation reaction, the amount of the peptide attached to PP slides was indirectly determined by comparing the peak area in the RP-chromatograms. The data obtained from these analyses showed that the immobilization yield varied from 23% using a starting from a peptide concentration of 50 μM to 5% when 200 μM was used. The maximum peptide binding (31%) was obtained at 100 μM , which corresponded to a surface coverage of approximately 5.8 nmol/cm^2 , confirming that the initial amount of 1018K6 strongly influenced its binding to synthetic slides (**Figure 18**). Therefore, 100 μM was selected as peptide concentration to perform all the further experiments.

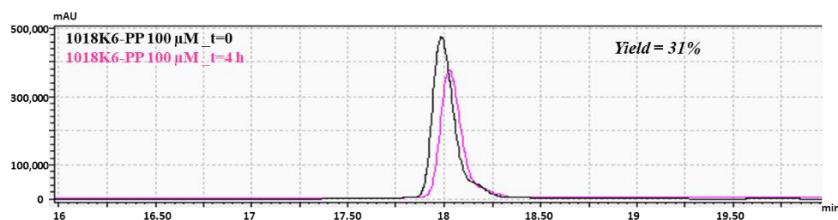


Fig. 18: Immobilization yield (%) of 1018K6 on PP surfaces determined by RP-HPLC chromatography on a C18 column after the coupling reaction. PP surfaces pre-activated by plasma treatment, were incubated with a water solution of 1018K6 (100 μ M). After the coupling reactions, the supernatants were recovered and analysed by RP-HPLC. The peptide solution (100 μ M) at time 0 ($t = 0$) was used as control. The reported chromatograms are representative of three independent experiments.

Concerning the low binding capacity associated with the highest peptide concentration used, it could be attributed to a steric hindrance effect, which limits polymer-peptide interactions and a phenomenon producing water-soluble microaggregates which can strongly reduce the availability of bioactive molecules for the immobilization reaction.

One of the most important requirements to apply an antimicrobial packaging in the food industries is the stability of the peptide immobilized on the polymers in the conditions of use, because in this way it does not require approval as food additive by EFSA (European Food Safety Authority). For this purpose, the slides functionalized with 100 μ M 1018K6 were incubated in pure water or in NaCl 1 M at 4 $^{\circ}$ C for 7 days and the potential release of the peptide from the polymeric support was monitored by RP-HPLC, using the free peptide as control. Following these analyses, no

peptide-release was observed during 7 days of incubation, confirming the strong attachment via the covalent coupling of the bioactive compound, preventing its release from the surface (data not shown) and highlighting the high stability of the system.

It is worth noting that the projected packaging was reused at least six times in all the subsequent analyses, after washing with EtOH 70% for 1 min, rinsing with water and exposition to UV radiations for 1 h. Surely, this represents an important advantage from the industrial point of view, allowing a substantial decrease in the environmental impact based on the concept that “reuse is better than recycling”.

4.1.2 Effects of 1018K6-PP on physical properties and on microbiological quality of Salmon fillets

It is known that the physicochemical characteristics of raw salmon fillets, such as pH (close to 6) and a high-water activity (a_w), make them highly susceptible to microbial growth, which affects the durability of these products [Bozaris, I.S. *et al.*, 2013]. Therefore, the fish industry is actively seeking methods of preservation to improve quality and marketability of this luxury marine food while economizing on costs. To this aim, the antimicrobial effects of 1018K6-PP on the spoilage microbiota and the intrinsic properties of fresh salmon fillets during refrigerated storage were assessed, using the pre-activated and not-functionalized PP slides as control (CTR). In **Figure 19**, a representative scheme of the different steps

applied for the preparation of salmon fillets employed in the microbiological and physico-chemical analyses, was shown.



Fig. 19: Representative scheme of the experimental preparation of salmon fillets.

As reported in **Table 3**, the initial pH values ($\text{pH} > 6$) for both samples (CTR and 1018K6-PP) were similar to those reported by other authors [Alves, V.L. *et al.*, 2018]. Throughout storage, the pH of salmon fillets in contact with the not-functionalized PP slides (CTR) and 1018K6-PP slightly decreased, recording a significant difference between the two groups on the 4th day. This result could be justified by an increase of acid production due to the homogenous proliferation of *Lactic Acid Bacteria* occurring in these samples during the experimental analysis (data not shown) [Kitundu, E. *et al.*, 2021], although Gonzalez-Rodriguez [Gonzalez-Rodriguez M.N. *et al.*, 2001] registered an increase of alkalinity in prepacked salmon slices because of the ammonia and amines production by bacteria. As far as the water activity is concerned, no significant differences were observed among the experimental groups, with only a minor increase on the fourth day (**Table 3**). From the microbiological point of view, the initial concentrations of TAB (Total Aerobic Bacteria) at both 30 °C and 7 °C in raw

salmons were somewhat higher compared with values reported in previous works [Lerfall, J. *et al.*, 2018; Mace, S. *et al.*, 2012], probably due to poor handling practices during processing of fish fillets. However, similar data were reported by Wiernasz N. *et al.*, 2020, which referred a concentration of 4.3 ± 0.2 Log (CFU/g) for total mesophilic bacteria. Indeed, the performed analyses showed that 1018K6-PP samples did not display significant differences ($p > 0.05$) in the growth kinetics of TAB at 30 °C and 7 °C compared with the control samples at the end of the storage period, indicating that the antimicrobial packaging did not have any effect, neither positive nor negative, on the microbiota of salmon fillets (**Table 3**). Albeit the total bacterial count represents a key factor in assessing the microbiological quality and safety of foods, it is well known that *Pseudomonas* spp., *Enterobacteriaceae*, and *Brochothrix thermosphacta* are the main microbial family and genera responsible for the off-flavours and the unpleasant odours typical of deterioration of fish and fish products [Geeroms, N. *et al.*, 2008]. As far as the evolution of these bacteria is concerned, the samples stored in 1018K6-PP packaging revealed a significant slowdown in the replication of these microorganisms at the 4th day of conservation. Specifically, the sensitivity of bacteria belonging to *Enterobacteriaceae* family to antimicrobial activity of the active packaging could make this product interesting for the food industry and promote its applicability as a potential “controller tool” for *Escherichia coli*. Indeed, the inhibitory effect of the innovative packaging was also evident towards beta-glucuronidase-positive *E.*

coli, whose levels in treated samples were always below 1.0 Log (CFU/g) in contrast to the CTR [> 2.0 Log (CFU/g)]. This finding becomes more relevant when the microbiological limits recommended for *E. coli* (1.0 and 2.7 Log (CFU/g) for minimum and maximum limit, respectively) by the International Commission on Microbiological Specifications for Foods (ICMSF) for the commercialization of fish and fish products [Roberts, T.A. *et al.*, 1986], are considering. Actually, the innovative packaging makes the salmon fillets hygienically suitable throughout the storage period.

Regarding total coliforms and *Enterococcus faecalis*, the growth curves were very similar for control and treated groups, but a significant antimicrobial effect of the 1018K6-PP was observed only on the 4th day of storage. Finally, the microbiological results pointed out the ability of the bound peptide to affect the growth of bacteria belonging to *Staphylococcus* genera. Therefore, the antimicrobial coating appears to successfully act on the survival and replicative capacity of this class of microorganisms, showing a significant ($p < 0.01$) difference between the control groups and the treat one on 4th and 7th days. All these findings confirm the results previously obtained with the peptide 1018K6 in the free status [Colagiorgi, A. *et al.*, 2020]. It is worth noting that the same microbiological analyses were performed on salmon fillets packaged in PP films that were not subjected to any surface modification. Interestingly, the obtained results were comparable to those achieved with the pre-activated and not-funzionalized PP

films, thus excluding the occurrence of a potential antimicrobial effect determined by the polymeric surfaces activated by plasma alone (data not shown).

It should be pointed out that the microbiological results were not obvious on the basis of two main considerations: 1) the antimicrobial packaging could be unable to kill microbes under conditions of intended use due to the complexity of the fish matrix which can inactivate the bioactive compound; 2) 1018K6 could not retain its antimicrobial activity when bound to PP polymers, because the immobilization process could restrict its conformational freedom and influence its orientation, both of which are important features for the peptide activity.

As far as the potential antimicrobial mechanism, two factors could play a dominant role of the bound 1018K6 respect to its soluble form:

- 1) the high local concentration of the peptide tethered to the polymeric surface;
- 2) the strong electrostatic interaction between the cationic peptide chains and anionic bacteria cell membranes (instead of membrane insertion), thus leading to an alteration of the potential across the bacterial membrane, which ultimately triggers the cellular death.

To sum up, 1018K6-PPs can be considered a promising instrument to positively affect the quality of perishable products such as fresh salmon based on the microbial effects observed. This suggestion is supported by the important antimicrobial data that the new package

Chapter II

exerts against specific spoilage microorganisms responsible for spoilage processes in fish and fish products. However, a potential role of 1018K6-PP in the food safety cannot be excluded taking into account its action against *Enterobacteriaceae* and *Staphylococcus* spp. In this scenario, the introduction of 1018K6-PP into the food marketplace could guarantee the availability of safe and natural tools capable of limiting damages of bacterial origin.

Table 3: Evaluation of microbiological counts [Log (CFU/g)] in salmon fillets packaged in active PP films functionalized with 1018K6 by storage time.

		Day	0	4	7
			<i>m</i> ± <i>sem</i>	<i>m</i> ± <i>sem</i>	<i>m</i> ± <i>sem</i>
TAB 30°C	CTR		4.76±0.06 ^A	6.77±0.07 ^B	6.89±0.02 ^B
	1018K6-PP		4.76±0.06 ^A	6.73±0.01 ^B	6.88±0.01 ^C
TAB 7°C	CTR		2.91±0.04 ^A	4.24±0.01 ^{B,X}	5.32±0.04 ^C
	1018K6-PP		2.91±0.04 ^A	4.56±0.04 ^{B,Y}	5.28±0.04 ^C
<i>Coliforms</i>	CTR		1.91±0.05 ^A	3.91±0.04 ^{aB,X}	3.44±0.19 ^{bB}
	1018K6-PP		1.91±0.05 ^A	3.56±0.07 ^{B,Y}	3.44±0.18 ^B
<i>Enterobacteriaceae</i>	CTR		0.96±0.01 ^A	3.86±0.07 ^{B,X}	3.07±0.04 ^{C,X}
	1018K6-PP		0.96±0.01 ^A	3.66±0.04 ^{B,Y}	3.96±0.04 ^{C,Y}
<i>Pseudomonas</i> spp.	CTR		4.31±0.09 ^A	7.32±0.10 ^{B,X}	7.44±0.16 ^{B,X}
	1018K6-PP		4.31±0.09 ^A	6.28±0.05 ^{B,Y}	6.91±0.04 ^{C,Y}
<i>E. coli</i>	CTR		<i>ni</i> ^A	2.07±0.09 ^{B,X}	2.95±0.03 ^{C,X}
	1018K6-PP		<i>ni</i>	<i>ni</i> ^Y	<i>ni</i> ^Y
<i>Enterococcus faecalis</i>	CTR		3.32±0.08 ^A	3.96±0.01 ^{B,X}	5.07±0.12 ^{C,X}
	1018K6-PP		3.32±0.08 ^{aA}	2.96±0.12 ^{bA,Y}	4.74±0.06 ^{bB,Y}
<i>B. thermosphacta</i>	CTR		4.98±0.07 ^A	5.98±0.03 ^{B,X}	7.36±0.14 ^{C,X}
	1018K6-PP		4.98±0.07 ^A	6.81±0.04 ^{B,Y}	5.96±0.19 ^{C,Y}
<i>Staph.coagulase positive</i>	CTR		<i>ni</i> ^A	2.26±0.09 ^{B,X}	3.19±0.05 ^{C,X}
	1018K6-PP		<i>ni</i> ^A	<i>ni</i> ^{A,Y}	1.96±0.02 ^{B,Y}
pH	CTR		6.25±0.01 ^A	6.18±0.02 ^{B,X}	6.07±0.03 ^C
	1018K6-PP		6.25±0.01 ^A	6.11±0.01 ^{B,Y}	6.02±0.01 ^C
<i>a_w</i>	CTR		0.973±0.003 ^a	0.981±0.001 ^b	0.982±0.002 ^b
	1018K6-PP		0.973±0.003 ^a	0.979±0.000 ^b	0.980±0.002 ^b

*ni: not isolated

In each storage day, three samples by experimental group were analyzed. Statistical analysis was performed comparing experimental groups at each sampling time and within each experimental group along the ripening period. All data were presented as mean (m) \pm standard error (sem).

Different superscript uppercase letters indicate a significant difference at $p < 0.01$.

Different superscript lowercase letters indicate a significant difference at $p < 0.05$.

a–c In the same row mean values (same group in different days) followed by different letters show significant differences.

x–y In the same column mean values (different groups on the same sampling time) followed by different letters show significant differences.

4.1.3 Instrumental colour analysis of salmon fillets

The colour in fish foods is one of the most important qualities influencing the consumer's decisions to purchase. Therefore, the impact of 1018K6-PPs on the colour of the packaged salmon fillets was investigated for various storage periods. As reported in **Table 4**, the lightness (L^*) was the only parameter to be influenced significantly using the active packaging, although this phenomenon did not visible affect the general appearance of the product. Indeed, chroma values are similar in all the samples during the whole experimental times. Our findings are in agreement with Merlo *et al.*, [Merlo, T.C. *et al.*, 2019], reporting that the use of chitosan film reduces the change in structure of proteins conferring a darker aspect to treated salmon fillets. This result was justified considering

the strong connection between the change in light scattering of the muscle and the variation in lightness. Furthermore, samples packed in 1018K6-PP were found to be slightly more reddish and yellowish (higher values of a^* and b^* , respectively) than the control ones. According to several authors [Merlo, T.C. *et al.*, 2019; Lerfall, J. *et al.*, 2015; Bjerkgeng, B. *et al.*, 2000] the main value considered for this fish family is the redness, which is associated to the consumer's preference and acceptability. Changes in a^* value in salmon are due to the addition of carotenoids, such as astaxanthin and cataxanthines, and related to reddish colour of salmonid fishes. However, the scientific community disagrees, and different opinions are reported in literature. Yeşilayer *et al.*, [Yeşilayer, N. *et al.*, 2020] demonstrated that fillets of farmed Atlantic salmon fed with feed containing carotenoids showed high values of yellowness, demonstrating that the typical red-orange color is represented by both redness and yellowness values. It is worth underling that a^* and b^* did not differ significantly among all samples by storage time, exhibiting similar ΔE (total colour differences), Δa^* , and Δb^* values. Therefore, 1018K6-PPs did not produce negative effects on colours parameters, potentially preserving the aspect of salmon samples.

Chapter II

Table 4: Changes in colour indices of the salmon fillets packaged in active PP films functionalized with 1018K6 by storage time.

		Day		
		0	4	7
		<i>m</i> ± <i>sem</i>	<i>m</i> ± <i>sem</i>	<i>m</i> ± <i>sem</i>
<i>L</i> *	CTR	43.51±1.47 ^a	45.93±0.63 ^{a,x}	48.23±0.67 ^{b,x}
	1018K6-PP	43.51±1.47 ^A	36.13±1.89 ^{b,y}	44.48±1.51 ^{A,y}
<i>a</i> *	CTR	16.78±0.83	19.75±1.41	15.94±1.44
	1018K6-PP	16.78±0.83	20.02±1.25 ^a	16.63±0.59 ^b
<i>b</i> *	CTR	21.15±1.68	23.55±2.86	15.94±1.99
	1018K6-PP	21.15±1.68	24.40±3.40	17.01±1.62
Chroma	CTR	27.01±1.82	30.76±3.06	22.55±2.43
	1018K6-PP	27.01±1.82	31.63±3.30	23.82±1.52
Hue angle	CTR	51.46±1.01 ^A	49.75±1.64 ^a	44.80±0.92 ^{bB}
	1018K6-PP	51.46±1.01 ^a	50.10±2.92	45.42±1.97 ^b
ΔE	CTR		6.31±2.26	7.22±0.88
	1018K6-PP		9.47±1.45	6.45±1.82
Δa^*	CTR		2.97±1.94	-0.83±0.61
	1018K6-PP		3.24±1.53	-0.14±1.21
Δb^*	CTR		2.40±3.14 ^a	-5.21±0.67 ^b
	1018K6-PP		3.24±2.55	-4.15±3.28

In each sampling day, three samples by experimental group were analyzed. Statistical analysis was performed comparing experimental groups at each sampling time and within each experimental group along the ripening period. All data were presented as mean (*m*) ± standard error (*sem*). Different superscript uppercase letters indicate a significant difference at $p < 0.01$. Different superscript lowercase letters indicate a significant difference at $p < 0.05$.

a–b In the same row mean values (same group in different days) followed by different letters show significant differences.

x–y In the same column mean values (different groups on the same sampling time) followed by different letters show significant differences.

4.1.4 Effect of 1018K6-PP on chemical parameters of Salmon fillets

It is common to evaluate the “age” of the food through the study of the microbiological community in order to evaluate the presence and the concentration of specific spoilage microorganisms (SSOs). However, the spoilage of fish and fish products is associated to the occurrence of off-odours due to the production of volatile substances as result of the bacterial metabolism. Changes in the odour affect the acceptability of consumers, who associate the freshness of fish products to typical organoleptic features. Due to perishable foods being sensitive to variations in appearance, some of the characteristic volatile organic compounds (VOCs) produced by bacteria can be used as potential chemical spoilage index (CSIs) in fish and fish products [Parlapani, F.F. *et al.*, 2015]. In this study, two chemical quality indicators were used to assess the ability of 1018K6-PP to preserve the quality and sensorial properties, such as the total volatile basic-nitrogen (TVB-N) and trimethylamine-nitrogen (TMA-N) (**Figure 20**). The choice to detect these two VOCs was dictated by key role that these chemicals play in the freshness of salmon, being the final products of protein degradation [Azizi-Lalabadi, M. *et al.*, 2020].

TVB-N includes the measurement of volatile basic nitrogenous compounds such as trimethylamine (TMA), dimethylamine (DMA), and other nitrogenic substances, which are produced by bacterial or tissue enzymes from the deamination of amino acids. In the current study, the initial amount of TVB-N in all salmon fillets analyzed was 7.89 ± 0.21 mg/100 g (**Figure 20 A**). Significant

differences ($p < 0.01$) between salmon samples packaged with CTR-PP and 1018K6-PP slides were observed after 4 days of storage. Specifically, 1018K6-PP appeared to slow down indirectly the protein degradation in salmon fillets through the control of the microbial growths. Indeed, the great amount of free amino acids in fish [Bramstedt, F. *et al.*, 1961; Jacquot, R. *et al.*, 1961] are used as substrate by bacteria in their metabolism with the final production of organic acids, sulfur compounds, ammonia, and biogenic amines (BAs) [Jorgensen, L.V. *et al.*, 2000; Rodrigues, M.J. *et al.*, 2003]. Overall, albeit 1018K6-PP demonstrated to be efficient in reducing the protein degradation, throughout the entire storage period TVB-N values never reached and overcame the legislative limit of 35 mg/100 g specified by the EU 2019/627 for this fish typology [Commission Implementing Regulation (EU) 2019/627 of 15 March 2019].

The TMA-N originates by decomposition of trimethylamine N-oxide (TMAO), used from bacteria as donor of oxygen molecules in their respiratory metabolism in fish and fish products stored at refrigeration temperature [Dalgaard, P. *et al.*, 1993; Boskou, G. *et al.*, 1997; Giménez, B. *et al.*, 2005]. Due to the importance of the initial amount of TMAO in the muscle, the concentration of TMA-N is strongly related to the species of fish, and *Salmo salar* is naturally rich in trimethylamine N-oxide [Chung, S.W.C. *et al.*, 2009]. In **Figure 20 B**, the trends of TMA-N over time are displayed. Specifically, the samples packed with 1018K6-PPs showed the lowest TMA-N values ($p < 0.01$) at both 4 and 7 days of

storage in agreement with the above reported values of TVB-N, thus reinforcing the hypothesis that active slides affect the spoilage microbial communities. In fact, it is well-known that the TMA production is mainly operated by bacteria belonging to the Enterobacteriaceae family, which resulted to be sensitive to the antimicrobial activity of the bound peptide, as already reported in **Table 3** [Dalgaard, P. *et al.*, 1995; Gram, L. *et al.*, 2002]. Although TMA is considered as a good indicator of the deterioration progress, no maximum legislative limits for TMA concentrations were defined and different values were proposed. However, according to Shumilina *et al.*, (2016) who reported 4.2 mg/100 g as the acceptability limit for fish, the freshness was preserved only in salmon fillets put in contact with 1018K6-PP (TMA < 5 mg/100g). Finally, measurements of thiobarbituric acid reactive substances (TBARS) expressed as Malonyldialdehyde (MDA) levels, were performed in order to investigate on the lipid oxidation, which is a very important event leading to the quality of foods, especially of those containing highly unsaturated fats like fish [Raeisi, M. *et al.*, 2015; Secci, G. *et al.*, 2016]. As shown in **Figure 20 C**, the TBARS values in control fillets increased significantly during refrigerated storage in contrast to that observed in the packaged fillets with 1018K6-PP slides. Therefore, 1018K6-PP is able to exert antioxidant properties, but this finding is not surprising given the well-known correlation between lipid oxidation and bacterial contamination [Remya, S. *et al.*, 2016].

Chapter II

Indeed, the MDA is the main aldehyde produced as result of the decomposition of unsaturated fatty acids also operated by bacteria, thus remarking the antimicrobial efficacy of the active films. The chemical analyses performed on the salmon fillets packaged in unmodified PP films, demonstrated that the plasma activation by itself was not able to allow the polymers to affect the quality of these fish products (data not shown).

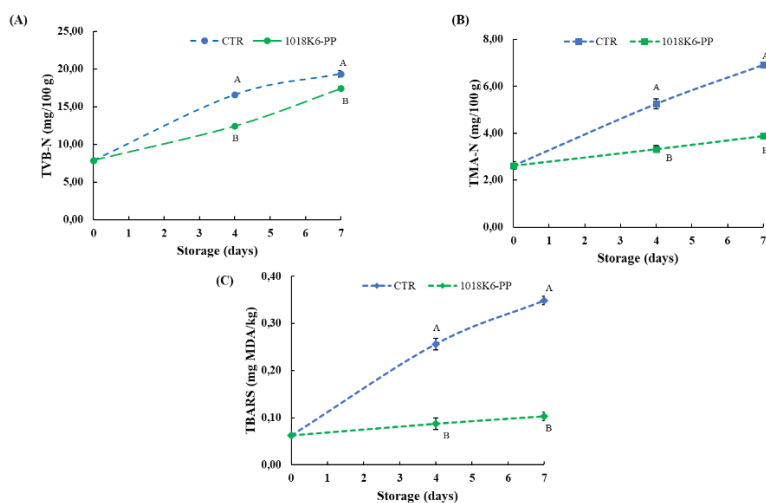


Fig. 20: Effects of 1018k6-PP surfaces on the Chemical Quality of *Salmon salar* fillets. Changes in TVB-N (A), TMA-N (B), and TBARS (C) of *Salmon salar* fillets packaged in active 1018K6-PP films during storage at 4 °C. CTR (blue lines): PP films without 1018K6; 1018K6-PP (green lines): PP films functionalized with 1018K6. Results are means of three independent experiments and error bars represent the standard error (sem). Different letters at each sampling time are used for significantly different samples, according to Tukey test (uppercase letters: $p < 0.01$; lowercase letters: $p < 0.05$).

Overall, the comprehensive analyses of microbiological and chemical parameters pointed out two main aspects: the key role of TVB-N, TMA, and MDA as chemical spoilage indices in perishable food and the effectiveness of 1018K6-PP in preserving salmon fillets. As reported by Prabhakar *et al.*,(2020), the assumption of the interconnection among bacterial concentrations and chemical metabolites production is already consolidated as well as the link between TVB-N/TMA levels and quality. Therefore, our findings confirmed this strong link and candidate 1018K6-PP as a valuable packaging technology capable of guaranteeing longer durability for highly perishable foods such as raw salmon.

4.1.5 *Panelists' sensory evaluation*

Sensory perception is the tool through which the consumers choose the food at a store, trusting in their senses and adopting an immediate and easy system for evaluating freshness and quality [Rasekh, J. *et al.*, 1970]. In this study, the organoleptic features appeared to be partially influenced by the packaging technology used. As reported in **Figure 21**, the representation of observed sensory characteristics highlighted an important repercussion of the use of antimicrobial slides on the production of off-odours. Despite the initial good quality of all samples, the salmon fillets belonging to the control groups showed signs of spoilage as early as the 4th day of storage at refrigeration temperature. The judges

rated the control samples as “poor freshness quality” products, due to the score of odor and general appearance obtained at the end of the trial. On the contrary, the treated samples maintained good sensory characteristics over time. In agreement with those reported above for VOCs, the demonstrated antimicrobial activity (**Table 3**) of 1018K6-PP seems to indirectly control the negative changes in the chemical structure and metabolites production of salmon fillets occurring during the storage [Karabagias, I. *et al.*, 2011; Françoise, L. *et al.*, 2010]. Furthermore, the scores of overall appearances of treated samples pointed out the absence of negative influences of the novel active packaging on the sensory features, due to the colourless and odourless nature of the 1018-K6 molecules.

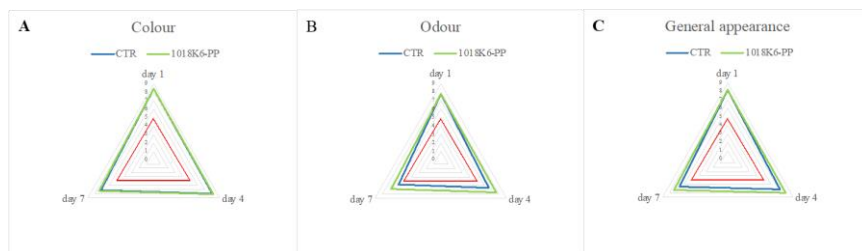


Fig. 21: Changes in colour (A), odour (B), and overall appearance (C) of salmon fillets during storage period. CTR (blue lines): PP films without 1018K6; 1018K6-PP (green lines): PP films functionalized with 1018K6.

4.1.6 Microbial challenge testing of *L. monocytogenes* on salmon fillets packaged with 1018K6-PP.

Foodborne diseases are a reality affecting thousands of people in industrialized countries every year. Amongst the bacterial pathogens responsible of severe human toxi-infections, *Listeria monocytogenes* is considered one of the most dangerous. Due to their origin and the way in which they are processed, fish products show an increased incidence rate of listeriosis, and then they represent typical food vehicles of high levels of microbiological contamination, considering that this bacterium is able to grow also at refrigeration temperatures. Therefore, challenge testing of the food products with *L. monocytogenes* is recommended to assess the potential for growth both qualitatively and quantitatively in the foods at risk.

In this context, the anti-listerial efficacy of 1018K6-PP was evaluated in salmon fillets stored at 5 °C for 96 h (**Figure 22**). In order to confer greater confidence in the assessment of the likelihood of a particular strain to compromise food safety, mixed cultures of three *L. monocytogenes* strains isolated from fish was used at a concentration of ca. 150 CFU/mL. This value of inoculum is representative for the natural contamination of *L. monocytogenes* commonly encountered in fresh foods, considering that 100 CFU/mL is the threshold limit considered as low risk for causing listeriosis. In addition, the use of food isolates is recommended because it is likely to represent better the behavior of naturally contaminating strains.

Chapter II

The results of challenge test performed on salmon fillets indicated that the antimicrobial packaging was effective in inhibiting the growth and survival of the pathogen on the surface of the fresh food during storage in contrast to the untreated control. Indeed, a complete inhibition of *L. monocytogenes* was observed after 72 h incubation, with a slight decrease (95%) at the end of the assay (96 h), thus suggesting that our system could be used to preserve the safety of fish products during their storage.

Overall, our results show the positive impact of the effectiveness of 1018K6-PP packaging on food safety when the target microorganism is a foodborne pathogen of great present concern, such as *L. monocytogenes*.

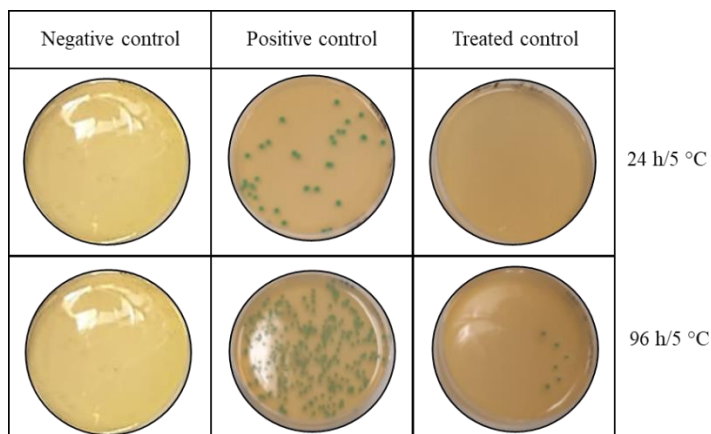


Fig. 22: Bactericidal activity of polymer functionalized with 1018K6 against *L. monocytogenes* on salmon fillets. Negative control: untreated salmon fillets; Positive control: salmon fillets treated with not-functionalized PP; Treated control: salmon fillets treated with 1018K6-PP.

4.1.7 Evaluation of 1018K6-PPs slides on physico-chemical, microbial and sensorial properties of *Sarda sarda* burgers

In order to evaluate the versatility of our active packaging, a different typology of food matrices was included in the experimental design. To this aim, microbiological, physico-chemical and sensorial analyses were performed on fish burgers of bonito (*Sarda sarda*) packaged with 1018K6-PP slides. This analysis was aimed to verify the effectiveness of 1018K6-PP also against minced fish meat, which is notoriously characterized by higher level of microorganisms than fillets because of the shredding process underlying their manufacture [Roohinejad, S. *et al.*, 2017]. The scheme used to set up the *Sarda sarda* hamburger employed in the experimental trials, is shown in **Figure 23**.

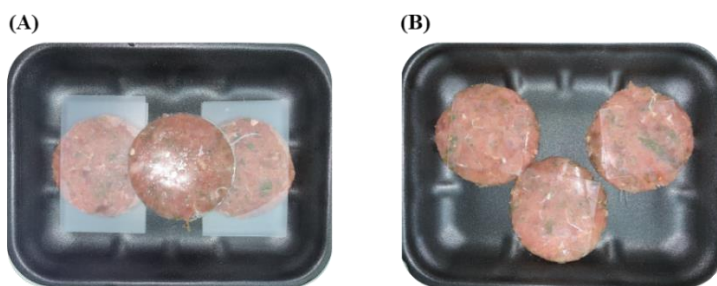


Fig. 23: Representative scheme of preparation of *Sarda sarda* burgers employed in the microbiological and physico-chemical analyses. (A) Burgers of *Sarda sarda* treated with PPs films not-functionalized with 1018K6 (CTR); (B) Burgers of *Sarda sarda* treated with PPs films functionalized with 1018K6 (1018K6-PP).

Chapter II

As reported in **Table 5**, the initial amounts of TAB were significant different between salmon fillets (**Table 3**) and fish burgers (**Table 5**), in which more than 1 Log (CFU/g) of mesophilic bacteria were enumerated. For this reason, fish burgers represent a difficult challenge. Regarding the antimicrobial activity, 1018K6-PPs showed to negatively affect the growth of specific microorganisms, including the total bacterial count. During the storage, the mesophilic TAB increased significantly in control samples until to reach a concentration greater than 8 Log (CFU/g) at 7th day in contrast to that observed in the samples packaged with the antimicrobial slides, in which the maximum acceptable limit set by ICMSF for TAB [7 Log (CFU/g)] was never exceeded during 7 days of storage. Furthermore, due to the key role of mesophilic bacteria in the production of metabolites and off-odours, the antimicrobial activity of 1018K6-PP produced a beneficial effect on the overall appearance of fish burgers and their chemical profile. Therefore, our findings not only confirmed the effectiveness of the new package in slowing the growth of the same bacterial communities described for salmon fillets but also the obtained results enhanced the potential role of 1018K6-PP as tool for monitoring microbiologic contaminations.

Chapter II

Table 5: Evaluation of microbiological counts (Log CFU/g) in *Sarda sarda* burgers packaged in active PP films functionalized with 1018K6 by storage time.

		Day	0	3	5	7
			<i>m</i> ± <i>sem</i>	<i>m</i> ± <i>sem</i>	<i>m</i> ± <i>sem</i>	<i>m</i> ± <i>sem</i>
<i>TAB 30°C</i>	CTR		6.25±0.02 ^{aA}	6.52±0.17 ^A	6.74±0.17 ^{bA}	8.14±0.08 ^{bB}
	1018K6-PP		6.25±0.02	6.17±0.12	6.22±0.22	6.37±0.34 ^y
<i>TAB 7°C</i>	CTR		5.16±0.09 ^A	6.36±0.08 ^B	6.79±0.07 ^{cX}	8.17±0.04 ^{dX}
	1018K6-PP		5.16±0.09 ^A	6.01±0.16 ^B	5.94±0.19 ^{bY}	6.50±0.39 ^{bY}
<i>Coliforms</i>	CTR		4.61±0.02 ^A	5.39±0.09 ^{aB,X}	4.90±0.04 ^C	5.15±0.06 ^{bX}
	1018K6-PP		4.61±0.02	4.60±0.23 ^y	4.62±0.16	4.35±0.25 ^y
<i>Enterobacteriaceae</i>	CTR		3.26±0.17 ^A	5.96±0.57 ^{bC,X}	4.98±0.10 ^B	5.26±0.00 ^C
	1018K6-PP		3.26±0.17 ^A	3.63±0.46 ^{aA,Y}	4.97±0.16 ^{bB}	5.11±0.15 ^B
<i>Pseudomonas spp.</i>	CTR		5.91±0.02 ^{aA}	6.51±0.20 ^{bB,X}	5.79±0.10 ^{aX}	8.59±0.09 ^{cX}
	1018K6-PP		5.91±0.02 ^A	5.91±0.13 ^y	5.47±0.08 ^{bY}	6.44±0.36 ^y
<i>E. coli</i>	CTR		1.50±0.12 ^a	1.80±0.20 ^A	1.62±0.11 ^A	1.11±0.09 ^{bB}
	1018K6-PP		1.50±0.12	1.32±0.18	1.19±0.23	1.28±0.16
<i>Enterococcus faecalis</i>	CTR		4.39±0.13 ^A	4.41±0.09 ^{A,X}	3.21±0.23 ^B	3.96±0.00 ^C
	1018K6-PP		4.39±0.13 ^{aA}	3.39±0.13 ^{b,Y}	3.81±0.39	3.87±0.21 ^b
<i>B. thermosphacta</i>	CTR		<i>ni</i> ^A	<i>ni</i> ^A	1.98±0.00 ^{b,X}	1.98±0.00 ^{b,X}
	1018K6-PP		<i>ni</i>	<i>ni</i>	<i>ni</i> ⁱ	<i>ni</i> ⁱ
<i>S. coagulase positive</i>	CTR		4.45±0.01 ^A	5.64±0.08 ^{B,X}	4.23±0.14 ^{A,X}	4.37±0.26 ^{A,X}
	1018K6-PP		4.45±0.01 ^A	4.12±0.16 ^{aA,Y}	3.6±0.08 ^{bB,Y}	3.19±0.22 ^{b,Y}
<i>pH</i>	CTR		6.20±0.01 ^A	6.18±0.00 ^{A,X}	6.24±0.01 ^B	6.39±0.03 ^{C,X}
	1018K6-PP		6.20±0.01 ^a	6.21±0.01 ^y	6.23±0.00 ^b	6.26±0.03 ^{b,Y}
<i>a_w</i>	CTR		0.976±0.006	0.969±0.001 ^a	0.972±0.001	0.974±0.001 ^b
	1018K6-PP		0.976±0.006	0.963±0.009	0.973±0.000	0.974±0.002

**ni*: not isolated

In each sampling day, three samples by experimental group were analyzed. Statistical analysis was performed comparing experimental groups at each sampling time and within each experimental group along the ripening period. All data were presented as mean (*m*) ± standard error (*sem*).

Different superscript uppercase letters indicate a significant difference at *p* < 0.01.

Different superscript lowercase letters indicate a significant difference at *p* < 0.05.

a–d In the same row mean values (same group in different days) followed by different letters show significant differences.

x–y In the same column mean values (different groups on the same sampling time) followed by different letters show significant differences.

Chapter II

It is worth noting that the same analyses were performed on bonito burgers packaged in PP films not subjected to any surface modification and no discrepancy in the results was observed respect to those obtained with the pre-activated PP films alone (data not shown).

As far as the determination of colour values, the changes in this parameter in fish burgers over time overlapped the data collected for salmon fillets (**Table 6**). Specifically, the samples belonging to the control group appeared less dark than the others, affirming the hypothesis of an increase in proteolysis. Moreover, no differences were highlighted among samples in a^* and b^* values and, consequently, in total colour differences (ΔE), variations in a^* (Δa^*), and in b^* (Δb^*).

Table 6: Changes in colour indices of *Sarda sarda* burgers packaged in active PP films functionalized with 1018K6 by storage time

		Day	0	3	5	7
			<i>m</i> ± <i>sem</i>	<i>m</i> ± <i>sem</i>	<i>m</i> ± <i>sem</i>	<i>m</i> ± <i>sem</i>
L^*	CTR		42.68±1.09	41.07±0.51 ^A	42.95±1.20	45.04±0.77 ^{B,x}
	1018K6-PP		42.68±1.09 ^a	39.76±0.74 ^{ba}	42.32±0.80 ^a	42.79±0.70 ^{By}
a^*	CTR		6.12±0.89	4.93±0.20 ^A	4.87±0.47 ^{A,x}	7.46±0.27 ^{B,x}
	1018K6-PP		6.79±0.34 ^{aA}	4.74±0.37 ^B	5.95±0.20 ^{ba,y}	6.12±0.63 ^y
b^*	CTR		12.42±0.38 ^{aA}	15.61±0.31 ^{B,x}	10.71±0.77 ^A	10.93±0.60 ^{ba}
	1018K6-PP		12.42±0.38 ^{aA}	14.50±0.37 ^{By}	12.29±0.38 ^{aA}	10.53±0.70 ^{ba}
<i>Chroma</i>	CTR		13.89±0.44 ^{aA}	16.37±0.33 ^{B,x}	11.79±0.83 ^{ba,x}	13.24±0.61 ^A
	1018K6-PP		14.15±0.43	15.28±0.35 ^{A,y}	13.66±0.37 ^{By}	12.21±0.86 ^B
<i>Hue angle</i>	CTR		63.86±3.54 ^a	72.47±0.62 ^{ba}	65.48±1.87 ^B	55.51±1.09 ^{BB,x}
	1018K6-PP		61.34±1.08 ^A	71.86±1.45 ^B	64.11±0.97 ^A	60.06±1.83 ^{A,y}
ΔE	CTR			4.20±0.60 ^A	3.61±0.88 ^B	4.06±0.91 ^B
	1018K6-PP			4.60±0.80 ^A	2.79±0.70 ^{ab}	3.65±0.76 ^{BB}
Δb^*	CTR			3.10±0.00	-1.71±0.91	-1.49±0.54
	1018K6-PP			2.09±0.39	-0.13±0.37	-1.88±0.75

In each sampling day, three samples by experimental group were analyzed. Statistical analysis was performed comparing experimental groups at each sampling time and within each experimental group along the ripening period. All data were presented as mean (m) \pm standard error (sem).

Different superscript uppercase letters indicate a significant difference at $p < 0.01$.

Different superscript lowercase letters indicate a significant difference at $p < 0.05$.

a–b In the same row mean values (same group in different days) followed by different letters show significant differences.

x–y In the same column mean values (different groups on the same sampling time) followed by different letters show significant differences.

The graph reported in **Figure 24** showed the positive effect of the active packaging on the redness on 3rd and 7th day, although slightly.

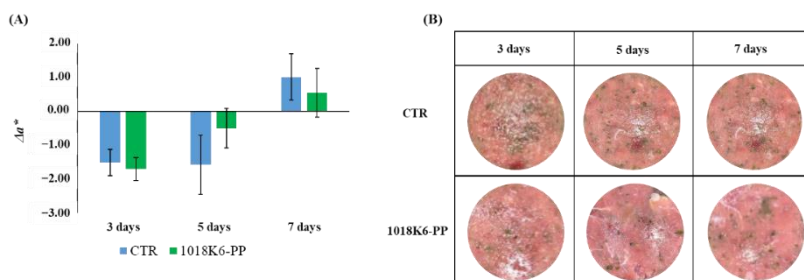


Fig. 24. (A) Analysis of a^* variation (Δa^*) in bonito fish burgers during the storage period. Results are means of three independent experiments and error bars represent the standard error (sem). CTR (blue): PP films without 1018K6; 1018K6-PP (green): PP films functionalized with 1018K6. (B) Photos of *Sarda sarda* burgers packaged with the control and functionalized slides at each sampling time.

Moreover, the experimentation on fish burgers marked the important contribution of the antimicrobial molecule in slowing down the protein degradation. Indeed, significant differences were found among samples packed in active films and control ones and the gap recorded between the corresponding TMA-N and TVB-N values proved the concrete beneficial effect of the 1018K6-PP (Figure 25).

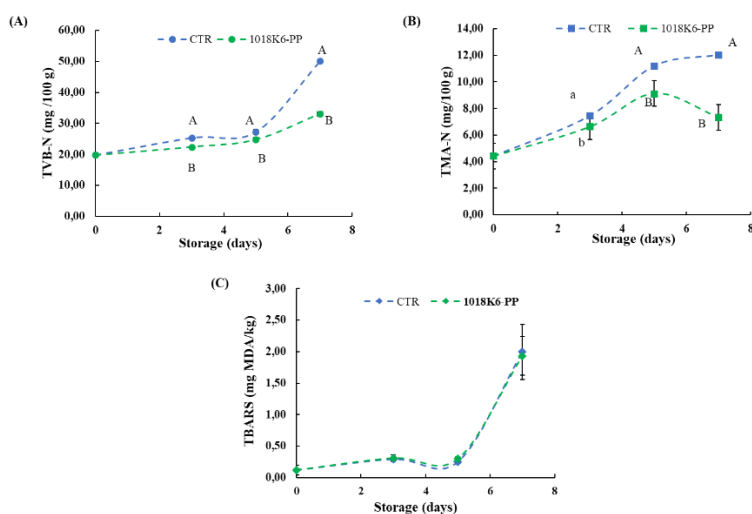


Fig. 25: Effects of 1018K6-PP slides on the Chemical Quality of *Sarda sarda* burgers. Changes in TVB-N (A), TMA-N (B), and TBARS (C) of *Sarda sarda* burgers packaged in active 1018K6-PP films during storage at 4 °C. CTR (blue lines): PP films without 1018K6; 1018K6-PP (green lines): PP films functionalized with 1018K6. Results are means of three independent experiments and error bars represent the standard error (sem). Different letters at each sampling time are used for significantly different samples, according to Tukey test (uppercase letters: $p < 0.01$; lowercase letters: $p < 0.05$).

At last, the off-odours drastically affected the judgments (**Figure 26**), which labelled the control samples as unpleasing foods, probably due to their content in TVB-N and TMA-N. This result is expected considering that the odour weight on the panelist choices is the most critical sensory characteristic for fish products [Wang, T. *et al.*, 2007].

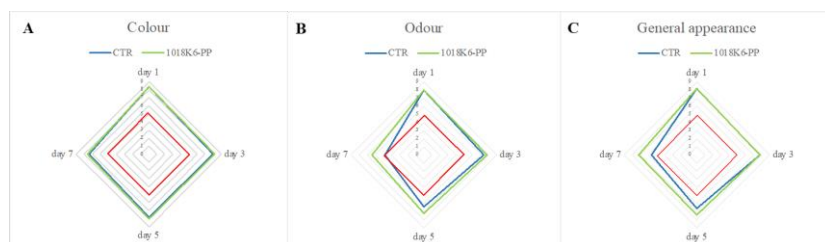


Fig. 26: Changes in colour (A), odour (B), and overall appearance (C) of bonito fish burgers during storage period. CTR (blue lines): PP films without 1018K6; 1018K6-PP (green lines): PP films functionalized with 1018K6.

Lastly, our findings allowed to suppose a positive effect of 1018K6-PP also on the quality parameters of bonito burgers considering the significant differences between the two experimental groups in microorganisms concentrations and CSIs levels, which strongly affected on the sensory appearance of samples. The off-odours and the changes in lightness have demonstrated to be the main visible properties associated to the spoilage processes, so that they could be considered alarm bells for the consumers.

4.2 ANTIMICROBIAL PEPTIDE RiLK1

4.2.1 Conformational characterization of RiLK1

It has been reported that the interactions of an AMP with membrane components should induce conformational changes of the peptide [Pasupuleti, M. *et al.*, 2008; Galanth, C. *et al.*, 2009]. In this context, to investigate on the conformational behavior of RiLK1 in membrane-mimetic environments, the temporal changes in the secondary structure of the peptide over a period of 24 h were studied by Circular Dichroism (CD) spectroscopy in the presence of Sodium Dodecyl Sulfate (SDS), which has been used extensively to mimic the anionic composition of the outer leaflet of the membrane bacteria cells [Tulumello, D.V. *et al.*, 2009].

As shown in **Figure 27 A**, RiLK1 exhibited a prevailing disordered structure in aqueous solution only, as revealed by the typical far-UV CD spectrum, which was characterized by a strong negative band below 200 nm and a weak positive band at 230 nm. After addition of SDS, the dichroic spectrum immediately underwent a dramatic shape change resulting in a more ordered structure with the appearance of a negative peak at ~218 nm and a positive peak at ~195 nm, suggesting that RiLK1 adopted predominantly a β -sheet conformation that was well conserved during the time. These findings are consistent with the previous results showing that almost all linear antimicrobial peptides are unstructured in water solution and adopt their active folding when in contact with the biological membranes [Harmouche, N. *et al.*, 2017]. To calculate the related

contents of the secondary structures of the peptide, the deconvolution of the CD spectra was performed using two different databases and the corresponding results are listed in **Table 7**. Both analyses confirmed the folding of RiLK1 upon interaction with SDS, evidencing a slight decrease of the α -helical and unordered structure content and a subtle increase of β -structures over experimental time span, revealing a high structural stability of the peptide in the assay conditions.

The conformational studies on RiLK1 were carried out also by fluorescence spectroscopy, taking advantage of the presence of two tryptophan residues in the peptide sequence. Indeed, this amino acid is the mainly natural fluorophore in proteins that can be selectively excited at 295 nm, and whose fluorescence is strongly influenced by the polarity of its local microenvironments [Ghisaidoobe, A.B. *et al.*, 2014]. Consequently, tryptophan can report on environmental changes during events, such as folding or unfolding and its maximal wavelength ($\lambda_{\text{emi, max}}$), can be used to study the interactions between Tryptophan (Trp)-containing peptides and membrane-mimetic systems [Moon, C.P *et al.*, 2011]. In aqueous solution, the maximum fluorescence emission was observed at approximately 350 nm that is the typical value for Trp residue when it is fully exposed to a hydrophilic environment (**Figure 27 B**). Immediately after SDS addition ($t = 0$), an increase in the fluorescence intensity and a shift to lower wavelength (“blue shift”) were observed, consistent with a decreased flexibility of Trp residues, which were more sterically confined and a change in the polarity of the microenvironments

surrounding the Trps, becoming more hydrophobic. Furthermore, a gradual large decrease in the peak fluorescence intensity evidenced by RiLK1 during the time could be indicative of the establishment of strong interactions between the peptide and the negatively charged SDS structures, which partly sequestered the two Trps; thus, resulting in a fluorescence quenching effect. Therefore, these results suggested that the two tryptophan residues in our peptide sequence likely play a critical role in its antimicrobial activity, anchoring the peptide into membranes to drive its permeation.

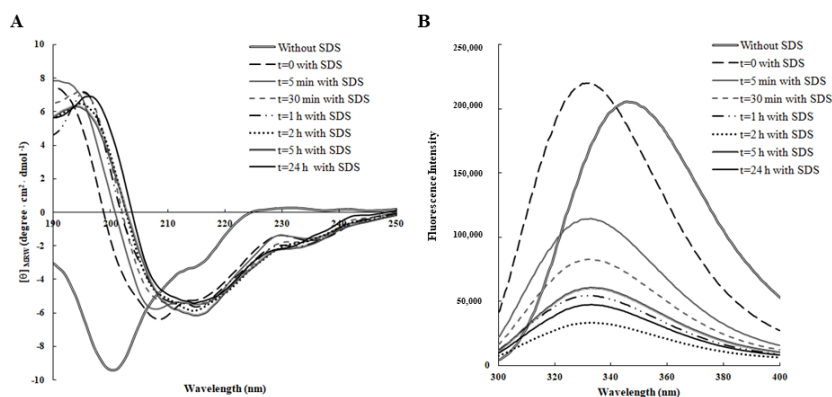


Fig. 27: Time-dependent effect of SDS on the secondary and tertiary structure of RiLK1 monitored by spectroscopic analyses. (A) Far-UV Circular Dichroism (CD) spectra of the peptide (0.1 mg/mL) were recorded in 10 mM Tris-HCl buffer pH 7.0 in the presence or absence of SDS (3 mM) over the time at 25 °C. **(B)** Intrinsic fluorescence emission spectra of RiLK1 (0.1 mg/mL) in 10 mM Tris-HCl buffer, pH 7.0 in the presence or absence of SDS (3 mM) over the time at 25 °C.

Table 7: Secondary structure contents of RiLK1 in the absence or presence of SDS (3 mM) determined by BeStSel (Beta Structure Selection) and DichroWeb server.

Incubation time	BeStSel			DichroWeb CONTIN-LL		
	α -helix	β -sheet	Random	α -helix	β -sheet	Random
Without SDS	1.2%	47.3%	51.5%	4%	35%	61%
t = 0_min_with SDS	7.4%	51.4%	41.3%	22%	38%	40%
t = 5_min_with SDS	4.4%	53.4%	42.2%	22%	42%	36%
t = 30_min_with SDS	11%	48.7%	40.3%	25%	38%	37%
t = 1_h_with SDS	9.8%	51.1%	39.1%	23%	38%	39%
t = 5_h_with SDS	6.7%	54%	39.3%	19%	43%	38%
t = 6_h_with SDS	8%	52%	40.1%	19%	44%	37%
t = 24_h_with SDS	8.4%	53.6%	38%	29%	47%	24%

It has been pointed out that the antibacterial activity of some AMPs is greatly attenuated by certain physical parameters, such as pH, high salt, and high temperature [Travis, S.M. *et al.*, 2000]. Therefore, the real efficacy of functional application of these peptides depends on their structural stability in specific environments [Ghisaidoobe, A.B. *et al.*, 2014]. To this aim, peptide samples were incubated for 24 h at different temperatures or pH values with SDS and the changes in the secondary structure were analyzed by CD spectroscopy. As shown in **Figure 28**, the thermal treatment did not induce significant changes in the shape of the spectra, which was consistent with a stable β -sheet folding conformation at the three temperatures investigated, although the β -structures seemed to be less thermally stable at 90 °C, with respect to those at 4 °C and 25 °C after 24 h incubation (**Table 8**).

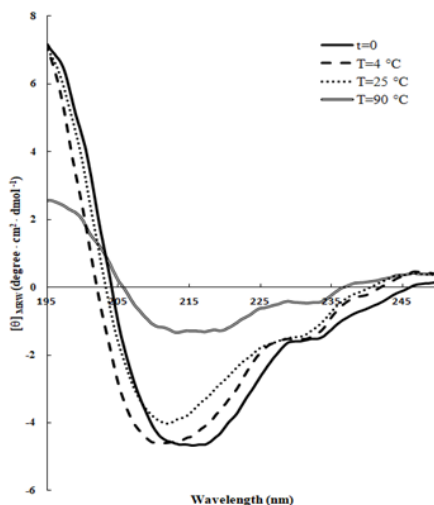


Fig. 28: Effect of the temperature on the secondary structure of RiLK1. Far-UV CD spectra of the peptide (0.1 mg/mL) were acquired in 10 mM Tris-HCl buffer pH 7.0 in the presence of 3 mM SDS at three different temperatures (4 °C, 25 °C, and 90 °C) after 24 h incubation.

Table 8: Secondary structure contents of RiLK1 at different temperatures in the absence or presence of SDS (3 mM) determined by BeStSel and DichroWeb server.

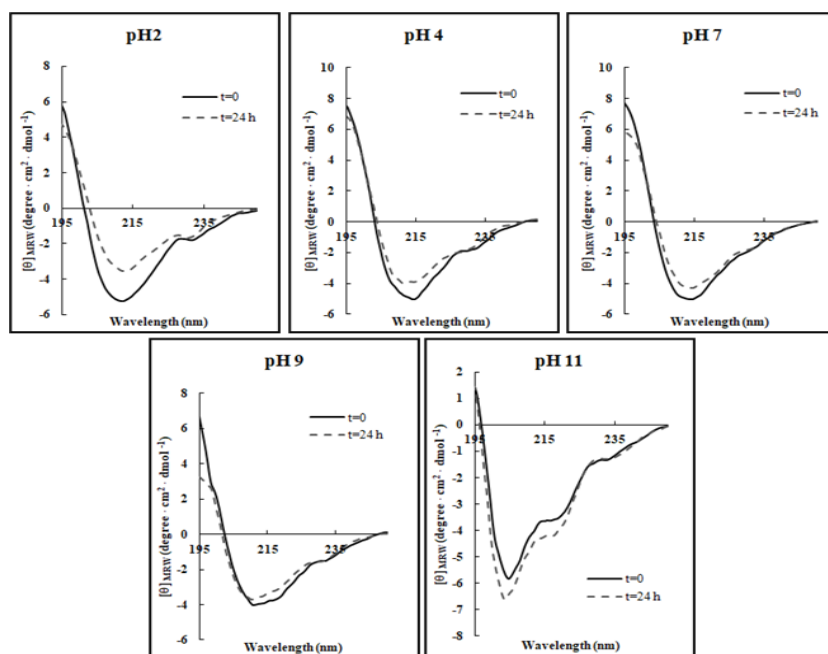
Temperature (°C)	BeStSel			DichroWeb CONTIN-LL		
	α -helix	β -sheet	Random	α -helix	β -sheet	Random
t = 0	17.9%	37.1%	44.9%	21%	43%	36%
T = 4 °C	6.5%	46%	47.5%	25%	37%	38%
T = 25 °C	6.8%	49.7%	43.6%	24%	39%	37%
T = 90 °C	3%	50.4%	46.7%	6%	52%	42%

As far as the effect of pH is concerned, it is known that the net charge of antimicrobial peptides, which depends by the presence and

Chapter II

richness of basic and acidic amino acids, is recognized as playing a key role in their function and an increase in the overall net positive charge leads usually to an improvement in the antimicrobial activity. Therefore, small changes in the pH can interfere with the peptide net charge as each amino acid has an exclusive pKa and isoelectric value.

As depicted in **Figure 29**, only slight structural perturbations were observed in all the conditions investigated, indicating that in general the pH does not markedly affect the β -sheet integrity of RiLK1 over 24 h incubation in the range investigated, as also evidenced in **Table 9**. Only at extreme alkaline conditions (pH 11.0), there was a noticeable variation in the CD spectrum of RiLK1, which was more inclined to assume a random-coil intermediate structure.



Chapter II

Fig. 29: Effect of pH on the secondary structure of RiLK1. Far-UV CD spectra were obtained by incubating the peptide (0.1 mg/mL) in buffers at different pHs for 24 h at 25 °C, and in the presence of SDS at a final concentration of 3 mM.

Table 9: Secondary structure contents of RiLK1 at different pH values determined by BeStSel and DichroWeb server.

pH	BeStSel			DichroWeb CONTIN-LL		
	α -helix	β -sheet	Random	α -helix	β -sheet	Random
pH 2 t = 0	18.5%	37%	44.4%	22%	39%	39%
pH 2 t = 24 h	13.2%	42.5%	44.3%	17%	44%	39%
pH 4 t = 0	7.7%	39.8%	52.4%	23%	41%	36%
pH 4 t = 24 h	13.3%	45.5%	41.2%	24%	41%	35%
pH 7 t = 0	15%	39.5%	45.4%	25%	39%	36%
pH 7 t = 24 h	15.5%	43.8%	40.8%	19%	44%	37%
pH 9 t = 0	13.7%	42%	44.4%	19%	42%	39%
pH 9 t = 24 h	13.4%	43.8%	42.9%	29%	47%	24%
pH 11 t = 0	14.5%	35.3%	50.2%	16%	31%	53%
pH 11 t = 24 h	5.2%	26%	68.8%	14%	33%	53%

One of the multiple obstacles to develop AMPs for biotechnological applications is a significantly reduced antibacterial potency in physiological salt conditions [Wang, B. *et al.*, 2018]. Therefore, salt sensitivity of RiLK1 was evaluated in the presence of 1 M NaCl and its stability in saline solution was quantitatively monitored up to 9 days by Reverse-Phase High-Performance Liquid Chromatography (RP-HPLC) analysis. As shown in the chromatographic profiles reported in **Figure 30**, no precipitation or aggregation phenomena occurred during the incubation periods in 1 M salt, thus indicating a

high lifetime and stability of the peptide solution over the incubation period, at saline concentrations that are higher than the human physiological values (150 mM), or those typical of some food preservative solutions, such as cheese brine.

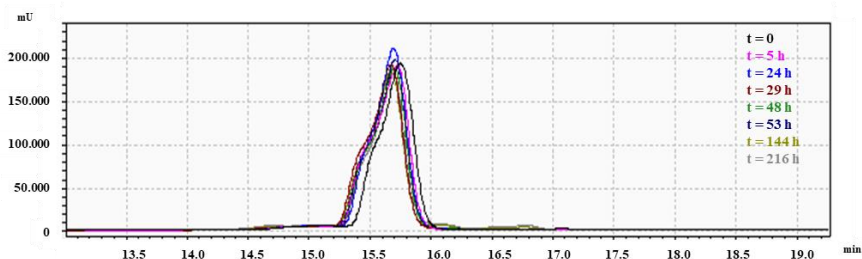


Figure 30: Stability in saline solution of RiLK1 determined by Reverse-Phase High-Performance Liquid Chromatography (RP-HPLC) on a C18 column. The peptide at final concentration of 50 μM was incubated in the presence of NaCl (1M) until 9 days at 25 $^{\circ}\text{C}$. At each incubation time, the peptide solutions were recovered and analyzed by RP-HPLC. The solution at time 0 ($t = 0$) was used as control. The chromatograms are representative of three independent experiments.

4.2.2 *In Vitro* Antimicrobial Activities of RiLK1

The evaluation of the antibacterial efficacy of RiLK1 was determined against some of the most representatives Gram-positive (*Staphylococcus aureus* and *Listeria monocytogenes* LM3) and Gram-negative (*Escherichia coli* and *Salmonella* Typhimurium) pathogens associated with food poisoning. Since bacteria are remarkably resilient and can adapt rapidly in response to a change in the environment changes increasing their virulence and resistance,

all of the strains under investigation were isolated from food products [Beceiro, A. *et al.*, 2013]. The antibacterial efficacy of RiLK1 was tested using the kinetic growth-inhibition assay, which represents an alternative dynamic method to the static Minimum Inhibitory Concentration (MIC) [Ng, V. *et al.*, 2018]. Indeed, since this value is determined at a fixed point in time after exposure to drug concentrations that do not change during the entire incubation interval, it is not possible to get many details on how the growth rate of bacteria is affected by the antimicrobial at different concentrations [Ng, V. *et al.*, 2018].

As represented in **Figure 31**, the sigmoidal dose-response curves of RiLK1 showed a sharp drop in bacterial (expressed as percentage) growth as its concentration was increased and allowed to determine the half-maximal inhibitory concentrations (IC₅₀), which ranged from $0.46 \pm 0.01 \mu\text{M}$ to $1.98 \pm 0.25 \mu\text{M}$, with respect to those measured for 1018-K6, ranging from $0.30 \pm 0.02 \mu\text{M}$ to $2.30 \pm 0.27 \mu\text{M}$ (**Table 10**).

Chapter II

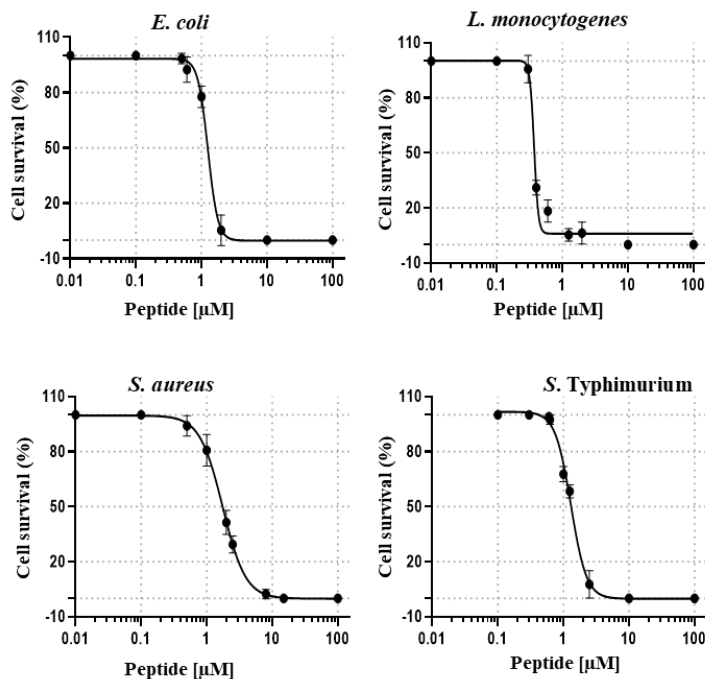


Figure 31: Dose-response effect of RiLK1 on the survival of different foodborne pathogens. Bacteria were incubated in the presence of increasing concentrations of the peptide. Data were determined by enumeration of the surviving colony forming units (CFU) on plates seeded with the pathogen incubated with the different peptide concentrations. Results were expressed as the percentage of colony forming units (CFU) survival, with respect to the colony counted in the control plates. The half-maximal inhibitory concentrations (IC50) and Minimal Bactericidal Concentration (MBC) values of the tested peptide against each bacterial strain were calculated using GraphPad Prism version 6.00. Data are presented as means \pm standard deviation (s.d.) of three separate experiments performed in triplicate.

Chapter II

Table 10: IC₅₀ and MBC values of the tested peptides against the bacterial strains.

Strain	RiLK1		1018-K6	
	IC ₅₀ [μM]	MBC [μM]	IC ₅₀ [μM]	MBC [μM]
<i>E. coli</i>	1.20±0.10	2.0	1.50±0.17	2.0
<i>L. monocytogenes</i> (LM3)	0.46±0.01	2.0	0.30±0.02	8.0
<i>S. Typhimurium</i>	1.30±0.14	2.5	2.30±0.27	25.0
<i>S. aureus</i>	1.98±0.25	16.0	0.92±0.07	16.0

Additionally, the bactericidal activity of RiLK1 was evaluated against all the bacteria strains in comparison to the parental peptide 1018-K6 by quantifying the minimum bactericidal concentration (MBC). As shown in **Table 10**, the short derivative peptide exhibited a bactericidal activity equal to that of 1018-K6 against *S. aureus* (MBC = 16.0 μM) and *E. coli* (MBC = 2.0 μM) strains. On the contrary, RiLK1 displayed a stronger killing efficiency than the parental peptide against *L. monocytogenes* and *S. Typhimurium*, with MBC values 4- and 10-times lower than those of 1018-K6, respectively.

Representative plates of RiLK1 against all the tested pathogens were reported in **Figure 32**.

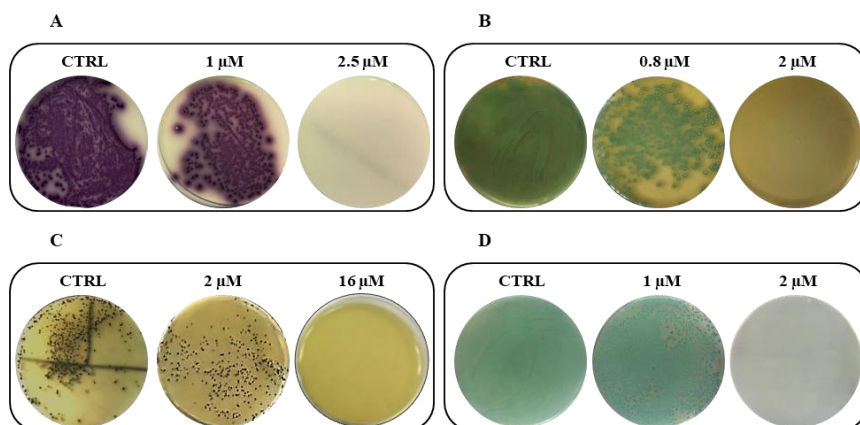


Fig. 32: Antibacterial activity of RiLK1 against different foodborne pathogens: (A) *S. Typhimurium*, (B) *L. monocytogenes*, (C) *S. aureus*, and (D) *E. coli*. CTRL: each tested pathogen without treatment. Bacterial cultures treated, or not, with different concentrations of peptides were seeded on selective plates. The photographs are representative of three independent experiments performed in triplicate.

It is worth noting that one of the most susceptible strains to the RiLK1 action resulted to be *L. monocytogenes* LM3, belonging to the serotype 4b based on the PFGE (Pulsed Field Gel Electrophoresis) profile [Palmieri, G. *et al.*, 2018]. This is notable considering that this serotype has been involved in most of reported human listeriosis cases (more than 95%) and displayed strong adaptation or resistance phenomena to antibiotics and disinfectants [Cossart, P. *et al.*, 2002]. Altogether, these findings pointed out a strong inhibitory and bactericidal activity of RiLK1 against all the pathogens tested, confirming its broad spectrum of action. In addition, the replacement and nature of the N-terminal residues in

the 1018-K6 sequence, together with the reduction of the chain length effectively enhanced the potency of our lead compound, suggesting that the first six amino acids at the N-terminus can be modified to further improve the antibacterial activity.

In order to check whether the peptide under investigation retained its bactericidal activity against multidrug-resistant strains, preliminary antibacterial experiments were performed using a clinical multidrug-resistant ampicillin, chloramphenicol, streptomycin, sulfonamides, and tetracycline (ACSSuT) isolate of *Salmonella* as the representative strain, which is considered one of the major zoonotic and human pathogens worldwide [Yu, C.Y. *et al.*, 2008]. Remarkably, the findings demonstrated that RiLK1 exerted potent killing effects against the clinical isolate (MBC = 1.25 μ M), two-fold lower than those observed against the strain isolated from food products and those determined with the parental peptide 1018-K6 against ACSSuT strain, thus, suggesting that RiLK1 might have a high potential also in the medical field.

4.2.3 *In Vitro* Antifungal Activities of RiLK1

The incidence of serious infections caused by pathogenic fungi that are resistant to the commonly used antifungal drugs is increasing dramatically, and the development of new antifungal agents is becoming an urgent need to avoid a global collapse in the ability to control this type of infections at different levels ranging from human health to food security [Fisher, M.C. *et al.*, 2018; They, T. *et al.*, 2019].

Chapter II

For a long time, besides altering food properties, fungi were not considered as particularly harmful to human health and it is only in recent periods that several mycotoxin-producing fungi have been considered as a major threat to human and animal health, being responsible for different adverse effects [Shephard, G.S. *et al.*, 2008]. Therefore, industrials and scientists are looking for efficient solutions to avoid and/or control the fungal spoilage and their associated infections. Among the 40 fungal species usually considered as pathogens, *Aspergillus spp.* and *Candida spp.* represent two of most relevant genera of mold and yeasts, which are responsible for most fungal infections [Thery, T. *et al.*, 2019].

In this study, to preliminary investigate whether RiLK1 possessed antifungal activity, the effects of the peptide on the growth of the two reference fungal strains *C. albicans* ATCC 14053 and *A. brasiliensis* ATCC 9341, were investigated in comparison with 1018-K6. Notably, susceptibility testing clearly showed that RiLK1 was very effective, being able to inhibit 100% growth of both fungi at 25 μ M concentration (Minimal Fungicidal Concentration - MFC), whereas the parental peptide 1018-K6 exerted no detectable antifungal activities even at the highest concentration (50 μ M) used in the assay (**Figure 33**).

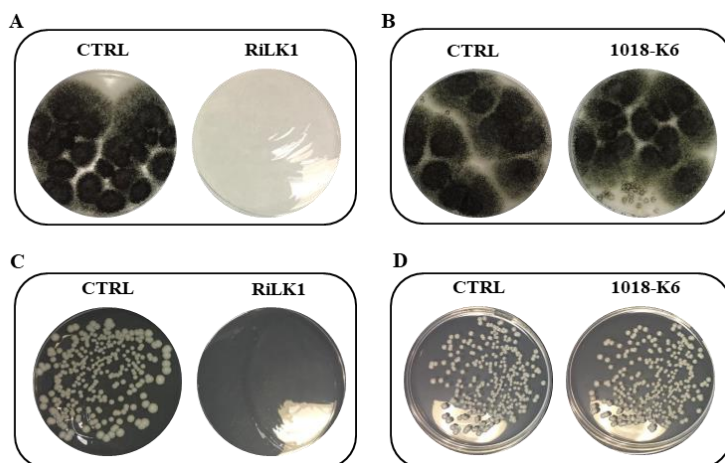


Figure 33: Antifungal activity of RiLK1 and 1018-K6 against pathogenic fungi. (A, B) *Aspergillus brasiliensis* and (C, D) *Candida albicans*. The fungal cultures untreated (CTRL) or treated with the peptides at 25 μ M concentration were seeded on DG18 (Dichloran 18% Glycerol Agar) plates. The photographs are representative of three independent experiments performed in triplicate.

It can be argued that the different inhibitory activity of 1018-K6 across microbial species could be attributed to the differences in the cell membrane composition displayed by bacteria and fungi.

Altogether, these results further emphasized the effectiveness of the modifications introduced in the sequence of 1018-K6 both in terms of chain length and nature of the residues. Indeed, the 10-mer peptide RiLK1 exhibited excellent antibacterial and antifungal activities in contrast to its parent, thus offering important advantages in a lot of applications as it would be helpful to have a single agent able to treat bacterial and fungal co-infections, including those caused by pathogens that are resistant to currently available drugs.

4.2.4 Evaluation of Detrimental Effects of RiLK1 on Mammalian Cells

The inherent risks of the use of antimicrobial agents, which include the determination of cytotoxicity towards human cells, should be addressed in order to consider them for practical applications, specifically in the medical field and food safety [Paiva, A.D. *et al.*, 2012]. In this study, the potential of RiLK1 to affect the cell morphology was evaluated against human keratinocytes (HaCAT), and fetal (WI-38) and adult (TIG-3) lung fibroblast-like cell lines, by incubating the cells with increasing concentrations (1–10 μM) of RiLK1 for 24 h followed by light microscopy. As shown in the micrographs reported in Figure 8, RiLK1 did not induce any change or alterations in the morphology of all the three human cells, similarly to that already observed with the parent 1018-K6 (**Figure 34**) [Palmieri, G. *et al.*, 2018].

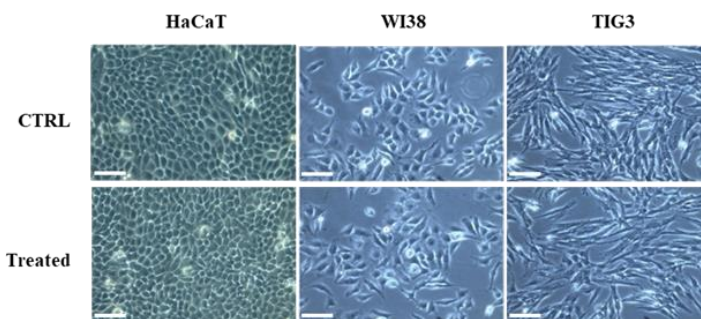


Fig. 34: Morphological observation of different human cell lines treated with RiLK1 under phase-contrast microscope. Keratinocyte (HaCAT), embryonic (WI38), and fetal (TIG3) lung fibroblastic cell lines were incubated at 37 °C for 24 h in absence (CTRL) or in presence (treated)

Chapter II

of RiLK1 at the maximum concentration tested (10 μM). The microscope images are representative of three independent experiments performed in triplicate. Bar is equal 100 μm .

Indeed, the same experiments were performed on WI-38 and TIG-3 cell lines exposed to 1018-K6 at the standard concentration of 10 μM . The obtained results demonstrated that the morphology of both cell lines of interest was not affected by the treatment with the parent peptide (**Figure 34**).

Moreover, the cytotoxic potential of RiLK1 on mammalian cells was initially investigated in vitro by Neutral Red Uptake (NRU) assay using the mammalian BALB 3T3 clone A31 fibroblast cell line. Following the treatment with increased concentrations of RiLK1 (10, 25, and 50 μM), it was observed that the cell viability was recorded as 98%, 98.7%, and 98.9%, respectively, which was calculated by using the equation (1) reported in Material and Methods. Therefore, these findings demonstrated that RiLK1 did not exert any cytotoxic effects against the mammalian cells under investigation at the tested concentrations, even at the highest concentration employed (50 μM), which was sufficiently high to kill all the target pathogen bacteria.

It is noteworthy that although both fungi and host cells are eukaryotic organisms, RiLK1 showed high selectivity towards fungi over mammalian cells, possibly attributable to the different membrane lipid components in this kind of cells. Moreover, the significant differences in the composition of eukaryotic membranes in

comparison to prokaryotic membranes could highlight the important selectivity of RiLK1 for microbial cells. Indeed, the cationic peptide will preferentially bind to the negatively charged phospholipid bilayer of bacterial cells rather than to that overall neutrally charged in eukaryotic [Lavery, G. *et al.*, 2011]. This is advantageous regarding wider potential use of RiLK1 for biotechnological and clinical applications.

4.2.5 Peptide binding to Multilamellar vesicles (MLVs) and lipid binding assay.

The interaction of membrane-binding compounds with model or biological membrane systems can be calculated by determining the amount of ligand bound to the lipid bilayer or free in the aqueous medium. To this aim, different methods can be performed, such as the physical separation of bound and free molecules and the titration methods [White, S.H. *et al.*, 1998].

In this study, the binding parameters of the peptide RiLK1 to pre-formed membranes were evaluated by separating the bound and free peptide through centrifugation [Alvarez, R. *et al.*, 2017], which allows to rapidly calculate the fraction of peptide partitioned, ranging from 0 to 100%. However, to avoid the interfering with the vesicle sedimentation due to density of lipids, the samples were centrifuged at high speed and Multilamellar Vesicles (MLVs) were used instead of Small Unilamellar Vesicles (SUVs), commonly used in partitioning studies [Fox, C.F. *et al.*, 1970]. Even if the determination of the mole fraction partition coefficient (K_p) is

Chapter II

commonly used in binding studies, a more accurate means to describe the interactions between peptide and lipids is the Scatchard analysis [Scatchard, G. 1949], which allows the estimation of dissociation constant K_d (binding affinity) and the number of binding sites B_{max} , [Jain, M.K. *et al.*, 1985; Ito, A.S. *et al.*, 1993]. However, several authors believe that the latter method alone cannot describe the phenomenon, due to the absence of specific receptors on the membranes for peptides, and therefore it is important to calculate both the K_p and K_d . However, the Scatchard method could be appropriate to analyze this type of interactions if the lipid bilayer is considered itself as a receptor and the peptide as a ligand [Escribá, P.V. *et al.*, 1990].

In the present study, the ability of peptide Rilk1 to bind to phospholipid bilayers was studied by carrying out saturation binding experiments. The concentration of peptide in the aqueous (supernatant-free ligand) and lipidic (pellet-bound ligand) phases, was measured using fluorescence spectroscopy, exploiting the generation of Trp signals in both phases [Palmieri, G. *et al.*, 2018]. As it can be seen in both figures, the behavior of the cation peptide clearly differed from one type of model membrane to another, possibly attributable to the differences in lipid composition, and mainly dependent on the membrane's surface charge. Indeed, a widely accepted notion is that electrostatic interactions between the positively charged residues of AMPs and the negatively charged phospholipid head groups of the target pathogen cell membrane, such as phosphatidylserine, phosphatidyl glycerol, or cardiolipin

Chapter II

[Bessalle, R. et al., 1992; Matsuzaki, K. et al., 1997; Dathe, M. et al., 2001; Melo, M.N. et al., 2009], are involved in the first step of interaction of the peptides (binding and accumulation) with the membrane.

Knowing that the 10-mer peptide RiLK1 has net positive charge [Agrillo, B. *et al.*, 2020], the potential interaction of this molecule with lipids containing net negative charges had already been hypothesized. This hypothesis was supported by the results shown in the present study where membranes composed of zwitterionic Phosphatidylcholine (PC) [Matsuno, R. *et al.*, 2011], simulating the bulk fluid phases in eukaryotic cell, were compared with those that mimic the anionic bacterial cells. The receptor density study confirmed a very low affinity of RiLK1 for the membranes with net neutral charge or low negative charge (PC and PC40:POPE40:SM15:PS5, respectively). Furthermore, the peptide seemed to prefer model membranes resembling that of *Staphylococcus aureus*, respect to those of *Salmonella Typhimurium*, reaching the highest value of Bmax as determined by using fluorescence spectroscopy methods (**Figure 35**).

In fact, it was necessary to increase the maximum peptide dose until 120 μM (**Figure 35**) to carry out saturation binding experiments, suggesting the propensity for the peptide to bind to Gram-positive bacterial cells much more easily than to Gram-negative ones. From the interactional point of view, it can be argued that the *Staphylococcus*-like membrane contains more binding sites and/or that its affinity is higher than that of the eukaryotic like membrane.

Chapter II

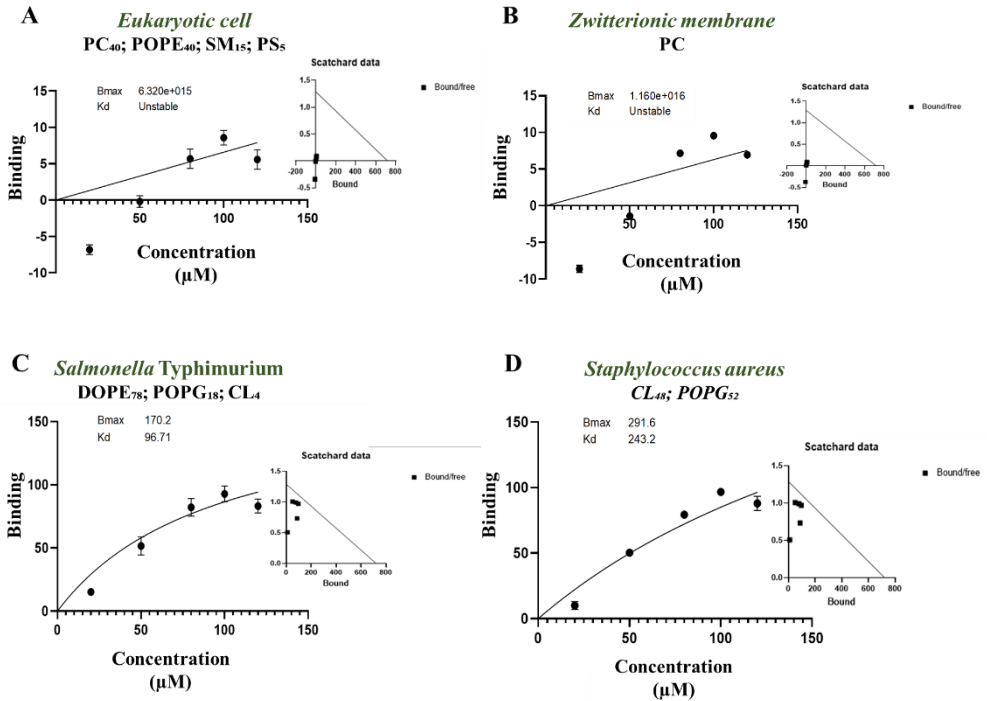


Fig. 35: Saturation binding assay curves and Scatchard plots transformation for fluorescence spectroscopy data of Rilk1 in model membranes of (A) eukaryotic cell, (B) zwitterionic lipids, (C) *S. aureus*, (D) *S. Typhimurium*. Results are means of three independent experiments.

5. CONCLUSIONS

The increase in consumer demand for fresh, minimally processed and “natural” foods, together with the requirements for maintenance and improvement of safety, quality and shelf-life features, has fueled research for the identification of new antimicrobials to develop innovative and alternative packaging solutions.

This represents an important and urgent need specifically for perishable foods, such as fish products which are characterized by a short shelf-life. In the present study, two different kinds of fish foods, such as *Salmon salar* fillets and *Sarda sarda* burgers, were used to test the feasibility for applying 1018K6-PP packaging in the food industry. The obtained results have shown that the developed 1018K6-PP helps to maintain the chemical and microbial quality of this kind of products without induce sensory alterations during the refrigerated storage. Therefore, this antimicrobial packaging can represent an excellent and promising option for the preservation of fish foods due to its antimicrobial, non-toxic and re-use properties, reducing the occurrence of foodborne illness.

Following the success of these findings, in order to achieve a new generation of AMPs able to work at lower dosages, with higher efficacy, fewer side effects, and, especially, with lower production costs, a decapeptide named RiLK1 was *de novo* designed by specifically modifying the antimicrobial peptide 1018-K6. In this work, RiLK1 was structural and functional characterized, revealing its high efficiency against both fungi and Gram-positive and -negative bacteria without

Chapter II

causing human cell cytotoxicity, being able to preserve its structural features under a wide range of physical conditions, such as pH, temperature, and high salt concentrations.

Moreover, preliminary studies on potential molecular interaction between RiLK1 and some bacterial or eukaryal membrane models were conducted and it was demonstrated that the peptide was highly selective towards bacterial membranes such as those of *S. aureus* compared to eukaryotic ones.

Collectively, our findings strongly support that the projected RiLK1 holds potential as a promising candidate for the development of a novel class of antimicrobial agents for further biotechnological and clinical applications, helping to overcome serious problems that prevent the use of AMPs, such as low stability, toxicity to mammalian cells, high cost of production, and induction of antibiotic-resistance phenomena.

Further works are in progress to verify the possibility to conjugate RiLK1 to polymeric surfaces, in order to develop more eco-sustainable and efficient antimicrobial packaging.

6. REFERENCES

- Agrillo B, Proroga YTR, Gogliettino M, Balestrieri M, Tatè R, Nicolais L, Palmieri G. A Safe and Multitasking Antimicrobial Decapeptide: The Road from De Novo Design to Structural and Functional Characterization. *Int J Mol Sci.* 2020 Sep 22;21(18):6952.
- Agrillo, B.; Balestrieri, M.; Gogliettino, M.; Palmieri, G.; Moretta, R.; Proroga, Y. T.; Cornacchia, A.; Capuano, F.; Smaldone, G.; De Stefano, L. Functionalized polymeric materials with bio-derived antimicrobial peptides for “active” packaging. *Int. J. Mol. Sci.* 2019, 20(3), 601.
- Agrillo, B.; Balestrieri, M.; Gogliettino, M.; Palmieri, G.; Moretta, R.; Proroga, Y. T.; Cornacchia, A.; Capuano, F.; Smaldone, G.; De Stefano, L. Functionalized polymeric materials with bio-derived antimicrobial peptides for “active” packaging. *Int. J. Mol. Sci.* 2019, 20(3), 601.
- Alvarez R, Casas J, López DJ, Iburguren M, Suari-Rivera A, Terés S, Guardiola-Serrano F, Lossos A, Busquets X, Kakhlon O, Escribá PV, 2017. Triacylglycerol mimetics regulate membrane interactions of glycogen branching enzyme: implications for therapy. *J lipid res* 58(8), 1598-1612.
- Alves, V.L.; Rico, B.P.; Cruz, R.M.; Vicente, A.A.; Khmelinskii, I.; Vieira, M.C. Preparation and characterization of a chitosan film with grape seed extract-carvacrol microcapsules and its effect on the shelf-life of refrigerated Salmon (*Salmo salar*). *LWT*, 2018, 89, 525-534.
- Angelini, A. et al., Bicyclic peptide inhibitor reveals large contact interface with a protease target, *ACS Chem. Biol.*, 2012, 7(5), 817–821.
- Angiolillo, L.; Conte, A.; Del Nobile, M.A. A new method to bio-preserve sea bass fillets. *Int. J. Food Microbiol.* 2018, 271, 60–66
- Apostolopoulos, V. Joanna Bojarska, Tsun-Thai Chai, “A Global Review on Short Peptides: Frontiers and Perspectives”, *Molecules.* 2021 January.
- Arun K. Bhunia *Foodborne Microbial Pathogens Mechanisms and Pathogenesis* Second Edition. Springer New York, (2018).
- Azizi-Lalabadi, M.; Rafiei, L.; Divband, B.; Ehsani, A. Active packaging for Salmon stored at refrigerator with Polypropylene nanocomposites containing 4A zeolite, ZnO nanoparticles, and green tea extract. *Food Sci. Nutr.* 2020, 8(12), 6445-6456.
- Bahar, A.A. & Ren, D. (2013) Antimicrobial peptides. *Pharmaceuticals*, 6, 1543–1575.
- Baniya, H.B.; Shrestha, R.; Guragain, R.P.; Kshetri, M.B.; Pandey, B.P.; Subedi, D.P. Generation and characterization of an atmospheric-pressure plasma jet (APPJ) and its application in the surface modification of polyethylene terephthalate. *Int. J. Polym. Sci.*, 2020.
- Barbosa, S.C.; Nobre, T.M.; Volpati, D.; Cilli, E.M.; Correa, D.S.; Oliveira, O.N. The Cyclic Peptide Labaditin Does Not Alter the Outer Membrane Integrity of *Salmonella enterica* Serovar Typhimurium. *Sci. Rep.* 2019, 9, 1993.
- Barreiro M., Carocho M., Morales P., Ferreira I. C. R. F. 2014. Adding Molecules to Food, Pros and Cons: A Review on Synthetic and Natural Food Additives.
- Beceiro, A.; Tomás, M.; Bou, G. Antimicrobial resistance and virulence: a successful or deleterious association in the bacterial world? *Clin. Microbiol. Rev.* 2013, 26, 185–230.
- Bessalle R, Haas H, Gorla A, Shalit I, Fridkin M. Augmentation of the antibacterial activity of magainin by positive-charge chain extension. *Antimicrob Agents Chemother* 1992, 36, 313- 317.

Chapter II

- Bi, X.; Wang, C.; Dong, W.; Zhu, W.; Shang, D. Antimicrobial properties and interaction of two Trp-substituted cationic antimicrobial peptides with a lipid bilayer. *J. Antibiot.* 2014, 67, 361–368.
- Bjerkeng, B. Carotenoid pigmentation of salmonid fishes—recent progress 1. In: *Avances en Nutricion Acuicola V Memorias del V. Simposium Internacional de Nutricion Acuicola*. Merida, Yucatan, Mexico, 19-22 November 2000., pp. 71-89.
- Bockus A. T., C. M. McEwen and R. S. Lokey, Form and function in cyclic peptide natural products: a pharmacokinetic perspective, *Curr. ToMed. Chem.*, 2013, 13(7), 821–836.
- Bontems, F., Roumestand, C., Gilquin, B., Menez, A. & Toma, F. (1991) Refined structure of charybdotoxin: common motifs in scorpion toxins and insect defensins. *Science*, 254, 1521–1523.
- Boskou, G.; Debevere, J. Reduction of trimethylamine oxide by *Shewanella* spp. under modified atmospheres in vitro. *Food Microbiol.* 1997, 14, 543–553.
- Bozariis, I.S.; Stamatou, A.P.; Nychas, G.J. Microbiological aspects and shelf life of processed seafood products. *J. Sci. Food Agric.* 2013, 93, 1184-1190.
- Bramstedt, F.; Auerbach, M. The Spoilage of Fresh-Water Fish. In: *Fish as Food*, Borgstram, G., Ed., Academic Press Inc.: San Diego, 1961, vol. 1, pp. 613–637.
- Bulet, Phippe, et al. "Enlarged scale chemical synthesis and range of activity of drosocin, an O-glycosylated antibacterial peptide of *Drosophila*." *European journal of biochemistry* 238.1 (1996): 64-69.
- Capuano, F.; Mancusi, A.; Capparelli, R.; Esposito, S.; Proroga, Y.T.R. Characterization of Drug Resistance and Virulotypes of Salmonella Strains Isolated from Food and Humans. *Foodborne Pathog. Dis.* 2013, 10, 963–968.
- Carocho M., Morales P., Ferreira I. C. R. F. 2015. Natural food additives: Quo vadis? DOI:10.1016/j.tifs.2015.06.007.
- Casares, D.; Escribá, P.V.; Rosselló, C.A. Membrane Lipid Composition: Effect on Membrane and Organelle Structure, Function and Compartmentalization and Therapeutic Avenues. *Int. J. Mol. Sci.* 2019, 20, 2167.
- Casteels, Peter, and Paul Tempst. "Apidaeicin-type peptide antibiotics function through a nonporeforming mechanism involving stereospecificity." *Biochemical and biophysical research communications* 199.1 (1994): 339-345.
- Chen, Y., Mant, C.T., Farmer, S.W., Hancock, R.E.W, Vasil, M.L. & Hodges, R.S. (2005) Rational design of α -helical antimicrobial peptides with enhanced activities and specificity/therapeutic index. *Journal of Biological Chemistry*, 280, 12316–12329.
- Chung, S.W.C.; Chan, B.T.P. Trimethylamine oxide, dimethylamine, trimethylamine and formaldehyde levels in main traded fish species in Hong Kong. *Food Addit. Contam. 2009, Part B*, 2(1), 44-51.
- Colagiorgi, A.; Festa, R.; Di Ciccio, P.A.; Gogliettino, M.; Balestrieri, M.; Palmieri, G.; Anastasio, A.; Ianieri, A. Rapid biofilm eradication of the antimicrobial peptide 1018-K6 against *Staphylococcus aureus*: A new potential tool to fight bacterial bio-films. *Food Control* 2020, 107, 106815.
- Commission Implementing Regulation (EU) 2019/627 of 15 March 2019 laying down uniform practical arrangements for the performance of official controls on products of animal origin intended for human consumption in accordance with Regulation (EU) 2017/625 of the European Parliament and of the Council and amending Commission Regulation (EC) No 2074/2005 as regards official controls, *Off. J. Eur. Union L* 131/51.
- Commission Regulation (EC) No 2073/2005 of 15 November 2005 on microbiological criteria for foodstuffs, *Off. J. Eur. Union L* 138.
- Conway, E. J.; Byrne, A. An absorption apparatus for the micro-determination of certain volatile substances: The micro-determination of ammonia. *Biochem. J.* 1933, 27(2), 419.

Chapter II

- Cossart, P. Molecular and cellular basis of the infection by *Listeria monocytogenes*: an overview. *Int. J. Med. Microbiol.* 2002, 291, 401–409.
- Craik D. J., Chemistry. Seamless proteins tie up their loose ends, *Science*, 2006, 311(5767), 1563–1564.6 A.
- Dalgaard, P. Qualitative and quantitative characterization of spoilage bacteria from packed fish. *Int. J. Food Microbiol.* 1995, 26, 319–333.
- Dalgaard, P.; Gram, L.; Huss, H.H. Spoilage and shelf life of cod fillets packed in vacuum or modified atmospheres. *Int. J. Food Microbiol.* 1993, 19, 283e294.
- Dathe M., Nikolenko H., Meyer J., Beyermann M., Bienert M. Optimization of the Antimicrobial Activity of Magainin Peptides by Modification of Charge. *FEBS Lett.* 2001; 501:146–150. doi: 10.1016/S0014-5793(01)02648.
- de la Fuente-Núñez, C., Reffuveille, F., Haney, E.F., Straus, S.K., Hancock, R.E.W., 2014a. Broad-spectrum anti-biofilm peptide that targets a cellular stress response. *PLoS Pathog.* 10 (5), e1004152.
- de la Fuente-Núñez, C., Mansour, S.C., Wang, Z., Jiang, L., Breidenstein, E.B.M., Elliott, M., Reffuveille, F., Speert, D.P., Reckseidler-Zenteno, S.L., Shen, Y., Haapasalo, M., Hancock, R.E.W., 2014b. Anti-biofilm and immunomodulatory activities of peptides that inhibit biofilms formed by pathogens isolated from cystic fibrosis patients. *Antibiotics* 3 (4), 509–526.
- De Oliveira Dias, R. & Franco, O.L. (2015) Cysteine-stabilized $\alpha\beta$ defensins: from a common fold to antibacterial activity. *Peptides*, 72, 64–72.
- Edwards, I.A., Elliott, A.G., Kavanagh, A.M., Zuegg, J., Blaskovich, M.A. & Cooper, M.A. (2016) Contribution of amphipathicity and hydrophobicity to the antimicrobial activity and cytotoxicity of β -hairpin peptides. *ACS Infectious Diseases*, 2, 442–450.
- Breukink, E. Ben de Kruijff. The lantibiotic nisin, a special case or not?, *Biochimica et Biophysica Acta (BBA) - Biomembranes*, Volume 1462, Issues 1–2, 1999, Pages 223–234.
- EFSA and ECDC (European Food Safety Authority and European Centre for Disease Prevention and Control), 2021. The European Union Summary Report on Antimicrobial Resistance in zoonotic and indicator bacteria from humans, animals and food in 2018/2019. *EFSA Journal* 2021;19(4):6490, 179 pp.
- Ehrenstein, G., & Lecar, H. (1977). Electrically gated ionic channels in lipid bilayers. *Quarterly Reviews of Biophysics*, 10(1), 1–34. doi:10.1017/S0033583500000123
- Ejsing CS, Sampaio JL, Surendranath V, Duchoslav E, Ekroos K, Klemm RW, Simons K, Shevchenko A. Global analysis of the yeast lipidome by quantitative shotgun mass spectrometry. *Proc Natl Acad Sci U S A.* 2009 Feb 17;106(7):2136–41. doi: 10.1073/pnas.0811700106. Epub 2009 Jan 27.
- Epand, R.M.; Epand, R.F. Bacterial Membrane Lipids in the Action of Antimicrobial Agents. *J. Pept. Sci.* 2011, 17, 298–305.
- Escriba PV, Ferrer-Montiel AV, Ferragut JA, Gonzalez-Ros JM. Role of membrane lipids in the interaction of daunomycin with plasma membranes from tumor cells: implications in drug-resistance phenomena. *Biochemistry* 1990, 29(31), 7275–7282.
- Falcigno L., D’Auria G., Palmieri G., Gogliettino M., Agrillo B., Tatè R., Dardano P., Nicolais L., Balestrieri M., “Key Physicochemical Determinants in the Antimicrobial Peptide RiLK1 Promote Amphipathic Structures”, *Int. J. Mol. Sci.* 2021.
- FAO. 2013. Food wastage footprint; impacts on natural resources. Summary Report. Rome. FAO. 2019.
- Fisher, M.C.; Hawkins, N.J.; Sanglard, D.; Gurr, S.J. Worldwide emergence of resistance to antifungal drugs challenges human health and food security. *Science* 2018, 360, 739–742.
- Floros, J. D., L. L. Dock and J. H. Han. 1997. "Active Packaging Technologies and Applications," *Food Cosmetics and Drug Packaging*, 20(1):10–17.

Chapter II

- Fox CF, Law JH, Tsukagoshi N, Wilson G. A density label for membranes. *P Natl A Sci*, 67(2), 598-605 1970.
- Françoise, L. Occurrence and role of lactic acid bacteria in seafood products. *Food Microbiol.* 2010, 27, 698–709.
- Fu, Y., Sarkar, P., Bhunia, A.K., Yao, Y. Delivery systems of antimicrobial compounds to food. *Trends Food Sci. Technol.* 2016. 57 (part A), 165–177.
- Gagnon, M.G., Roy, R.N., Lomakin, I.B., Florin, T., Mankin, A.S. & Steitz, T.A. (2016) Structures of proline-rich peptides bound to the ribosome reveal a common mechanism of protein synthesis inhibition. *Nucleic Acids Research*, 44, 2439–2450.
- Galanth, C.; Abbassi, F.; Lequin, O.; Ayala-Sanmartin, J.; Ladram, A.; Nicolas, P.; Amiche, M. Mechanism of antibacterial action of dermaseptin B2: interplay between helix-hinge-helix structure and membrane curvature strain. *Biochemistry* 2009, 48, 313–327.
- Garcha, S. "Control of food spoilage molds using lactobacillus bacteriocins". *Journal of Pure and Applied Microbiology.* (2018) 12 (3): 1365–1373.
- Geeroms, N.; Verbeke, W.; Van Kenhove, P. Consumers' health-related motive orientations and ready meal consumption behaviour. *Appetite* 2008, 51, 704–712.
- Ghisaidoobe, A.B.; Chung, S.J. Intrinsic tryptophan fluorescence in the detection and analysis of proteins: a focus on Förster resonance energy transfer techniques. *Int. J. Mol. Sci.* 2014, 15, 22518–22538.
- Giménez, B.; Roncalés, P.; Beltrán, J.A. The effects of natural antioxidants and lighting conditions on the quality of salmon (*Salmo salar*) fillets packaged in modified atmosphere. *J. Sci. Food Agric.* 2005, 85, 1033–1040.
- Goldrick, Barbara (2003). "Foodborne Diseases: More efforts needed to meet the Healthy People 2010 objectives". *The American Journal of Nursing.* 103 (3): 105–106. doi:10.1097/00004446-200303000-00043. PMID 12635640.
- Gonzalez-Rodriguez, M.N.; Sanz, J.J.; Santos, J.A.; Otero, A.; Garcia-Lopez, M.L. Bacteriological quality of aquacultured freshwater fish portions in prepackaged trays stored at 3 C. *J. Food Prot.* 2001, 64(9), 1399-1404.
- Gourama H, Bullerman LB, Bianchini A (2015). Toxigenic fungi and fungal toxins. In: Salfinger Y, Tortorello ML (eds) *Compendium of methods for the microbiological examination of foods.* American Public Health Association, Washington, DC, pp 583–594.
- Gram, L.; Dalgaard, P. Fish spoilage bacteria — problems and solutions. *Curr. Opin. Biotechnol.* 2002, 13, 262–266.
- Guzmán-Rodríguez J.J., Ochoa-Zarzosa A., López-Gómez R., López-Meza J., "Plant Antimicrobial Peptides as Potential Anticancer Agents", *BioMed Research International.* (2015).
- Han, J. H. (2000). Antimicrobial food packaging. *Food Technol.* **54(3)**, 56-65.
- Hancock, R. E. W., & Scott, M. G. (2000). The role of antimicrobial peptides in animal defenses. *Proceedings of the National Academy of Sciences*, 97(16), 8856–8861.
- Haney, E.F., Brito-Sánchez, Y., Trimble, M.J.; Mansour, S.C.; Cherkasov, A.; Hancock, R.E.W. Computer-aided Discovery of Peptides that Specifically Attack Bacterial Biofilms. *Sci. Rep.* 2018, 8, 1871.
- Harmouche, N.; Aisenbrey, C.; Porcelli, F.; Xia, Y.; Nelson, S.E.D.; Chen, X.; Raya, J.; Vermeer, L.; Aparicio, C.; Veglia, G.; et al. Solution and Solid-State Nuclear Magnetic Resonance Structural Investigations of the Antimicrobial Designer Peptide GL13K in Membranes. *Biochemistry* 2017, 56, 4269–4278.
- Hintz, T., Matthews, K.K., Di, R., 2015. The use of plant antimicrobial compounds for food preservation. *Biomed. Res. Int.* 2015, 1–12.
- Huan, Y. Qing Kong,* Haijin Mou, and Huaxi Yi, "Antimicrobial Peptides: Classification, Design, Application and Research Progress in Multiple Fields", *Front Microbiol.* 2020.

Chapter II

- Humphrey T, O'Brien S, Madsen M (2007) Campylobacters as zoonotic pathogens: A food production perspective. *Int J Food Microbiol* 117: 237–257.
- Isabel M López-Lara, Otto Geiger. "Bacterial lipid diversity", *Biochim Biophys Acta Mol Cell Biol Lipids*, 2017 Nov;
- Ito AS, Castrucci AML, Hruby VJ, Hadley ME, Krajcarski DT, Szabo AG, 1993. Structure – activity correlations of melanotropin peptides in model lipids by tryptophan fluorescence studies. *Biochemistry* 1993, 32, 12264 – 12272.
- Jacquot, R. Organic Constituents of Fish and Other Aquatic Animal Foods. In: *Fish as Food*, Borgstram, G., Ed., Academic Press Inc., San Diego, 1961, vol. 1, pp. 145–209.
- Jain MK, Rogers J, Simpson L, Gierasch LM, 1985. Effect of tryptophan derivatives on the phase properties of bilayers. *Biochim Biophys Acta* 816, 153 – 162.
- Jorgensen, L.V., Huss, H.H., Dalgaard, P., The effect of biogenic amine production by single bacterial cultures and metabiosis on cold-smoked salmon. *J. Appl. Microbiol.* 2000, 89, 920–934.
- Kalafatovic, D.; Giralt, E. Cell-Penetrating Peptides: Design Strategies beyond Primary Structure and Amphipathicity. *Molecules* 2017, 22, 1929.
- Karabagias, I.; Badeka, A.; Kontominas, M.G. Shelf life extension of lamb meat using thyme or oregano essential oils and modified atmosphere packaging. *Meat Sci.* 2011, 88, 109–116.
- Kitundu, E.; Young, O.; Seale, B.; Owens, A. Lactic fermentation of cooked, comminuted mussel, *Perna canaliculus*. *Food Microbiol.* 2021, 99, 103829.
- Laverty, G.; Gorman, S.P.; Gilmore, B.F. The potential of antimicrobial peptides as biocides. *Int. J. Mol. Sci.* 2011, 12, 6566–6596.
- Lemaire A., Limbourg S. 2019. How can food loss and waste management achieve sustainable development goals? DOI:10.1016/J.JCLEPRO.2019.06.226.
- Leirfall, J.; Bendiksen, E.A.; Olsen, J.V.; Østerlie, M. A comparative study of organic- versus conventional Atlantic Salmon. II. Fillet color, carotenoid- and fatty acid composition as affected by dry salting, cold smoking and storage. *Aquaculture* 2015, 451, 369–376.
- Leirfall, J.; Jakobsen, A.N.; Skipnes, D.; Waldenstrøm, L.; Hoel, S., Rotabakk, B.T. Comparative evaluation on the quality and shelf-life of Atlantic salmon (*Salmo salar* L.) filets using microwave and conventional pasteurization in combination with novel packaging methods. *J. Food Sci.* 2018, 83(12), 3099-3109.
- Listeria Monocytogenes* | Servizio di ispezione e sicurezza alimentare (usda.gov).
- Listeriosi - Relazione epidemiologica annuale 2017 (europa.eu).
- Mace, S.; Cornet, J.; Chevalier, F.; Cardinal, M.; Pilet, M.F.; Dousset, X.; Joffraud, J.J. Characterization of the spoilage microbiota in raw salmon steaks stored under vacuum or modified atmosphere packaging combining conventional methods and PCR-TTGE. *Food Microbiol.* 2012, 30(1), 164–172.
- Mardirossian, M., Pérébaskine, N., Benincasa, M., Gambato, S., Hofmann, S., Huter, P. et al. (2018). The dolphin proline-rich antimicrobial peptide Tur1A inhibits protein synthesis by targeting the bacterial ribosome. *Cell Chemical Biology*, 25, 530–539
- Marshall, Eleanor, Liliana M. Costa, and Jose Gutierrez-Marcos. "Cysteine-rich peptides (CRPs) mediate diverse aspects of cell–cell communication in plant reproduction and development." *Journal of experimental botany* 62.5 (2011): 1677-1686.
- Masalha M, Borovok I, Schreiber R, Aharonowitz Y, Cohen G. "Analysis of transcription of the *Staphylococcus aureus* aerobic class Ib and anaerobic class III ribonucleotide reductase genes in response to oxygen". *Journal of Bacteriology.* (2001). 183 (24): 7260–7272.
- Mathur, D.; Prakash, S.; Anand, P.; Kaur, H.; Agrawal, P.; Mehta, A.; Kumar, R.; Singh, S.; Raghava, G.P.S. PEPLife: A Repository of the Half-life of Peptides. *Sci. Rep.* 2016, 6, 36617.

- Matsuno R, Ishihara K. Integrated Functional Nanocolloids Covered with Artificial Cell Membranes for Biomedical Applications. *Nano Today* 2011, 6, 61–74.
- Matsuzaki K, Nakamura A, Murase O, Sugishita K, Fujii N, Miyajima K. Modulation of magainin 2-lipid bilayer interactions by peptide charge. *Biochemistry* 1997, 36, 2104–2111.
- Melo MN, Ferre R, Castanho MA. Antimicrobial peptides: linking partition, activity and high membrane-bound concentrations. *Nat Rev Microbiol* 2009, 7, 245–250.
- Merlo, T.C.; Contreras-Castillo, C.J.; Saldana, E.; Barancelli, G.V.; Dargelio, M.D.B.; Yoshida, C.M.P.; Ribeiro Junior, E.E.; Massarioli, A.; Venturini, A.C. Incorporation of pink pepper residue extract into chitosan film combined with a modified atmosphere packaging: Effects on the shelf-life of salmon fillets. *Food Res. Int.* 2019, 125, 108633.
- Miconai, A.; Wien F, Bulyáki, É.; Kun, J.; Moussong, É.; Lee, Y.H.; Goto, Y.;
- Moon, C.P.; Fleming, K.G. Using tryptophan fluorescence to measure the stability of membrane proteins folded in liposomes. *Methods Enzymol.* 2011, 492, 189–211.
- Ng, V.; Kuehne, S.A.; Chan, W.C. Rational Design and Synthesis of Modified Teixobactin Analogues: In Vitro Antibacterial Activity against *Staphylococcus aureus*, *Propionibacterium acnes* and *Pseudomonas aeruginosa*. *Chemistry* 2018, 24, 9136–9147.
- Oren, Ziv, and Yechiel Shai. "Mode of action of linear amphipathic α -helical antimicrobial peptides." *Peptide Science* 47.6 (1998): 451-463.
- Paiva, A.D.; de Oliveira, M.D.; de Paula, S.O.; Baracat-Pereira, M.C.; Breukink, E.; Mantovani, H.C. Toxicity of bovicin HC5 against mammalian cell lines and the role of cholesterol in bacteriocin activity. *Microbiology* 2012, 158, 2851–2858.
- Palmieri G, Balestrieri M, Capuano F, Proroga YTR, Pomilio F, Centorame P, Riccio A, Marrone R, Anastasio A. *Int J Food Microbiol.* 2018. "Bactericidal and antibiofilm activity of batenecin-derivative peptides against the food-pathogen *Listeria monocytogenes*: New perspectives for food processing industry."
- Palmieri, G.; Tatè, R.; Gogliettino, M.; Balestrieri, M.; Rea, I.; Terracciano, M.; Proroga, Y.T.; Capuano, F.; Anastasio, A.; De Stefano, L. Small synthetic peptides bioconjugated to hybrid gold nanoparticles destroy potentially deadly bacteria at sub-micromolar concentrations. *Bioconjugate Chem.* 2018, 29(11), 3877–3885.
- Parlapani, F.F.; Haroutounian, S.A.; Nychas, G.J.E.; Boziaris, I.S. Microbiological spoilage and volatiles production of gutted European sea bass stored under air and commercial modified atmosphere package at 2 C. *Food Microbiol.* 2015, 50, 44–53.
- Pasupuleti, M.; Walse, B.; Svensson, B.; Malmsten, M.; Schmidtchen, A. Rational design of antimicrobial C3a analogues with enhanced effects against *Staphylococci* using an integrated structure and function-based approach. *Biochemistry* 2008, 47, 9057–9070.
- Petruzzi L, Corbo MR, Sinigaglia M, Bevilacqua A. Microbial Spoilage of Foods. In *The Microbiological Quality of Food*, 2017. 1–21.
- Prabhakar, P.K.; Vatsa, S.; Srivastav, P.P.; Pathak, S.S. A comprehensive review on freshness of fish and assessment: Analytical methods and recent innovations. *Food Res. Int.* 2020, 133, 109157.
- Raeisi, M.; Tajik, H.; Aliakbarlu, J.; Mirhosseini, S.H.; Hosseini, S.M.H. Effect of carboxymethyl cellulose-based coatings incorporated with *Zataria multiflora* Boiss. essential oil and grape seed extract on the shelf-life of rainbow trout fillets. *LWT-Food Sci. Technol.* 2015, 64(2), 898–904.
- Rahman MS (eds). *Handbook of food preservation*. 2nd ed. Food science and technology. Boca Raton: CRC Press; 2007.
- Rasekh, J.; Kramer, A.; Finch, R. Objective evaluation of canned tuna sensory quality. *J. Food Sci.* 1970, 35(4), 417–423.

Chapter II

- Reffuveille, F., de la Fuente-Núñez, C., Mansour, S., Hancock, R.E.W., 2014. A broad-spectrum anti-biofilm peptide enhances antibiotic action against bacterial biofilms. *Antimicrob. Agents Chemother.* 58, 5363–5371.
- Remya, S.; Mohan, C.O.; Bindu, J.; Sivaraman, G.K.; Venkateshwarlu, G.; Ravishankar, C.N. Effect of chitosan based active packaging film on the keeping quality of chilled stored barracuda fish. *J. Food Sci. Technol.* 2016, 53, 685–693
- Roberts, T.A., Bryan, F.L., Christian, J.H.B., Kilsby, D., Olson Jr, J.C., Siliker, J.H. ICMSF: International Commission of Microbiological Specifications for Foods. Microorganisms in Foods. 2. Sampling for Microbial Analysis. Principles and Specific Applications, 2nd ed.; University of Toronto Press, Toronto, 1986.
- Rodrigues, M.J.; Ho, P.; Lopez-Caballero, M.E.; Vaz-Pires, P.; Nunes, M.L. Characterization and identification of microflora from soaked cod and respective salted raw materials. *Food Microbiol.* 2003, 20, 471–481.
- Roohinejad, S.; Koubaa, M.; Barba, F.J.; Saljoughian, S.; Amid, M.; Greiner, R. Application of seaweeds to develop new food products with enhanced shelf-life, quality and health-related beneficial properties. *Int. Food Res.* 2017, 99, 1066–1083.
- Roostita, R., & Fleet, G. H. (1996). Growth of yeasts in milk and associated changes to milk composition. *International Journal of Food Microbiology*, 31(1–3), 205–219. [https://doi.org/10.1016/0168-1605\(96\)00999-3](https://doi.org/10.1016/0168-1605(96)00999-3)
- Sathe, S. J., Nawani, N. N., Dhakephalkar, P. K., & Kapadnis, B. P. (2007). Antifungal lactic acid bacteria with potential to prolong shelf-life of fresh vegetables. *Journal of Applied Microbiology*, 103(6), 2622–2628.
- Scatchard G. The attractions of proteins for small molecules and ions. *Ann N Y Acad Sci* 51(4), 660-672, 1949.
- Secchi, G.; Parisi, G. From farm to fork: lipid oxidation in fish products. A review. *Ital. J. Anim. Sci.* 2016, 15(1), 124-136.
- Shephard, G.S. Impact of mycotoxins on human health in developing countries. *Food Addit. Contam. Part A Chem. Anal. Control Expo. Risk Assess.* 2008, 25, 146–151.
- Shumilina, E.; Slizyte, R.; Mozuraityte, R.; Dykyy, A.; Stein, T.A.; Dikiy, A. Quality changes of salmon by-products during storage: Assessment and quantification by NMR. *Food Chem.* 2016, 211, 803-811.
- Singh, A., Prasad, S.M. Reduction of heavy metal load in food chain: technology assessment. *Rev Environ Sci Biotechnol* 10, 199 (2011). <https://doi.org/10.1007/s11157-011-9241-z>
- Singh, R. P. Scientific principles of shelf-life evaluation. In: *Shelf-Life Evaluation of Foods*. Man, C. M. D., Jones, A. A., Eds. Blackie Academic and Professional, Glasgow. (1994) pp. 3–24.
- Sohrabi, C., A. Foster and A. Tavassoli, Methods for generating and screening libraries of genetically encoded cyclic peptides in drug discovery, *Nat. Rev. Chem.*, 2020, 4(2), 90–101.
- Soltani, Samira, et al. "Bacteriocins as a new generation of antimicrobials: toxicity aspects and regulations." *FEMS Microbiology Reviews* 45.1 (2021): fuaa039.
- Spohn, R.; Daruka, L.; Lázár, V.; Martins, A.; Vidovics, F.; Grézal, G.; Méhi, O.; Kintses, B.; Számel, M.; Jangir, P.K.; et al. Integrated evolutionary analysis reveals antimicrobial peptides with limited resistance. *Nat. Commun.* 2019, 10, 4538.
- Stotz, Henrik U., James Thomson, and Yueju Wang. "Plant defensins: defense, development and application." *Plant signaling & behavior* 4.11 (2009): 1010-1012.
- Suryawanshi, S.K.; Chouhan, U. Application of Bioinformatics in the Prediction and Identification of Potential Antimicrobial Peptides from *Curcuma Longa*. *Biosci. Biotechnol. Res. Commun.* 2016, 9, 216-224.
- Thery, T.; Lynch, K.M.; Arendt, E.K. Natural Antifungal Peptides/Proteins as Model for Novel Food Preservatives. *Compr. Rev. Food Sci. Food Saf.* 2019, 18, 1327–1360.

Chapter II

- Tossi, A., Scocchi, M., Skerlavaj, B. & Gennaro, R. (1994) Identification and characterization of a primary antibacterial domain in CAP18, a lipopolysaccharide binding protein from rabbit leukocytes. *FEBS Letters*, 339, 108–112.
- Travis, S.M.; Anderson, N.N.; Forsyth, W.R.; Espiritu, C.; Conway, B.D.; Greenberg, E.P.; McCray, P.B. Jr; Lehrer, R.I.; Welsh, M.J.; Tack, B.F. Bactericidal activity of mammalian cathelicidin-derived peptides. *Infect. Immun.* 2000, 68, 2748–2755.
- Tulumello, D.V.; Deber, C.M. SDS micelles as a membrane-mimetic environment for transmembrane segments. *Biochemistry* 2009, 48, 12096–12103.
- Waghu, F.H.; Barai, R.S.; Gurung, P.; Idicula-Thomas, S. CAMPR3: a database on sequences, structures and signatures of antimicrobial peptides. *Nucleic Acids Res.* 2016, 44, D1094–1097.
- Wang, B.; Xie, N.; Li, B. Influence of peptide characteristics on their stability, intestinal transport, and in vitro bioavailability: A review. *J. Food Biochem.* 2018, 43, e12571.
- Wang, G.; Li, X.; Wang, Z. APD3: the antimicrobial peptide database as a tool for research and education. *Nucleic Acids Res.* 2016, 44, D1087–D1093.
- Wang, T.; Sveinsdóttir, K.; Magnússon, H.; Martinsdóttir, E. Combined Application of Modified Atmosphere Packaging and Superchilled Storage to Extend the Shelf-life of Fresh Cod (*Gadus morhua*) Loins. *J. Food Sci.* 2007, 73, S11–S19.
- Weng, Y., Chen, M., and Chen, W. Antimicrobial food packaging materials from poly(ethyleneco-methacrylic acid). *Food Science and Technology* 32: 191–195. (1999).
- White SH, Wimley WC, Ladokhin AS, 1998. Energetics of Peptide–Bilayer Interactions. *Methods in enzymology* 295, 62-87.
- Whitmore, L.; Wallace, B.A. DICHROWEB, an online server for protein secondary structure analyses from circular dichroism spectroscopic data. *Nucleic Acids Res.* 2004, 32, W668–W673.
- Wiernasz, N.; Leroi, F.; Chevalier, F.; Cornet, J.; Cardinal, M.; Rohloff, J.; Pilet, M.F. Salmon gravlax biopreservation with lactic acid bacteria: A polyphasic approach to assessing the impact on organoleptic properties, microbial ecosystem and volatilome composition. *Front. Microbiol.* 2020, 10, 3103.
- World Health Organization. WHO Estimates of the Global Burden of Foodborne Diseases: Foodborne Disease Burden Epidemiology Reference Group 2007–2015; World Health Organization (WHO): Geneva, Switzerland, 2015; pp. 1–15.
- Yang, C.; Chen, Y.; Peng, S.; Tsai, A.; Jer-Fu Lee, T.; Yen, J.H.; Liou, J.W. An engineered arginine-rich α -helical antimicrobial peptide exhibits broad-spectrum bactericidal activity against pathogenic bacteria and reduces bacterial infections in mice. *Sci. Rep.* 2018, 8, 14602.
- Yeaman, Michael R., and Nannette Y. Yount. "Mechanisms of antimicrobial peptide action and resistance." *Pharmacological reviews* 55.1 (2003): 27-55.
- Yeşilayer, N. Comparison of Flesh Colour Assessment Methods for Wild Brown Trout (*Salmo trutta macrostigma*), Farmed Rainbow Trout (*Oncorhynchus mykiss*) and Farmed Atlantic Salmon (*Salmo salar*). *Pak. J. Zool.* 2020, 3, 52.
- Yu C.Y.; Chou, S.J.; Yeh, C.M.; Chao, M.R.; Huang, K.C.; Chang, Y.F.; Chiou, C.S.; Weill, F.X.; Chiu, C.H.; Chu, C.H.; et al. Prevalence and characterization of multidrug-resistant (type ACSSuT) *Salmonella enterica* serovar Typhimurium strains in isolates from four gosling farms and a hatchery farm. *J. Clin. Microbiol.* 2008, 46, 522–526.
- Zaslloff, M. (1987) Magainins, a class of antimicrobial peptides from *Xenopus* skin: isolation, characterization of two active forms, and partial cDNA sequence of a precursor. *Proc. Natl. Acad. Sci. USA* 84, 5449–5453.
- Zheng A., Lin, Q., Zhang D., Qin, P., Xu L., Ai P., Ding L., Wang Y., Chen Y., Liu Y., Sun Z., Feng H., Liang X., Fu R., Tang C., Li Q., Zhang J., Xie Z., Deng Q., Li S, Wang

Chapter II

- S., Zhu J., Wang L., Liu H., Li P. 2013. The evolution and pathogenic mechanisms of the rice sheath blight pathogen. *Nature Communications* volume 4, Article number: 1424.
- Zhu S. & Gao B., Tytgat J. (2005) Phylogenetic distribution, functional epitopes and evolution of the CS $\alpha\beta$ superfamily. *Cellular and Molecular Life Sciences*, 62, 2257–2269.
- Zhu, X., Zhang, L., Wang, J., Ma, Z., Xu, W., Li, J. et al. (2015) Characterization of antimicrobial activity and mechanisms of low amphipathic peptides with different α -helical propensity. *Acta Biomaterialia*, 18, 155–167.

